The U.S. GOVERNMENT

IS ABSOLVED

FROM ANY LITIGATION WHICH MAY

ENSUE FROM THE CONTRACTORS IN-

FRINGING ON THE FOREIGN PATENT

RIGHTS WHICH MAY BE INVOLVED.

UNCLASSIFIED

Recant, I. O. Aerodynamics (2) 20709
Wallace, A. R. Stability and Control (1)
Airplanes - Tail configurations MR L-779
(08490.3); Airplanes - Control characteristics (08393);
Airplanes - Performance (08478.6);*

Wind-tunnel tests of the 1/9-scale model of the Curtiss XP-62 airplane with various vertical tail arrangements

National Advisory Committee for Aeronautics, Washington, D. C.

U.S. Eng. Unclass. Jul'43 120 photos, tables, diagrs, graphs

The effect of various vertical tail arrangements upon the stability and control characteristics of an XP-62 fighter model was investigated. Rudder-free yaw characteristics with take-off power and flaps deflected were satisfactory after dorsal fin modifications. Directional stability was obtained with all modified vertical tails. Satisfactory rudder effectiveness resulted partly because the dual-rotation propellers produced no asymmetric yawing moments. Pedal forces in sideslips were undesirably large but may be easily reduced.

* Airplane models - Wind tunnel testing (08321.3); XP-62 (08321.3)

NOTE: Requests for copies of this report must be addressed to: N.A.C.A., Washington, D. C.

MR July 1943

NATIONAL ADVISORY COMMITTEE FOR AERONAUTICS

WARTIME REPORT

ORIGINALLY ISSUED
July 1943 as
Memorandum Report

WIND-TUNNEL TESTS OF THE 1/9-SCALE MODEL

OF THE CURTISS XP-62 AIRPLANE WITH

VARIOUS VERTICAL TAIL ARRANGEMENTS

By I. G. Recant and Arthur R. Wallace

Langley Memorial Aeronautical Laboratory
Langley Field, Va.

WASHINGTON

L – 779

L-779

NATIONAL ADVISORY COMMITTEE FOR AERONAUTICS

MEMORANDUM REPORT

for the

Army Air Forces, Materiel Command

WIND-TUNNEL TESTS OF THE 1/9-SCALE MODEL

OF THE CURTISS XP-62 AIRPLANE WITH

VARIOUS VERTICAL TAIL ARRANGEMENTS

By I. G. Recant and Arthur R. Wallace

INTRODUCTION

At the request of the Army Air Forces tests were made of the 1/9-scale model of the Curtiss XP-62 airplane in the LMAL 7- by 10-foot tunnel.

Yaw tests were made of the 1/9-scale model with power and with propeller windmilling. Enough variations of the vertical tail were tested to determine the following effects with rudder free or fixed:

1. Effect of vertical tail area, aspect ratio, and plan form
2. Effect of increasing vertical tail length
3. Effect of a variety of dorsal fins
4. Effect of end plates on horizontal tail
5. Effect of rudder chord
6. Effect of rudder balance
7. Effect of a bevel trailing edge
8. Effect of a balancing tab

The purpose of the tests was to determine the directional stability and rudder control characteristics with the above vertical tail variations.

MODEL

The 1/9-scale model of the Curtiss XP-62 airplane was furnished by the Curtiss company. It is shown in figures 1, 2(a), and 2(b). The model was not checked for accuracy but all surfaces were found to be fair and finished in a satisfactory manner.

The dual-rotation power plant was built and installed in the model at the Laboratory. The power plant consisted of a frame supporting two water-cooled induction motors, one for each propeller since the two propellers were not geared together. The front propeller was driven directly by an extension of one motor shaft, and the rear propeller was driven by two spur gears which can be seen in figures 2(a) and 2(b). The three-blade metal propellers and hubs were furnished with the model. The diameter of these propellers was not to scale, being 1.555 feet as compared to the scaled value of 1.462 feet. Both propellers were set at a 15° blade angle at 0.75 radius for all tests. Motor speed was measured by a cathode-ray oscillograph which indicated the output of a small alternator built into each motor.

Three additional vertical tail surfaces were supplied with the model, each of which has interchangeable rudder nose pieces and mating fin blocks so that the rudder balance could be changed. A bevel trailing edge was built up on one of the rudders. After testing, the bevel trailing edge was removed and a tab installed. One of the tails was tested in conjunction with end plates on the horizontal tail and also with the fuselage extended 4 inches on the model. Descriptions and other data pertaining to the various vertical tails tested are given in table I.

Several dorsal fins were made at the Laboratory and are shown in figure 16. Some of the dorsal fins are shown in place in several of the photographs. The dorsal fins are shown as attached to tail VR. When attached to other vertical tails the dorsal fins were cut so that they could be bent to fit the angle between fuselage and fins. The over-all length of the dorsals for tails other than VR thus departs from the length given in figure 16 but the area and shape were not materially changed. For some of the tests, antispin fillets were installed as shown in figures 17(a) and 17(b). The antispin fillets also appear on figures 13 and 15.

Rudder hinge moments were measured by an electrically indicating strain gage supplied by the Laboratory.

TESTS AND RESULTS

Test conditions. - The tests were made in the LMAL 7- by 10-foot tunnel at dynamic pressures of 16.37 and 9.21 pounds per square foot, corresponding to 80 and 60 miles per hour for standard sea-level conditions. The test Reynolds numbers were about 710,000 and 530,000 based on the wing mean aerodynamic chord of 11.63 inches. Because of the turbulence factor of 1.6 for the wind tunnel, the effective Reynolds numbers were about 1,100,000 and 850,000.

Coefficients and symbols. - The results of the tests are presented in standard NACA coefficients of forces and moments based on the model wing area, wing span, and wing mean aerodynamic chord. Rolling, yawing, and pitching-moment coefficients are given about the normal center-of-gravity location shown in figure 1 (26.7 percent of the mean aerodynamic chord). The data are referred to a system of axes in which the Z axis is in the plane of symmetry and perpendicular to the relative wind, the X axis is in the plane of symmetry and perpendicular to the Z axis, and the Y axis is perpendicular to the plane of symmetry (fig. 18).

The coefficients and symbols are defined as follows:

C_L lift coefficient (Z/qS)

C_{D_R} resultant-drag coefficient (X/qS)

C_Y lateral-force coefficient (Y/qS)

C_l rolling-moment coefficient (L/qSb)

C_m pitching-moment coefficient (M/qSc)

C_n yawing-moment coefficient (N/qSb)

C_h hinge-moment coefficient $(H/qb\bar{c}^2)$

T_c' effective thrust coefficient (T/qS)

V/nD propeller advance-diameter ratio

where

$\left.\begin{matrix}X\\Y\\Z\end{matrix}\right\}$ forces along X, Y, and Z axes, respectively

$\left.\begin{matrix}L\\M\\N\end{matrix}\right\}$ moments about X, Y, and Z axes, respectively

H control-surface hinge moments

T effective thrust

q dynamic pressure $(\frac{1}{2}\rho V^2)$

S wing area (5.18 sq ft)

c mean aerodynamic chord of wing (11.63 in.)

b wing span (5.96 ft)

$b\bar{c}^2$ product of the span and the square of the chord of a control surface, in which $\bar{c}$ is the root mean square chord back of the hinge line

D propeller diameter

n revolutions per second of propellers

and

ρ mass density of air

α angle of attack of thrust line, degrees

ψ angle of yaw, degrees

i_t angle of stabilizer setting with respect to thrust line, degrees; positive with trailing edge down

δ control-surface deflections, degrees

β_F front propeller blade angle at 0.75 radius (15°)

β_R rear propeller blade angle at 0.75 radius (15°)

I.A.S. indicated airspeed, miles per hour

Subcripts

e elevator

r rudder

f flap

t horizontal tail (tab when used with δ)

Corrections. - No corrections have been applied to the data for tares caused by the model support strut. No jet-boundary corrections have been applied to any of the data given except angles of attack and drag coefficients, which were corrected as follows:

$$\Delta\alpha = \delta_w \frac{S}{C} C_L \ 57.3$$

$$\Delta C_D = \delta_w \frac{S}{C} C_L^2$$

where

δ_w 0.113

S wing area (5.18 sq ft)

C wind-tunnel cross-section area (69.59 sq ft)

Test procedure. - Propeller calibrations were made by measuring the resultant drag with the model at zero angle of attack for a range of propeller speeds. Because there was a small difference between the speeds of the front and rear propellers, all the data were arbitrarily based on the speed of the rear propeller. The effective thrust coefficients were then computed from

$$T_c' = C_D - C_{D_R}$$

where C_D is the drag coefficient of the model with propeller removed. The propeller calibration is shown in figure 19.

The thrust coefficients required at any lift coefficient for various amounts of power were furnished by the Curtiss company and have been reproduced on figure 20. Since all the tests made in the present investigation were yaw tests, they were made at constant propeller rpm. No allowance was made for any variation of C_L with yaw or T_c' with yaw and pitch. (Any reference to military power in this report means military power at 20,000 feet as given on fig. 20.)

The first tests were made to determine the most severe conditions for rudder-free directional stability. Various dorsal fins were then tested at the determined critical condition; that is, take-off power, $\delta_f = 45^\circ$, and a high-lift coefficient. In general, subsequent tests were made with the smallest and best shaped dorsal fin which met requirement II-F-3 of reference 1. This requirement specifies that the yawing moment due to sideslip (rudder free) should be such that the airplane will always tend to return to zero sideslip regardless of the angle of sideslip to which it has been forced. The rudder tests for tail VR were made at conditions requested by the Curtiss company. All other rudder tests were made at the worst condition (determined from the tests) for rudder-free stability. A few additional tests were made to determine the directional stability in the high-speed condition for each tail. Tail-off tests were made for miscellaneous flight conditions so that the stability contributed by the vertical tail may be isolated.

Unless otherwise noted, the landing gear was extended when flaps were deflected, and was retracted when flaps were neutral. The stabilizer setting (i_t) was 2° and the elevator setting (δe) was 0° for all tail-on tests. In all cases the propeller blade angle was 15°.

Methods of comparing the characteristics of the various vertical tails. - The pedal forces and rudder deflections required to maintain a given angle of steady yaw were determined

L-779

from the curves of C_{h_r} and C_n. Pedal-force computations were first based on the assumption of ±4 inches of pedal travel for ±30° of rudder deflection, the rudder deflection being assumed to be linearly proportional to the pedal movement, and a wing loading of 35 pounds per square foot. Any pedal force resulting at zero yaw was assumed to be trimmed to zero.

In order to compare the various tails on a more equitable basis the rudder deflection for each tail was assumed to be limited to the angle which trimmed the model at 18° angle of yaw. The mechanical advantage for each tail was then based on a pedal movement of 4 inches to obtain the rudder deflection for trim at 18° of yaw. This angle of yaw was chosen because it was the angle held by the least effective rudder with 30° deflection.

A third basis for comparison of the various tails is the rudder angles and pedal forces required to overcome the adverse aileron yawing moments. The possibility of this requirement becoming critical is imminent inasmuch as the requirement for trim at zero yaw is no problem with a dual-rotation propeller. The yawing moment due to full aileron deflection was obtained from unpublished results of tests of a 0.27-scale model of the airplane in the Langley 19-foot pressure tunnel. The yawing moment due to rolling was evaluated by use of the theoretical charts of reference 2 for a wing-tip helix angle, $pb/2V$, of 0.09. Most of the tests were made with take-off power at a moderate angle of attack. The critical condition for rudder deflection, however, will be at a high angle of attack with the propeller windmilling, because the yawing moment due to rolling will be greater at the high angle and the rudder effectiveness lower with the propeller windmilling. The rudder effectiveness for each tail was therefore estimated from the power-on data for the windmilling condition by assuming that the change in effectiveness between the two conditions was a function only of the dynamic pressure at the tail. The rudder hinge-moment coefficients for the windmilling condition were estimated in a similar manner.

The rudder deflections required to overcome the adverse aileron yawing moment were computed from the estimated yawing moment and the rudder effectiveness. In computing the pedal forces, the mechanical advantage for each configuration was obtained by assuming 4 inches of pedal travel for the rudder deflection required to overcome the aileron yawing moment in the windmilling condition; that is, the mechanical advantage varied with each tail configuration but, for a given tail, was the same with propeller windmilling or with power on.

Summary of tests. - For convenience, an outline of the tests with the figures on which the results appear is given below: (The landing gear was up when $\delta_f = 0$ and down when $\delta_f = 45^\circ$ except as noted. $\beta_F = \beta_R = 15^\circ$. $i_t = 2^\circ$. $\delta_e = 0$. No ailerons.)

Type of test	Vertical Tail	Figure
I Rudder free to determine most critical condition		
A. $\delta_f = 45^\circ$, take-off power and windmilling	VR	21
B. $\delta_f = 0^\circ$, take-off power and windmilling	VR	22
II Tail off	- - - - - - - -	23
III Rudder free with various dorsal fins	VR	24
IV Effect of propellers, rudder free	VR	25
V Rudder free at most critical condition (take-off power, $\delta_f = 45^\circ$, $\alpha = 7.5^\circ$)		
A. Comparison of tails	All	26
B. Effect of end plates and tail extension	$V^{13}R^{13}$	27
C. Effect of antispin fins	$V^{14}R^{14}$	28
D. Effect of balance	$V^{16}R^{16}$, $V^{18}R^{18}$	29
E. Effect of balance	$V^{19}R^{19}$, $V^{20}R^{20}$	30
F. Effect of bevel trailing edge	$V^{14}R^{14.5}$	31
VI Rudder locked, miscellaneous tests and replots		
A.	VR	32
B.	$V^{13}R^{13}$	33
C. Comparison of tails, $\delta_f = 0^\circ$, military power 20,000 ft, $\alpha = 5.2^\circ$	All	34
VII Rudder deflection		
A. $\delta_f = 0^\circ$, military power, 20,000 ft, $\alpha = 5.2^\circ$	VR	35
B. $\delta_f = 45^\circ$, military power 20,000 ft, $\alpha = 2.7^\circ$, L.G. up	VR	36

	Type of tests	Vertical Tail	Figure
	C. $\delta_f = 45^\circ$ take-off power $\alpha = 7.5^\circ$	$V_{13}R_{13}$	37
	D. $\delta_f = 45^\circ$ ------do------ $\alpha = 7.5^\circ$ (end plates)	$V_{13}R_{13}$	38
	E. $\delta_f = 45^\circ$ take-off power $\alpha = 7.5^\circ$ (extended)	$V_{13}R_{13E}$	39
	F. $\delta_f = 45^\circ$ take-off power $\alpha = 7.5^\circ$	$V_{14}R_{14}$	40
	G. $\delta_f = 45^\circ$ ------do------ $\alpha = 7.5^\circ$	$V_{18}R_{18}$	41
	H. $\delta_f = 45^\circ$ ------do------ $\alpha = 7.5^\circ$	$V_{16}R_{16}$	42
	I. $\delta_f = 45^\circ$ ------do------ $\alpha = 7.5^\circ$	$V_{14}R_{14.5}$	43
	J. $\delta_f = 45^\circ$ ------do------ $\alpha = 7.5^\circ$	$V_{19}R_{19}$	44
	K. $\delta_f = 45^\circ$ ------do------ $\alpha = 7.5^\circ$	$V_{20}R_{20}$	45
VIII	Tab deflection	$V_{14}R_{14T}$	46
IX	Computation of rudder deflection and pedal forces for trim		
	A.	VR	47
	B. Effect of end plates and tail extension	$V_{13}R_{13}$	48
	C. Effect of balance	$V_{14}R_{14}$, $V_{16}R_{16}$, $V_{18}R_{18}$	49
	D. Balancing tab and bevel trailing edge	$V_{14}R_{14}$	50
	E. Effect of balance	$V_{19}R_{19}$, $V_{20}R_{20}$	51

DISCUSSION

Critical rudder-free condition. - An examination of variation of C_n with ψ on figures 21 and 22 shows that the worse flight condition from the standpoint of lack of restoring yawing moments at large angles of yaw is the take-off power condition, flaps down, and a high angle of attack. Placing rudder stops at ±25° improved the condition but still left the yawing moments far from satisfactory. (When no stops were present the rudder deflection was limited by striking the stabilizer at a few degrees beyond 30°.)

It may be noted that the data for propeller windmilling do not show the reversal of yawing moments shown by the take-off power data. This fact does not necessarily mean that the rudder for the former case does not have a destabilizing floating tendency at large angles of yaw. Examination of the tail-off curves (fig. 23) shows that the adverse increment in yawing moment caused by power is also present when the tail is off. Thus the yawing-moment reversal results largely from the effects of power on the wing-fuselage combination and it may be expected that it will be most severe when the power effects are greatest (low-speed, high-power condition).

Effect of dorsal fins. - All of the dorsal fins improved the rudder-free C_n at large yaw angles. In the two longest groups [length 1 and 2, figs. 24(a) and 24(b)] any of the dorsal fins eliminated the reversal of yawing moments for the yaw range tested. In the shortest groups (length 3, fig. 24(c)) the two deepest dorsal fins provided the model with restoring moments in yaw for angles of yaw to -40°, while the shallowest two gave restoring moments in yaw up to about -35° of yaw. It will be noted that the length of the fins along the fuselage is of more importance than the area of the fin. Thus dorsal D_{41} has about the same effectiveness as D_{13} in spite of the fact that the area of the former is about half that of the latter.

The dorsal fins produce a slight destabilizing tendency around zero yaw, an effect which cannot be explained at present. The slopes of the yawing-moment curves at $\psi = -40^\circ$ indicate that many of the dorsal fins tested were not sufficiently effective to maintain restoring moments beyond this angle. It is probable that a dorsal fin which is effective up to 40° of yaw will be satisfactory since conditions for which larger angles would be obtained will not very often be encountered. Dorsal fins D_{41}, D_{51}, and D_{32} were selected as the smallest which would meet the requirement that there be no reversal of yawing moment regardless of angle of yaw; hence, these dorsal fins were the ones used for subsequent tests.

Effect of propellers. - The effect of adding single- and dual-rotation propellers on the yaw characteristics with power off is shown in figure 25. The addition of the propellers progressively decreases the directional stability , which is to be expected in view of the side force produced by a yawed propeller. The change in side force as measured, however, is not sufficient to account for the decrease in the slope of yawing-moment curves.

Characteristics of various vertical tails with free rudder. - With all the tails a reversal of yawing moments occurred at large angles of yaw (fig. 26). The addition of end plates or extension of the fuselage (fig. 27) improved the situation but was no remedy. The addition of a sufficiently effective dorsal fin eliminated the reversal of yawing moments for all tails (figs. 24, 27, 28, 29, 30 and 31.)

The antispin fins had a small adverse effect on C_n at large angle of yaw (fig. 28). Comparison of figures 28 and 29 indicate that an increase in balance from minimum produces a small adverse increment in C_n at large yaw angles.

The use of bevel trailing edge (fig. 31) produces a very irregular rudder-free yawing-moment curve. This curve reflects the marked effect of the bevel on the floating tendencies of the rudder. The large yawing moments at zero yaw indicates that the rudder was floating at about 14° (see fig.43) probably as a result of an asymmetric bevel.

At small angles of yaw all the tails tested give about the same value of $\partial C_n/\partial\psi$ with rudder free as with rudder fixed. This is an indication that the rudder floating angles are about zero in the yaw range of $\pm 5°$.

Characteristics of various vertical tails with rudder fixed. - The results of the tests with vertical tail VR for several conditions are shown in figure 32. For the $\delta_f = 0°$ condition, power on or propeller windmilling, the model with this tail is neutrally stable directionally near zero yaw.

With $\delta_f = 45^\circ$, the stability is good for all power conditions, with $\partial C_n/\partial\psi$ becoming greater negatively with an increase in thrust. The sudden change in slope of C_n curve for the $T_c' = 0.81$, $\delta_f = 45^\circ$, $\alpha = 9.7^\circ$ condition at about 15° of yaw must be caused by the combined effects of the large tail-off instability for this condition, the vertical tail being near the edge of the slipstream and probably a vertical tail stall. A dorsal fin would be expected to improve the condition considerably. (This test was to have been run at military power at sea level. By mistake the tunnel speed was incorrect, causing a higher T_c' which corresponded to considerably more than take-off power.) With vertical tail $V^{13}R^{13}$ there is a similar reduction in directional stability, around zero yaw with flaps neutral (fig. 33(a)). The stability, however, does not reduce to zero as for tail VR. Adding end plates or extending the fuselage increased the stability as expected. With $\delta_f = 0^\circ$, the weathercock stability is good for all the other tails tested (fig. 34). Tail VR has good stability with $\delta_f = 45^\circ$, military power and $\alpha = 2.7^\circ$ (figs. 32 and 36). For $\delta_f = 45^\circ$, take-off power, $\alpha = 7.5^\circ$ directional stability is good for all other tails as shown on the rudder test figures (figs. 37 to 43). It is reasonable to assume that all tails tested will give satisfactory stability at small yaw angles (rudder fixed) with power on and $\delta_f = 45^o$. The model is stable in roll with all tails tested. Effective dihedral varied from about $1\frac{1}{2}^o$ for take-off power, $\delta_f = 45^o$, to about 6^o or 7^o for military power, $\delta_f = 0^o$, and windmilling, $\delta_f = 0^o$ or 45^o.

Comparison of vertical tails. - The following table summarizes the lateral-stability characteristics of the model with the various tail arrangements for both rudder-fixed and rudder-free conditions:

TABULATION OF LATERAL STABILITY SLOPES AT ZERO YAW

XP-62 (1/9-SCALE)

Vertical tail	Military power at 20,000 ft, $\delta_f = 0$, $\alpha = 5.2$, $\delta_r = 0$				Take-off power at S.L. $\delta_f = 45$, $\alpha = 7.5$, $\delta_r = 0$				Take-off power at S.L. $\delta_f = 45$, $\alpha = 7.5$, rudder free			
	$\frac{\partial C_n}{\partial \psi}$	$\frac{\partial C_Y}{\partial \psi}$	$\frac{\partial C_l}{\partial \psi}$	Fig.	$\frac{\partial C_n}{\partial \psi}$	$\frac{\partial C_Y}{\partial \psi}$	$\frac{\partial C_l}{\partial \psi}$	Fig.	$\frac{\partial C_n}{\partial \psi}$	$\frac{\partial C_Y}{\partial \psi}$	$\frac{\partial C_l}{\partial \psi}$	Fig.
VR	0	0.012	0.0011	22	-------	------	------	--	-0.0018	0.024	0.0003	21
$V^{13}R^{13}$	-.0003	.012	.0012	33	-0.0015	0.026	0.0003	37	-.0019	.026	.0005	26
$V^{13}R^{13}$ end plates	-.0008	.013	.0012	33	-.0026	.027	.0005	38	-.0027	.026	.0005	26
$V^{13}R^{13}E$ extended	-.0005	.012	.0012	33	-.0026	.026	.0005	39	-.0028[a]	.029	.0006	26
$V^{14}R^{14}$, $V^{16}R^{16}$, $V^{18}R^{18}$	-.0011	.015	.0014	40	-.0029	.029	.0007	40 41 42	-.0028	.029	.0007	27 28
$V^{14}R^{14.5}$	-.0008	.013	.0013	29	-.0026	.027	.0006	43	-.0028	.028	.0007	29
$V^{19}R^{19}$, $V^{20}R^{20}$	-.0011	.013	.0013	30	-.0029	.028	.0007	44 45	-.0028	.027	.0006	30
Tail off	.0011	.007	.0008	23	.0012	.016	-.0001	23	.0012	.016	-.0001	23

[a]Value for $V^{14}R^{14}$
$V^{16}R^{16}$, -0.0031
$V^{18}R^{18}$, -0.0036

It will be noted that tail $V^{19}R^{19}$ has the same effectiveness as $V^{14}R^{14}$ in spite of the fact that it has about 14 percent less area. Estimates made of the effectiveness of the two tails indicate this result is due to the higher aspect ratio of $V^{19}R^{19}$.

Rudder requirements. - The rudder control requirements of reference 1 state, in general, that the rudder should be powerful enough to overcome the adverse aileron yawing moments, to provide trim at all conditions, and to provide the required spin-recovery characteristics. The pedal force to meet these requirements should not exceed 180 pounds, and should show no overbalance. In addition to checking rudder control for the foregoing requirements, the variation of rudder angle and force with yaw were also considered as an indication of the ability with which cross-wind take-offs and landings and other maneuvers requiring sideslip could be made (figs. 47 to 51).

Rudder control at zero yaw. - Because of the dual-rotation propeller, there are no asymmetric moments at zero yaw in any steady condition, and the provision of trim is therefore no problem.

Rudder control to overcome adverse aileron yawing. - Estimated rudder angles and pedal forces required to overcome the adverse aileron yawing moment are given in the following table:

Tail	Power on							Prop. windmilling C_L=1.52, δ_f=45, α=12°		
	$\alpha°$	$\delta_f°$	C_L	Power	ΔC_n due to ailerons	$\delta_r°$ to overcome ΔC_n	Pedal force (lbs)	ΔC_n due to ailerons	$\delta_r°$ to overcome ΔC_n	Pedal force (lbs)
VR	5.2	0	0.54	Military	0.0067	6.7	87	------	------	-----
VR	2.7	45	.95	20,000 ft	.0085	7.0	61	0.0125	14.5	67
$V^{13}R^{13}$	7.5	↓	1.48	take off	.0106	5.7	34	↓	12.9	48
$V^{13}R^{13}$ end plates	↓	↓	↓	sea level	↓	6.6	40	↓	14.5	54
$V^{13}R^{13}$ ext. fus.	↓	↓	↓	↓	↓	5.1	23	↓	11.6	30
$V^{14}R^{14}$	↓	↓	↓	↓	↓	5.2	27	↓	11.7	38
$V^{14}R^{14.5}$	↓	↓	↓	↓	↓	6.2	-21[a]	↓	13.7	23
$V^{16}R^{16}$	↓	↓	↓	↓	↓	5.1	29	↓	11.5	38
$V^{18}R^{18}$	↓	↓	↓	↓	↓	5.1	16	↓	11.5	19
$V^{19}R^{19}$	↓	↓	↓	↓	↓	6.5	17	↓	14.9	24
$V^{20}R^{20}$	↓	↓	↓	↓	↓	6.6	20	↓	14.9	27

[a]Negative sign indicates overbalance.

All vertical tails easily meet the requirements for overcoming adverse aileron yawing moments. Even if the mechanical advantage were based on ±30° rudder deflection instead of the rudder deflection required to overcome adverse aileron yawing moments the pedal forces would still be well under 180 pounds. The table indicates that tail $V^{18}R^{18}$ and $V^{19}R^{19}$ give the lowest pedal forces while VR and $V^{13}R^{13}$ with end plates give the highest.

The angles to which the airplane would yaw due to adverse aileron yawing moment with rudder fixed were not computed because of insufficient data. The indications are, however, that the angles will be well below the 20° maximum specified by reference 1.

Rudder control for spin recovery. - Spin recovery tests were made on a 1/22-scale model of the XP-62 airplane in the NACA spin tunnel for certain vertical tails. The results, which are unpublished, are summarized in the following table:

Tail	Rudder range	Satisfactory	Est. pedal force, lb
VR	±30	Yes	300
VR with end plates and reduced rudder chord	±20	Yes	<120
$V^{11}R^{11}$.5 with area increased 10 percent	±25, ±20	No	
Same with antispin fillets	±20	Yes	
$V^{21}R^{21}$	±30	Yes	
$V^{21}R^{21}$	±20	Doubtful	
$V^{21}R^{21}$ with dorsal and antispin fillets	±30	Yes	

$V^{11}R^{11.5}$ with area increase 10 percent is practically identical with $V^{14}R^{14}$, $V^{16}R^{16}$, and $V^{18}R^{18}$.

$V^{21}R^{21}$ is the same as $V^{19}R^{19}$ and $V^{20}R^{20}$ except that balance area is 2.63 square feet for $V^{21}R^{21}$ full scale.

Satisfactory recovery depends on the pilot being able to quickly deflect the rudder full against the spin. Three hundred pounds pedal force is, of course, too large; 180 pounds, or less is acceptable. The dorsal fins are apt to have an adverse effect on spin recovery.

The indications are that the spin recovery requirements will be the critical requirement with regard to rudder control characteristics on this airplane.

Rudder control in sideslip. - The results of tests of the various tails with rudder deflected to several angles are shown in figures 35 to 46. The computed pedal forces and rudder deflections for trim plotted against angle of steady yaw are shown in figures 47 to 51. In general, $\partial C_h/\partial \psi$ is zero or slightly positive for small angles of yaw but becomes negative at large angles of yaw.

The estimated pedal forces for tail VR are shown in figure 47. Lack of stability with $\delta_r = 0^{\circ}$ and zero $\partial C_h/\partial \psi$ at small angles of yaw would result in a loss of control feel under this condition (fig. 35). Since tail VR was not tested under the same conditions of power and C_L as were the other tails no direct comparison is possible.

Tail $V^{13}R^{13}$ gave pedal forces up to 300 pounds. (See fig. 48.) These forces increased when the fuselage was extended, and when end plates were added to the horizontal tail. When, however, the deflection of $V^{13}R^{13}$ alone was restricted so that the maximum sideslip angle possible was 18° (the value for the most ineffective rudder at 30° deflection) and the mechanical advantage changed accordingly the pedal force was reduced to about 130 pounds. Only minimum balance was tested with $V^{13}R^{13}$, so that the pedal forces for this tail with extended fuselage or with end plates might be reduced by using a balanced rudder.

The effect of balance is shown in figures 40, 41, and 42 (vertical tails $V^{14}R^{14}$, $V^{16}R^{16}$, and $V^{18}R^{18}$). With the large balance ($V^{18}R^{18}$), 30° of rudder deflection will not trim the model with the particular dorsal fin used (D_{51}) in the yaw range tested so that it is not known how far beyond 40° the model will yaw. A reversal of pedal force also results for this case at about 28° yaw. Limiting the rudder angle below 27° should remove the reversal of pedal force. The large balance ($V^{18}R^{18}$) was effective in reducing pedal forces. The medium balance ($V^{16}R^{16}$), however, showed an increase in pedal force over that for the minimum balance at moderate angles of yaw. No explanation is forthcoming at present to account for the failure of the medium balance to decrease hinge moments. In this connection it may be pointed out that the

Reynolds number at which the tail was operating was very small and the effect of scale on hinge moments is known to be large. Thus, the hinge moments measured on the 1/9-scale model are probably not very reliable as indications of the exact magnitudes of the forces to be expected on the airplane. The results of tests of 0.45-scale models of tails $V^{14}R^{14}$, $V^{16}R^{16}$, and $V^{18}R^{18}$ (reference 3) indicate that the medium and large overhangs give the expected reductions in hinge moments. An analysis of the airplane pedal forces, using these data, will be made. When the maximum yaw (ψ_{max}) is limited to 18°, the pedal forces for all of the balances are substantially reduced.

With the bevel-trailing-edge rudder ($V^{14}R^{14.5}$) a reversal of pedal force occurs at small angles of yaw, and $\partial C_h/\partial\psi$ is hightly positive (fig. 43). This condition could probably be greatly improved by sealing the gap between the fin and rudder. The hinge-moment coefficient is quite large at zero rudder and zero yaw indicating some asymmetrical condition. Rough estimates indicate that a difference of about 7° between the two sides of the bevel could give the asymmetry shown in these results. Because of the small size of the model such a difference is possible.

For the tails $V^{19}R^{19}$, $V^{20}R^{20}$ (figs. 44 and 45) the effect of a small change in rudder balance on hinge moments was the same as for tails $V^{14}R^{14}$ and $V^{16}R^{16}$. Both $V^{19}R^{19}$

and $V^{20}R^{20}$ have pedal forces exceeding 180 pounds but the forces for $V^{20}R^{20}$ are somewhat reduced when ψ_{max} is limited to 18°. Comparing figures 49 and 51 (tails $V^{14}R^{14}$ and $V^{19}R^{19}$) the reduction in pedal forces resulting from the smaller chord is somewhat greater than would be expected through most of the yaw range. At large angles of yaw the force reduction is smaller than would be expected. The pedal force required to overcome the adverse aileron yawing moments is considerably reduced by using the smaller chord rudder.

The tab was very effective in reducing pedal forces when connected as a balancing tab (figs. 46 and 50). Pedal forces given on figure 50 for the tails $V^{14}R^{14.5}$ and $V^{14}R^{14}T$ are all below 180 pounds for a ψ_{max} of 18° but only $V^{14}R^{14}T$ with $\delta_t:\delta_r = -1:1$ requires less than 180 pounds for a 30° maximum rudder deflection. The fact that the pedal forces for the -1:1 tab are linear with ψ while the -1/2:1 tab are irregular with ψ is largley coincidental, because the results are derived from small differences of large values of C_{h_r} so cannot be considered very reliable. Presumably the addition of a balancing tab to any of the rudders would result in a similar reduction in pedal forces.

CONCLUSIONS

1. With take-off power and flaps deflected the model, with rudder free, showed reversal of yawing moments at large angles of yaw for all the vertical tails tested. The addition

of a proper dorsal fin improved this condition so that all vertical tails were satisfactory in this respect at least to 40° yaw.

2. Directional stability, with flaps neutral (rudder fixed) at small angles of yaw was obtained for all tails tested except the original tail (VR) which had very low or zero stability. On this basis, tail VR was considered unsatisfactory. When flaps were deflected and with power all tails gave satisfactory stability. Tail $V_{19}R_{19}$ was the smallest tail which would give satisfactory weathercock stability for all conditions considering a value of $\partial C_n/\partial\psi$ of about -0.001 as being the criterion for satisfactory directional stability.

3. All of the vertical tails tested had satisfactory rudder effectiveness for the flight conditions for which they were tested, and it is believed the tails tested would have satisfactory rudder effectiveness for all normal flight conditions.

This situation results partly from the fact that, because of the dual-rotation propeller, there are no asymmetric yawing moments at zero yaw which necessitate large rudder deflections for trim. Sufficient rudder control to overcome the adverse aileron yawing moments was supplied by all the vertical tails. Probably the most severe rudder requirement in the present case is the spin recovery requirement and any requirement which may be made as to cross-wind take-offs and landings.

4. Pedal forces in sideslips were undesirably large for some of the tails but may be easily reduced. The rudder with the bevel trailing edge gave a reversal in pedal forces at small angles of yaw. With flaps neutral tail VR would probably lack control feel at small angles of yaw.

5. The smallest pedal forces for overcoming adverse aileron yaw were given by tails $V^{18}R^{18}$ and $V^{19}R^{19}$.

Langley Memorial Aeronautical Laboratory,
National Advisory Committee for Aeronautics,
Langley Field, Va., July 1, 1943.

REFERENCES

1. Gilruth, R. R.: Requirements for Satisfactory Flying Qualities of Airplanes. NACA Rep. No. 755, 1943.

2. Pearson, Henry A., and Jones, Robert T.: Theoretical Stability and Control Characteristics of Wings with Various Amounts of Taper and Twist. NACA Rep. No. 635, 1938.

3. Lowry, John G., Turner, Thomas R., and Liddell, Robert B.: Aerodynamic Characteristics of Several Modifications of a 0.45-Scale Model of the Vertical Tail of the Curtiss XP-62 Airplane. NACA MR No. L6F27, 1946.

TABLE I

GEOMETRIC CHARACTERISTICS OF VERTICAL TAILS TESTED ON 1/9-SCALE MODEL OF XP-62 AIRPLANE

Vertical tail designation	Total area ft²		Rudder area ft²		Rudder r.m.s. chord ft		Effective balance area ft²		Aspect ratio	Remarks	Figure no.
	Full scale	1/9 scale	Full scale	1/9 scale	Full scale	1/9 scale	Full scale	1/9 scale			
VR	36.6	0.452	19.75	0.244	2.34	0.260	3.09	0.038	1.89	original	3,4
$V^{13}R^{13}$	36.6	.452	14.5	.179	1.71	.190	minimum		2.27		5,6
$V^{13}R^{13}$	36.6	.452	14.5	.179	1.71	.190	minimum		2.27	Endplates on horizontal tail	5,7,8,9
$V^{13}R^{13}{}_E$	36.6	.452	14.5	.179	1.71	.190	minimum		2.27	Vertical tail extended 4 in. on model	5,10,11
$V^{14}R^{14}$	50.8	.626	21.1	.261	1.94	.216	minimum		2.41		12,13
$V^{16}R^{16}$	50.8	.626	21.1	.261	1.94	.216	4.23	.0521	2.41		12,13
$V^{18}R^{18}$	50.8	.626	21.1	.261	1.94	.216	7.07	.0873	2.41		12,13
$V^{14}R^{14.5}$	50.8	.626	21.1	.261	1.94	.216	minimum		2.41	with bevel trailing edge	12
$V^{14}R^{14}{}_T$	50.8	.626	21.1	.261	1.94	.216	minimum		2.41	with tab	12
$V^{19}R^{19}$	43.4	.536	13.14	.162	1.27	.141	minimum		2.82		14,15
$V^{20}R^{20}$	43.4	.536	13.14	.162	1.27	.141	1.72	.0212	2.82		14,15

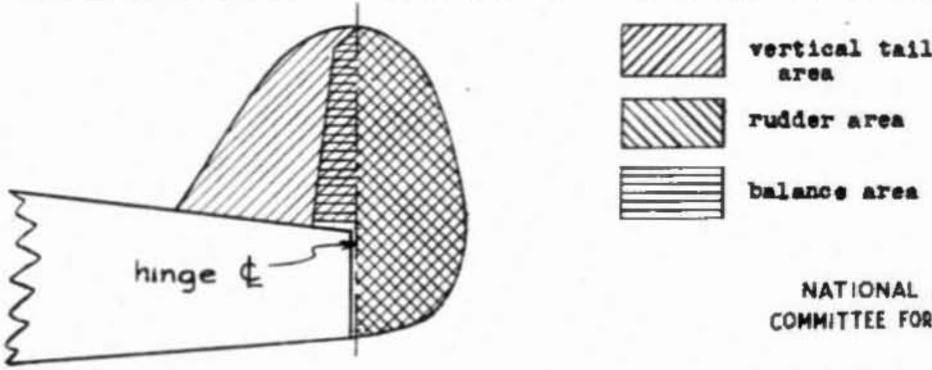

NATIONAL ADVISORY COMMITTEE FOR AERONAUTICS

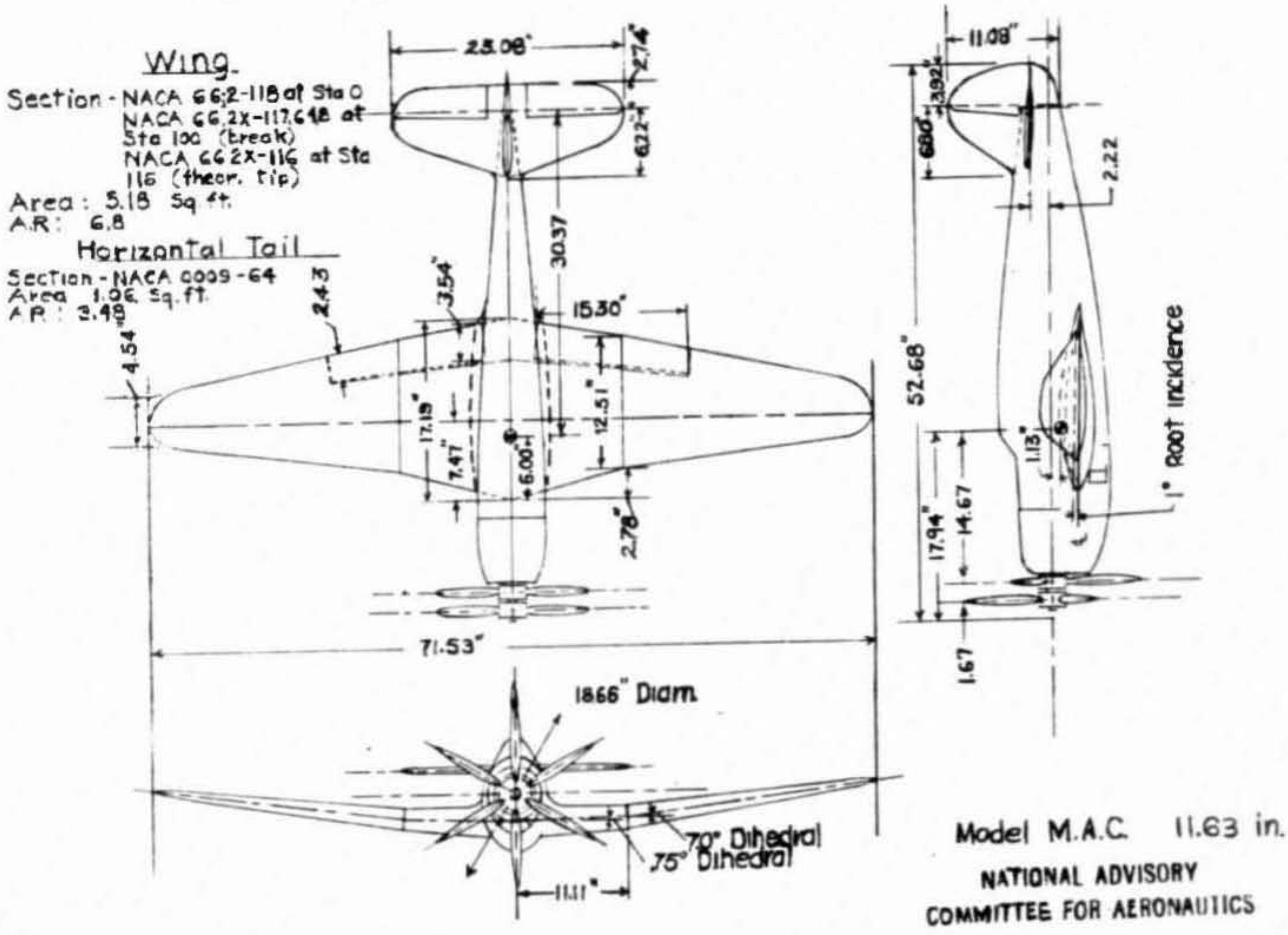

Figure 1-Three view drawing of the 1/9-scale XP-62 airplane model.

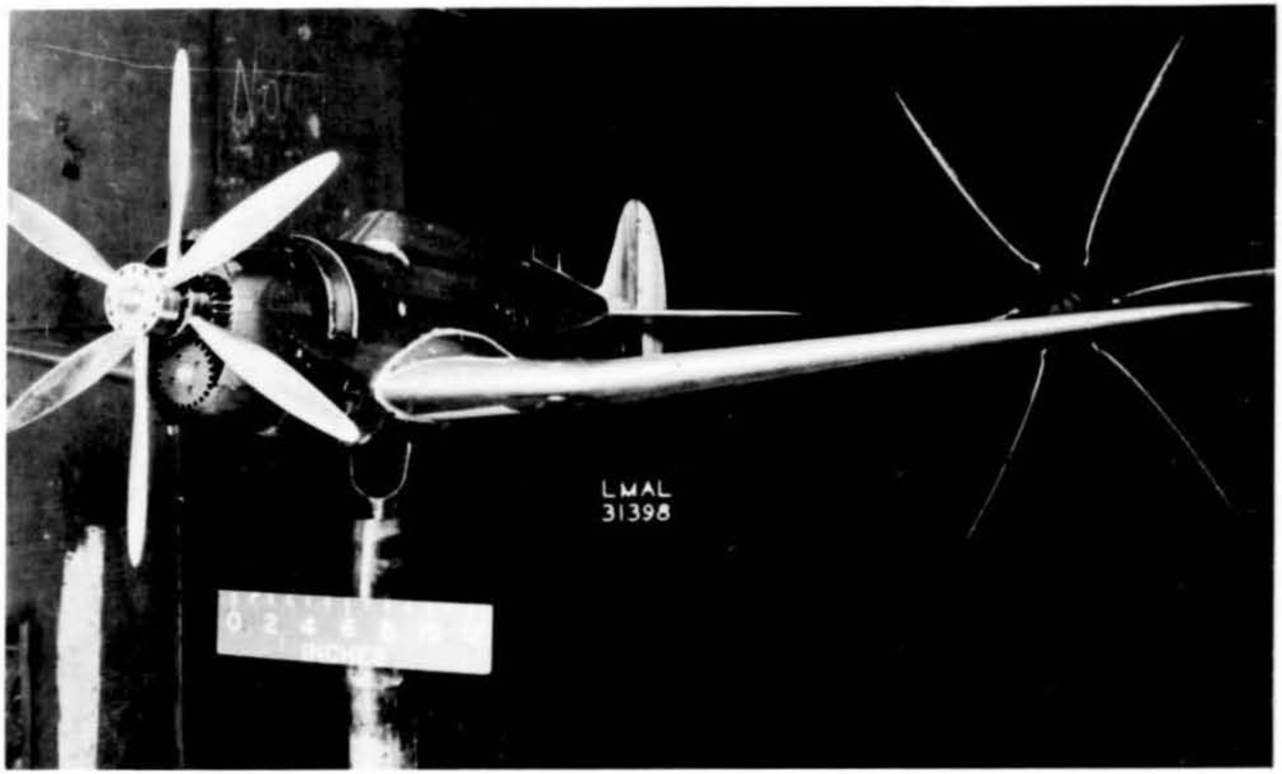

Figure 2(a).- Three-quarter view of $\frac{1}{9}$-scale model of XP-62 airplane.

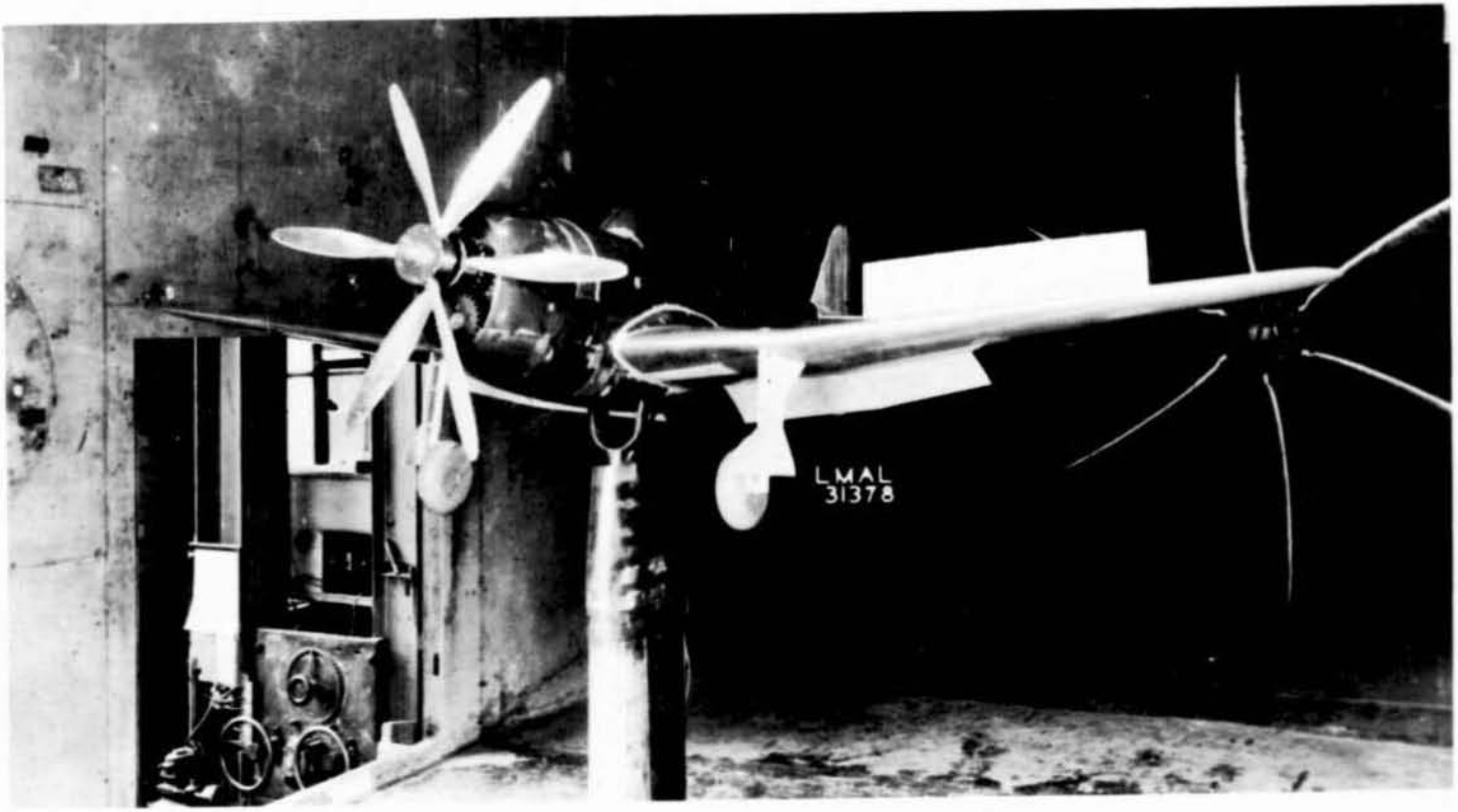

Figure 2(b).- Three-quarter view of $\frac{1}{9}$-scale model of XP-62 airplane. Flaps and landing gear extended.

L-779

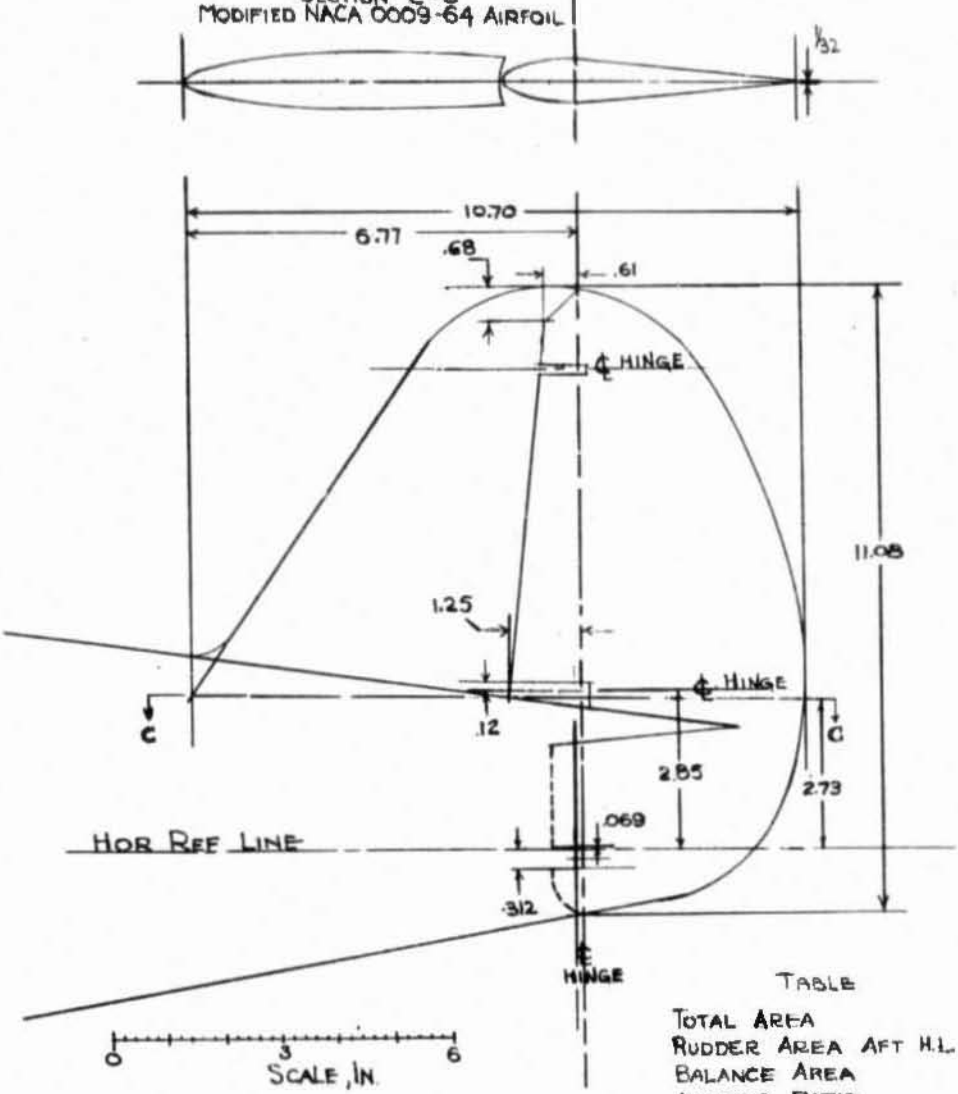

TABLE

TOTAL AREA	.452 ft²
RUDDER AREA AFT H.L.	.244 ft²
BALANCE AREA	.038 ft²
ASPECT RATIO	1.89
RMS RUDDER CHORD	.260 ft

NATIONAL ADVISORY
COMMITTEE FOR AERONAUTI

FIGURE 3.- PLAN AND SECTION VIEWS OF TAIL VR ON 1/8-SCALE XP-62 AIRPLANE MODEL.

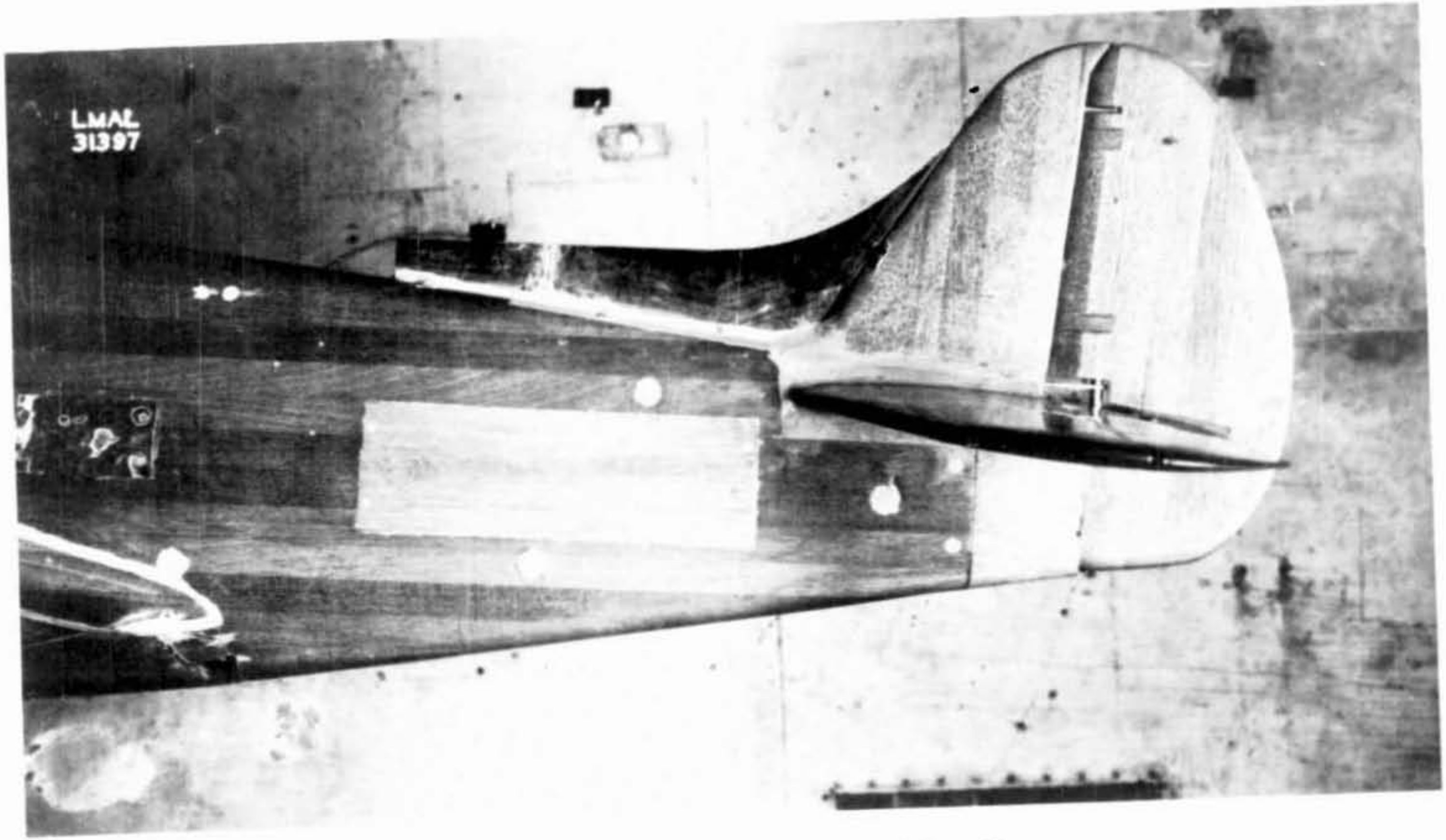

Figure 4.- Vertical tail VR with dorsal fin, D_{32}.

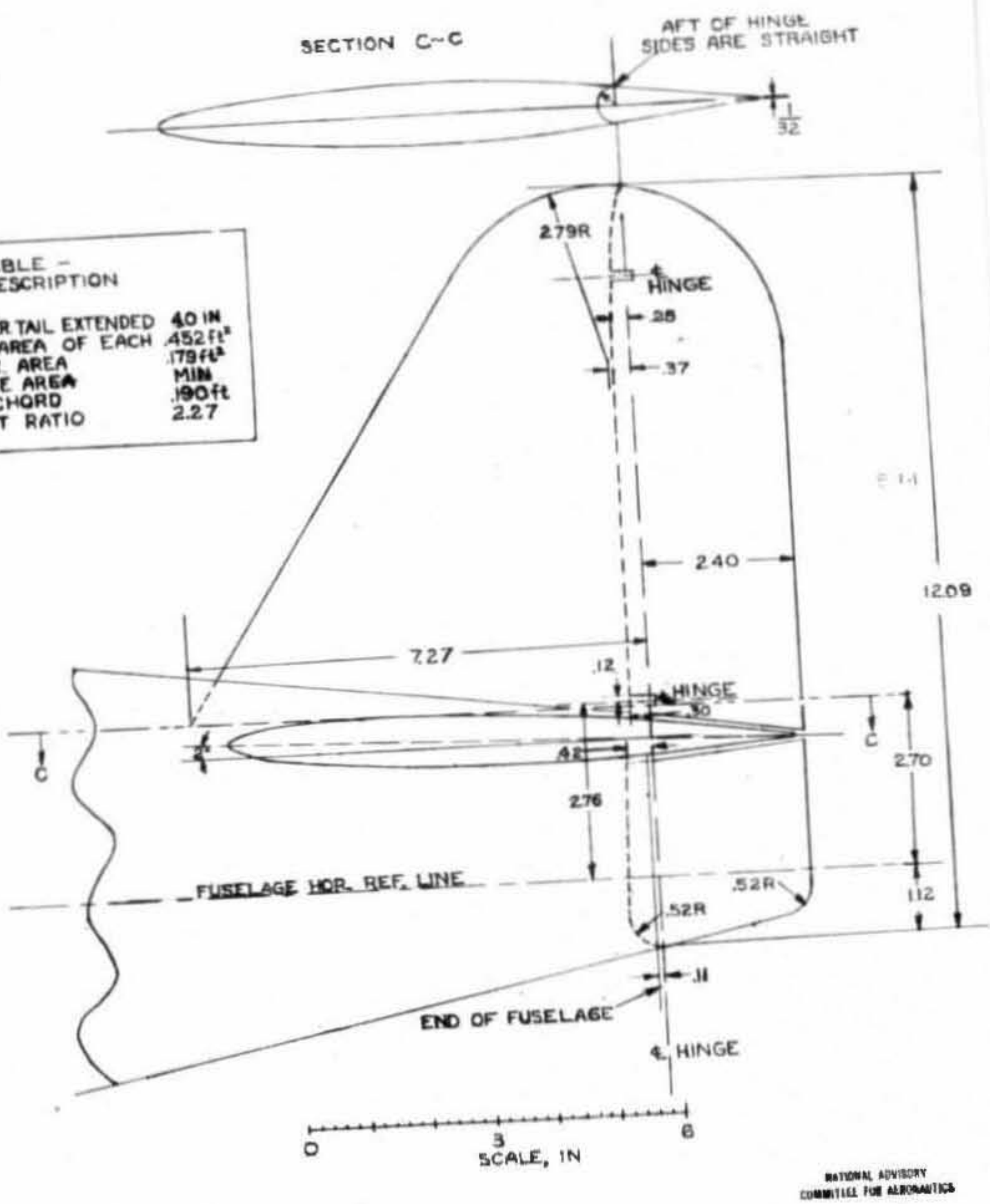

FIGURE 5.- PLAN AND SECTION VIEWS OF $V^{18}R^{18}$ AND $V^{18}R^{18}E$ VERTICAL TAILS ON 1/20-SCALE XP-62 AIRPLANE MODEL.

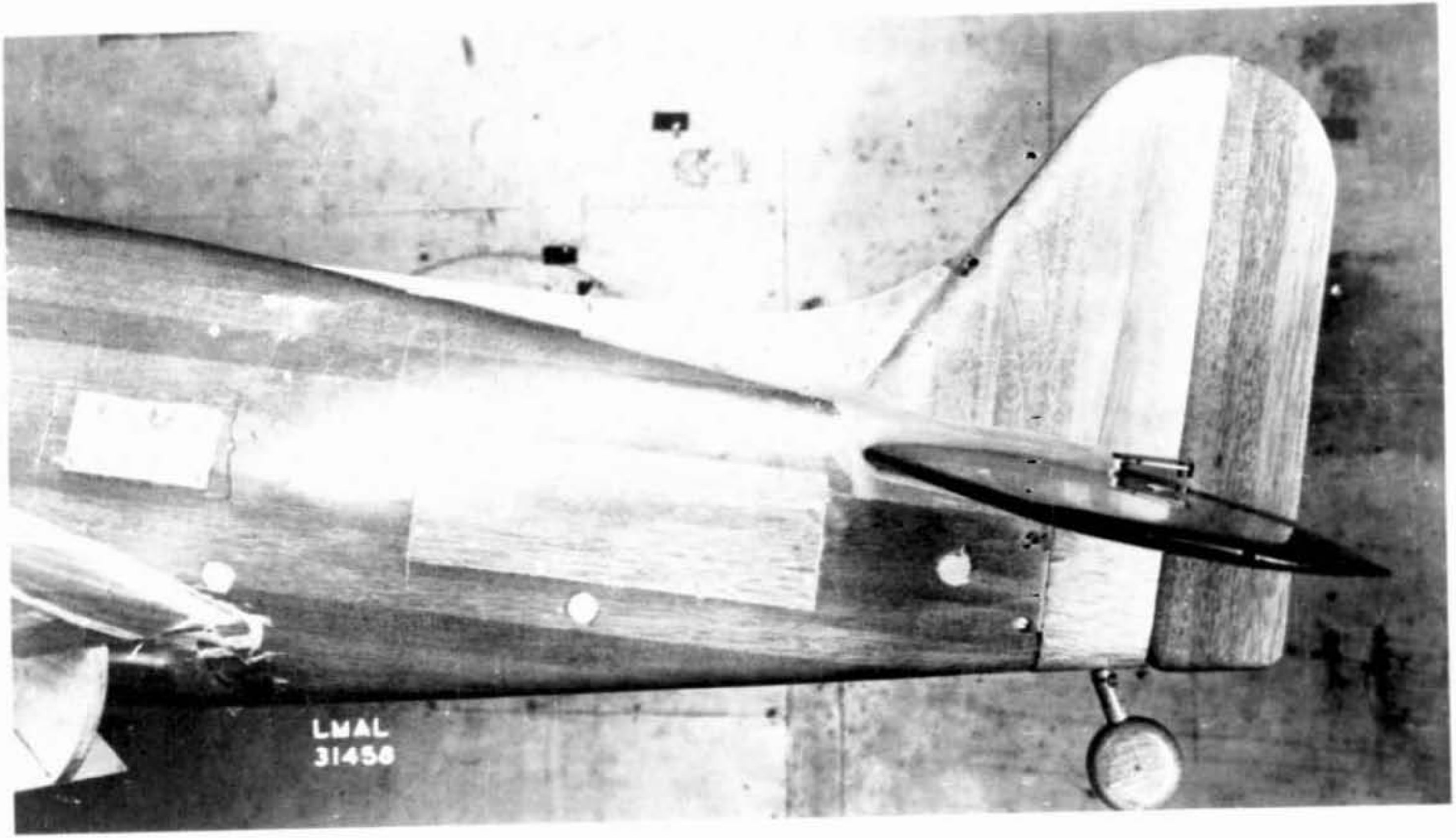

Figure 6.- Vertical tail $V^{13}R^{13}$ with dorsal fin D_{41}.

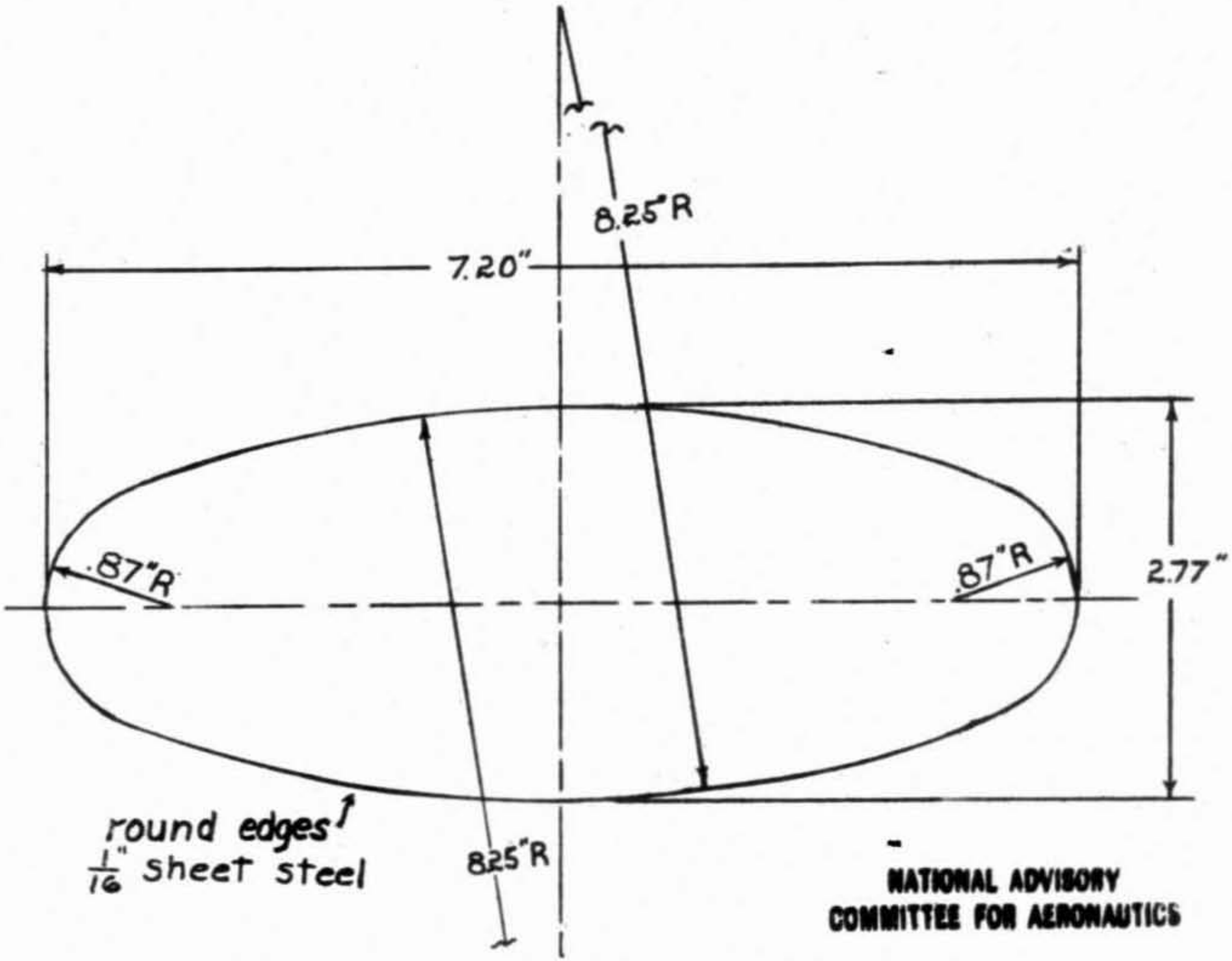

Figure 7.- Endplates tested on XP-62 model (1/9 scale)

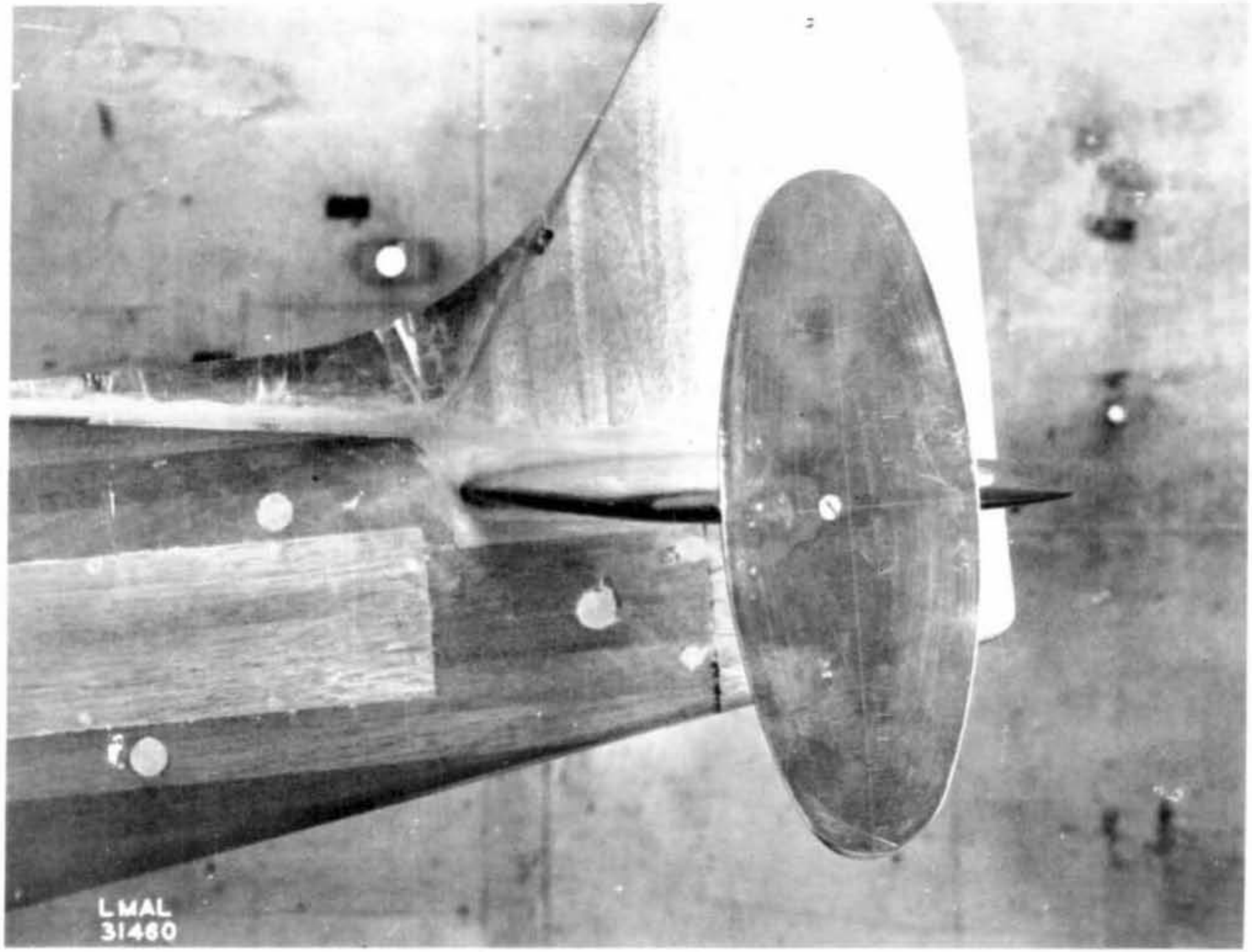

Figure 8.- Vertical tail $V^{13}R^{13}$ with endplates on horizontal tail and dorsal fin D_{41}.

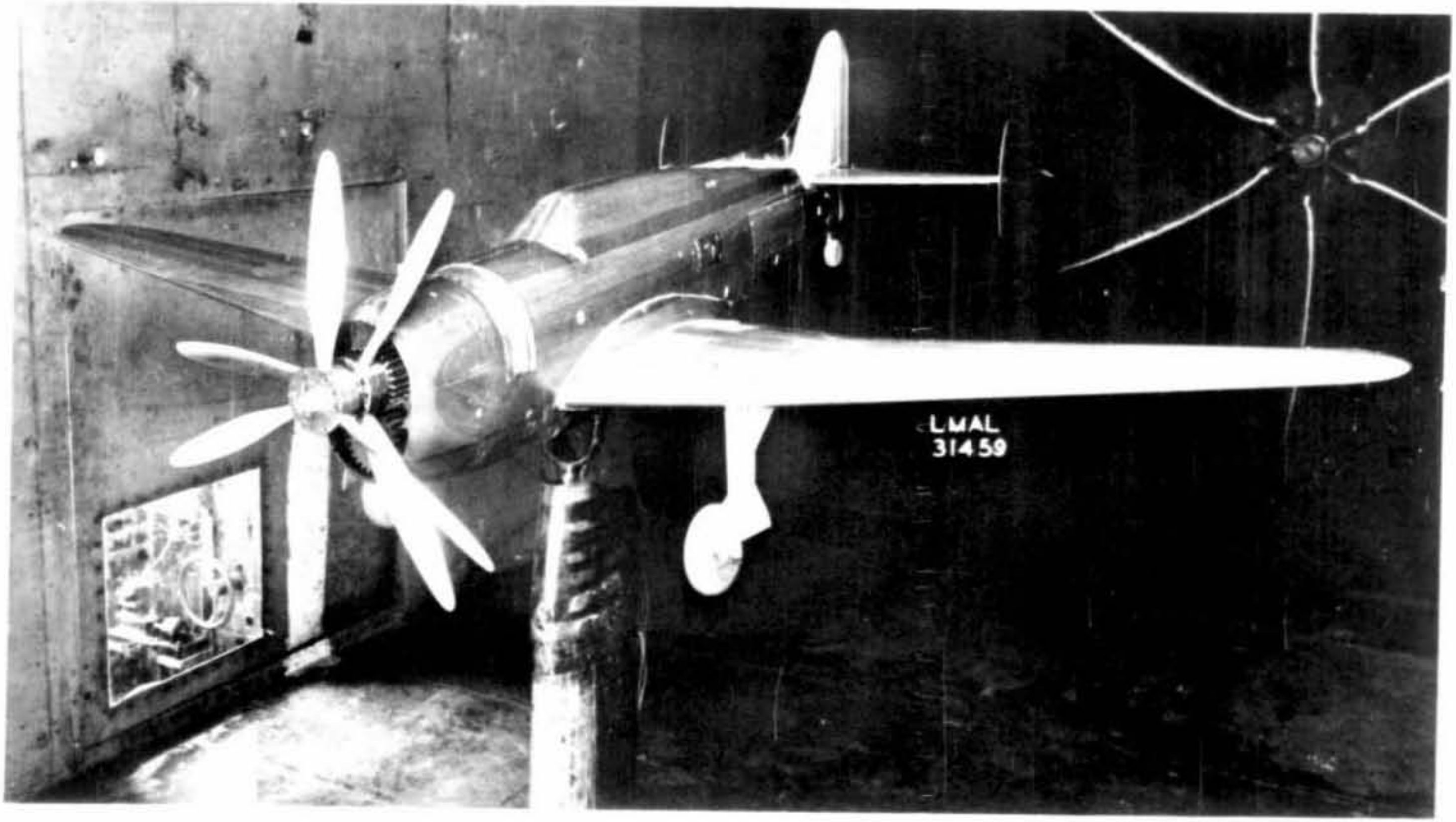

Figure 8.- Three-quarter view of $\frac{1}{8}$-scale model of XP-62 airplane with vertical tail $V^{13}R^{13}$, endplates on horizontal tail, and dorsal fin D_{41}.

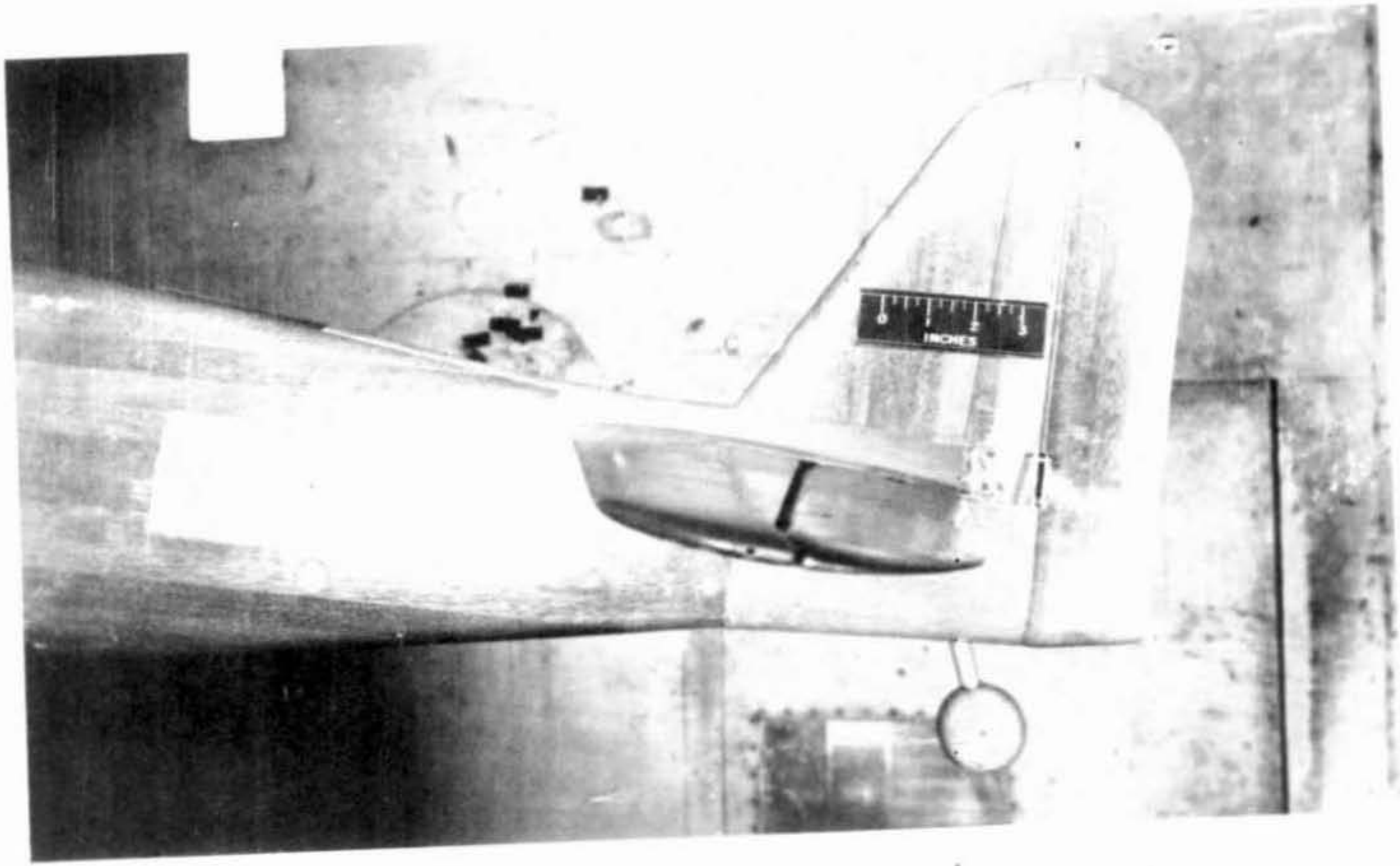

Figure 10.- Vertical tail $V^{13}R^{13}E$ ($V^{13}R^{13}$ extended 4 inches).

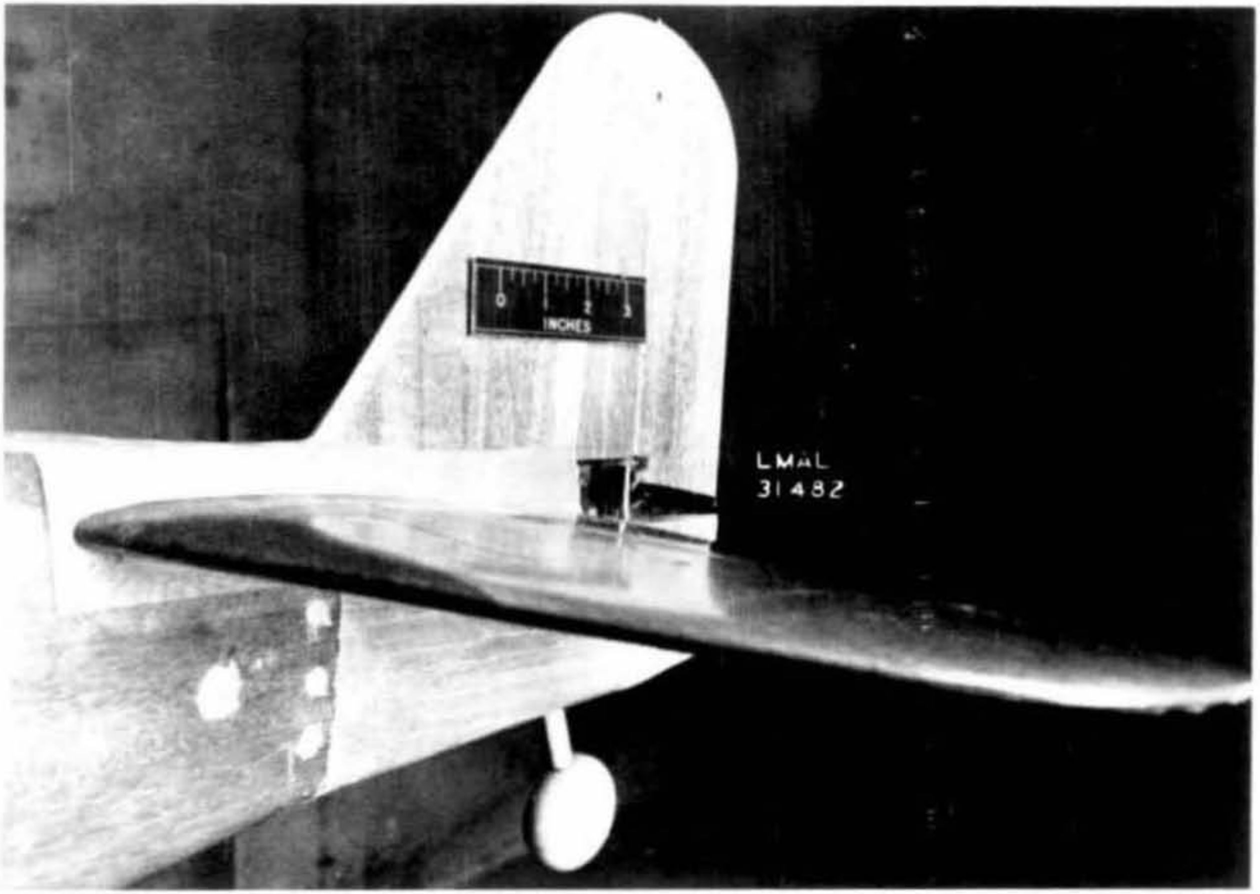

Figure 11.- Three-quarter view of vertical tail $V^{13}R^{13}F$.

L-779

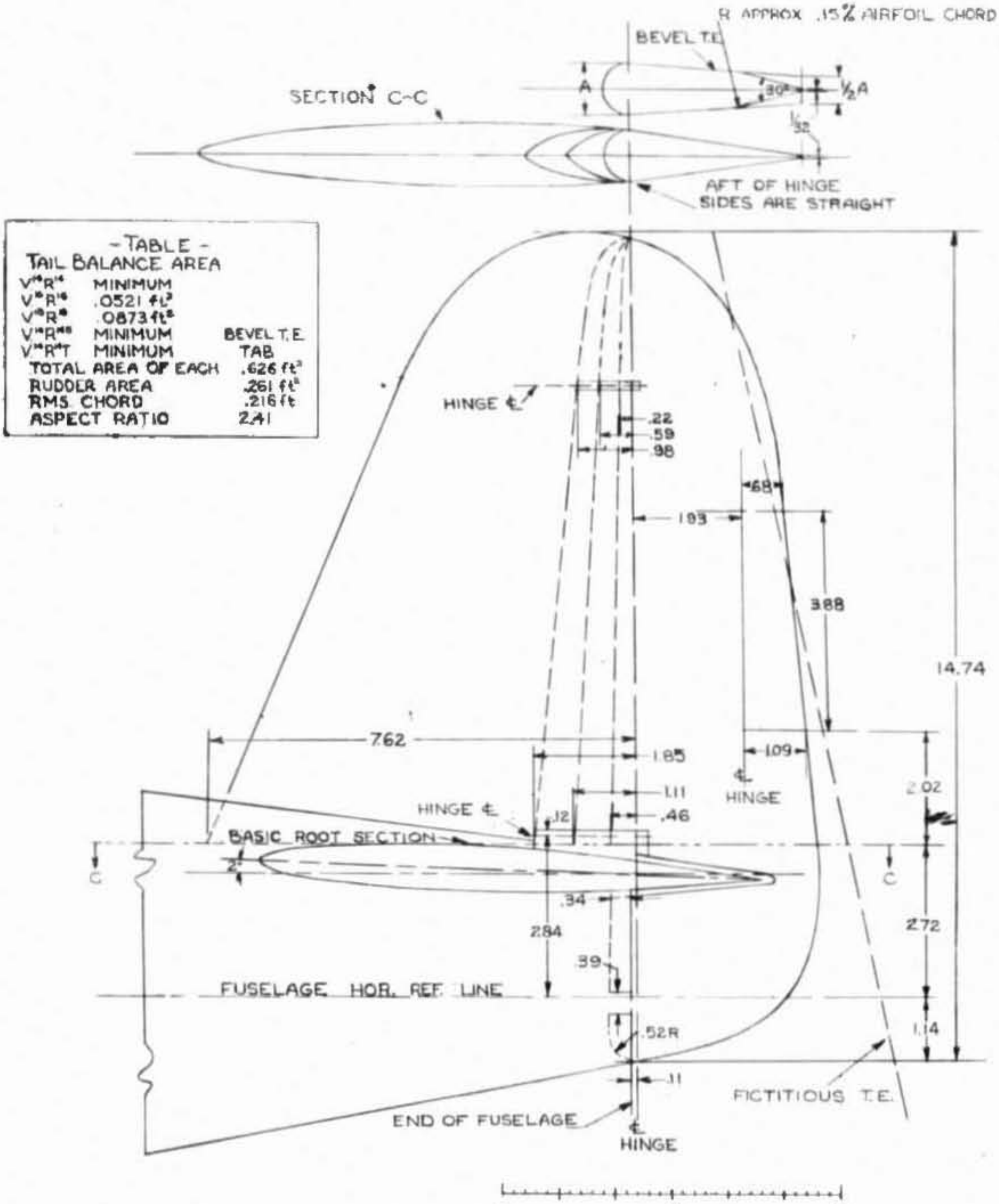

FIGURE 12.- PLAN AND SECTION VIEWS OF $V^{14}R^{14}$, $V^{14}R^{16}$, $V^{18}R^{18}$, $V^{14}R^{14.5}$ AND $V^{14}R^{14}T$ VERTICAL TAILS ON 1/9-SCALE XP-62 AIRPLANE MODEL.

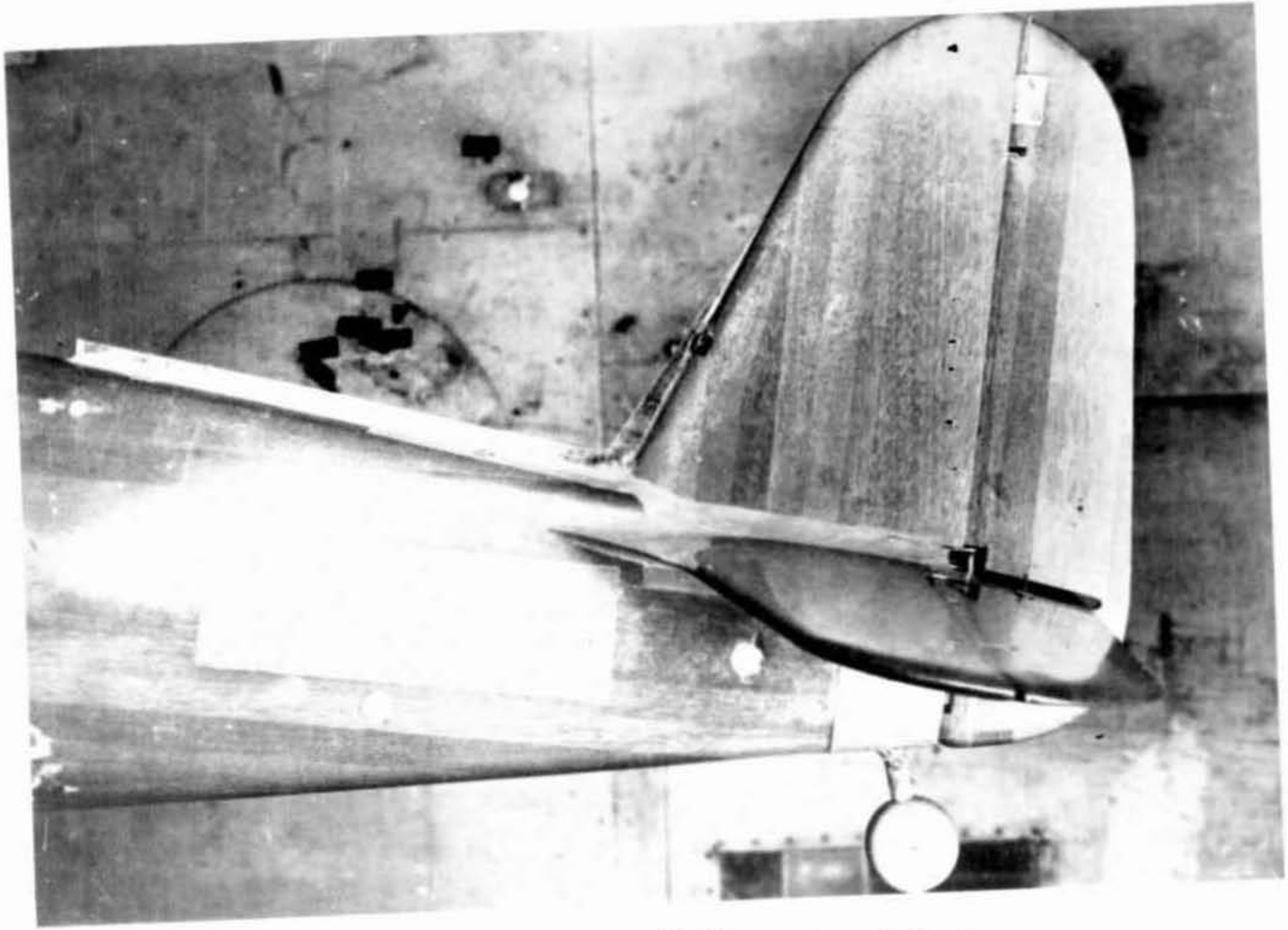

Figure 13.- Vertical tail $V^{14}R^{14}$ with dorsal fin D_{51}.

L-779

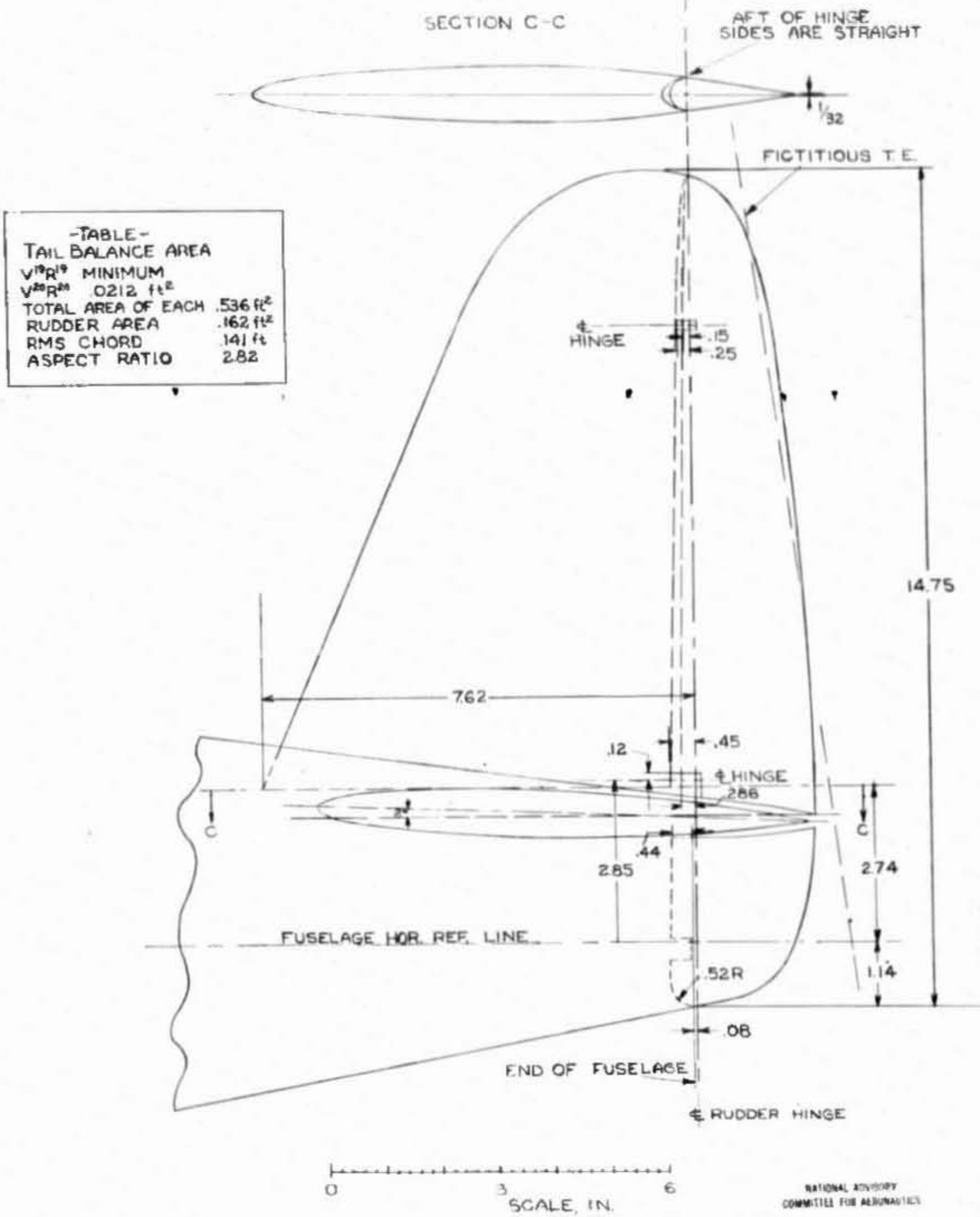

FIGURE 14.– PLAN AND SECTION VIEWS OF V19R19 AND V20R20 VERTICAL TAILS ON 1/6-SCALE XP-62 AIRPLANE MODEL.

L-779

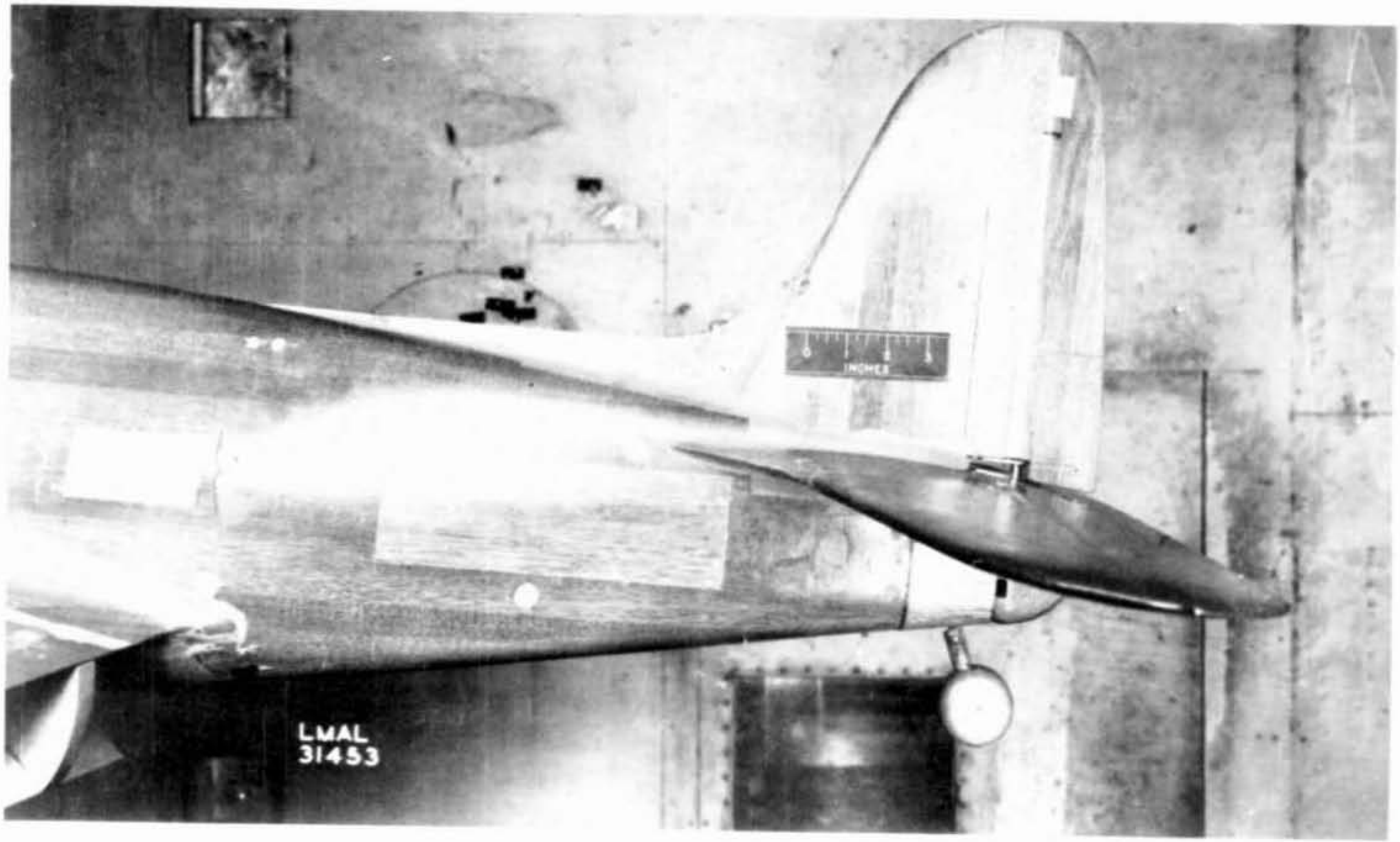

Figure 15.- Vertical tail $V^{20}R^{20}$ with dorsal fin D_{41}.

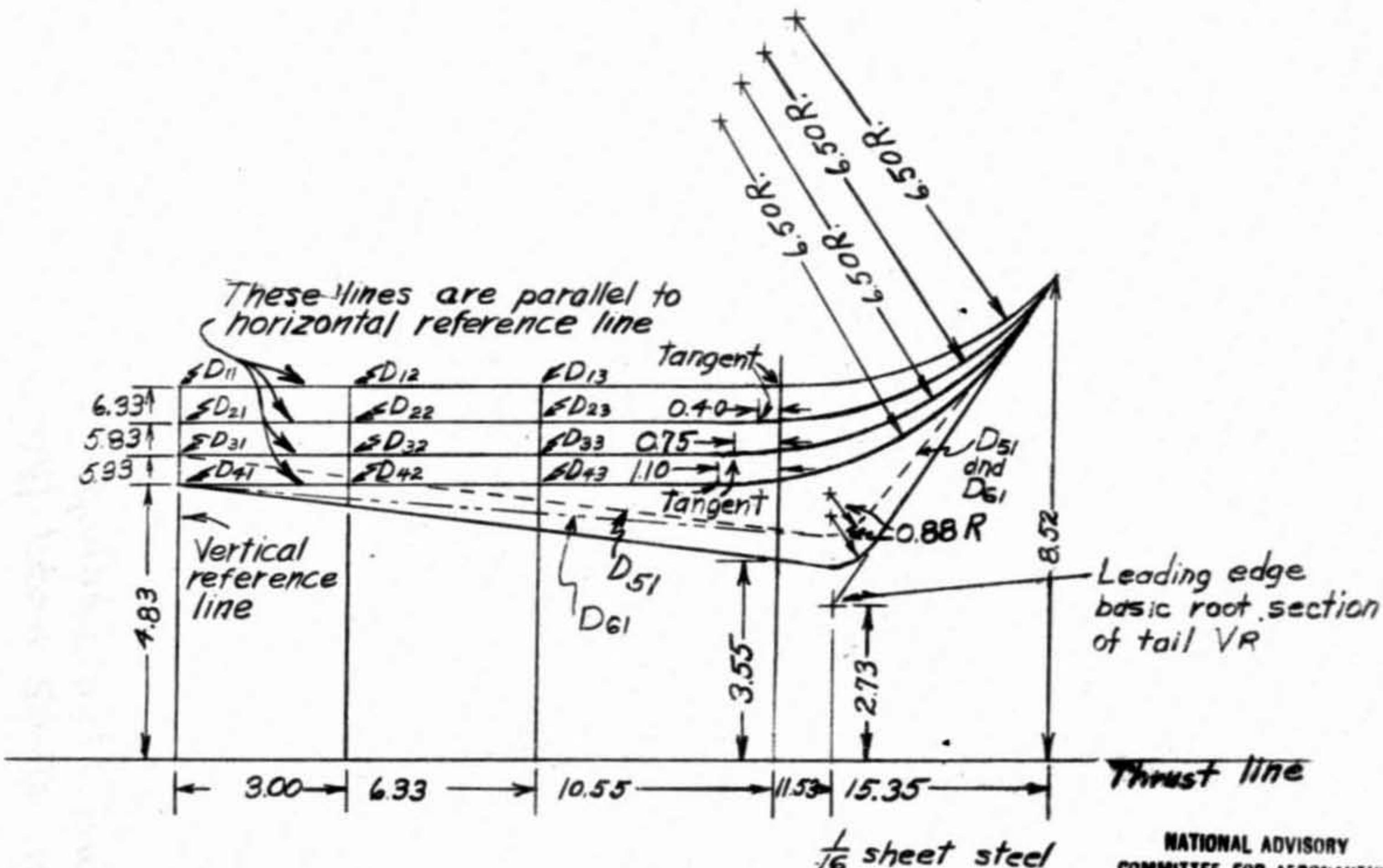

Figure 16.- Dorsal fins tested on 1/9-scale model of the XP-62 airplane.

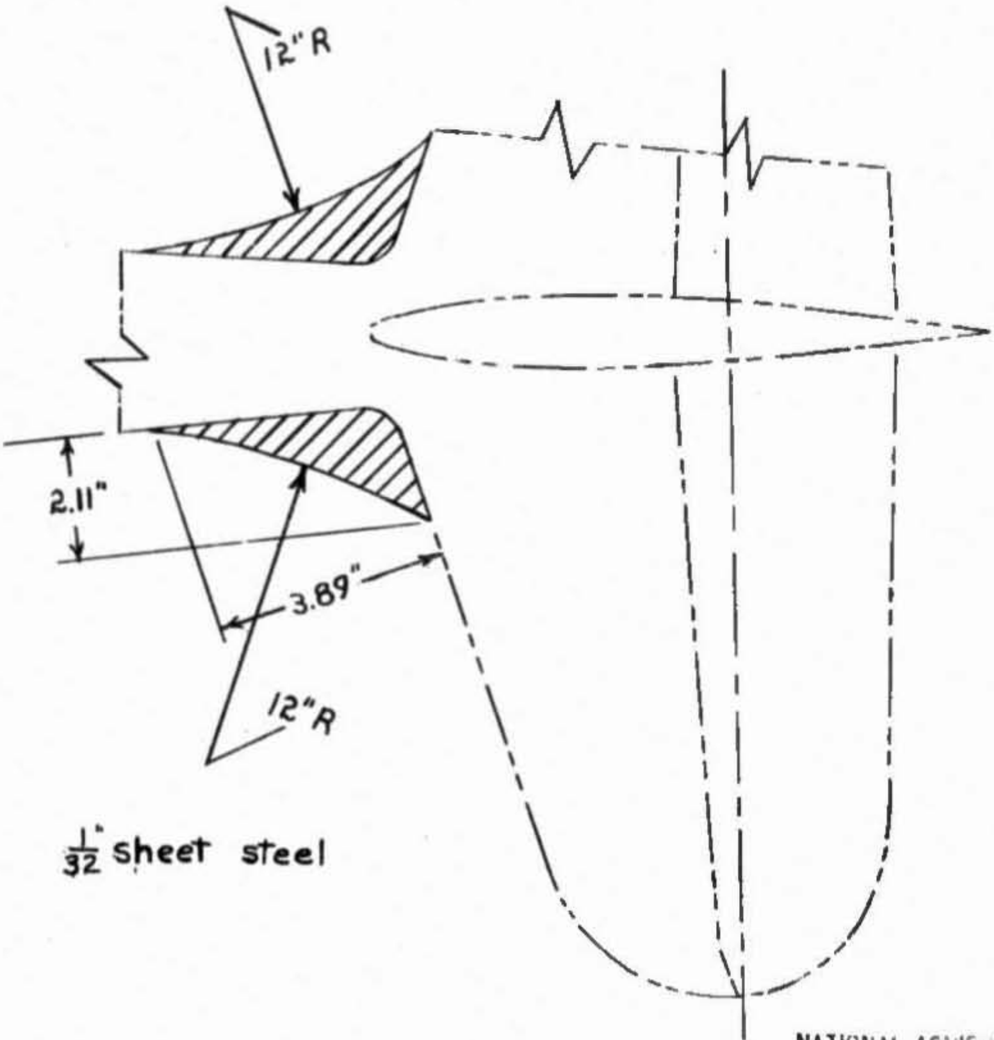

NATIONAL ADVISORY
COMMITTEE FOR AERONAUTICS

Figure 17(a). - Antispin fillets tested on XP-62 model (1/9 scale)

L-779

Figure 17(b).- Three-quarter top view of tail root showing antispin fillets and dorsal fin D_{51}.

L-779

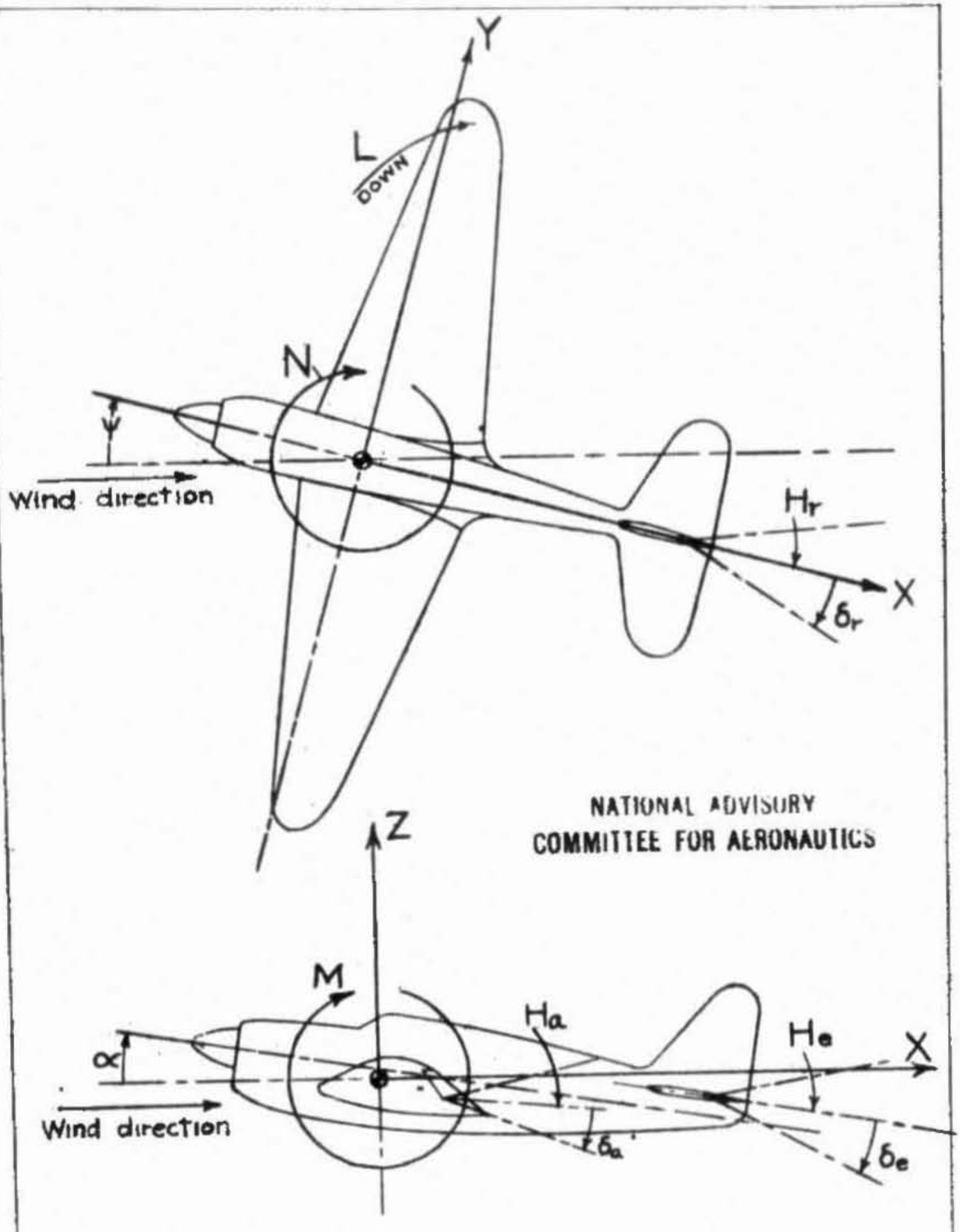

Figure 18.- Notation of the system of axes used and the control surface hinge moments and deflections. (Arrows indicate positive values.)

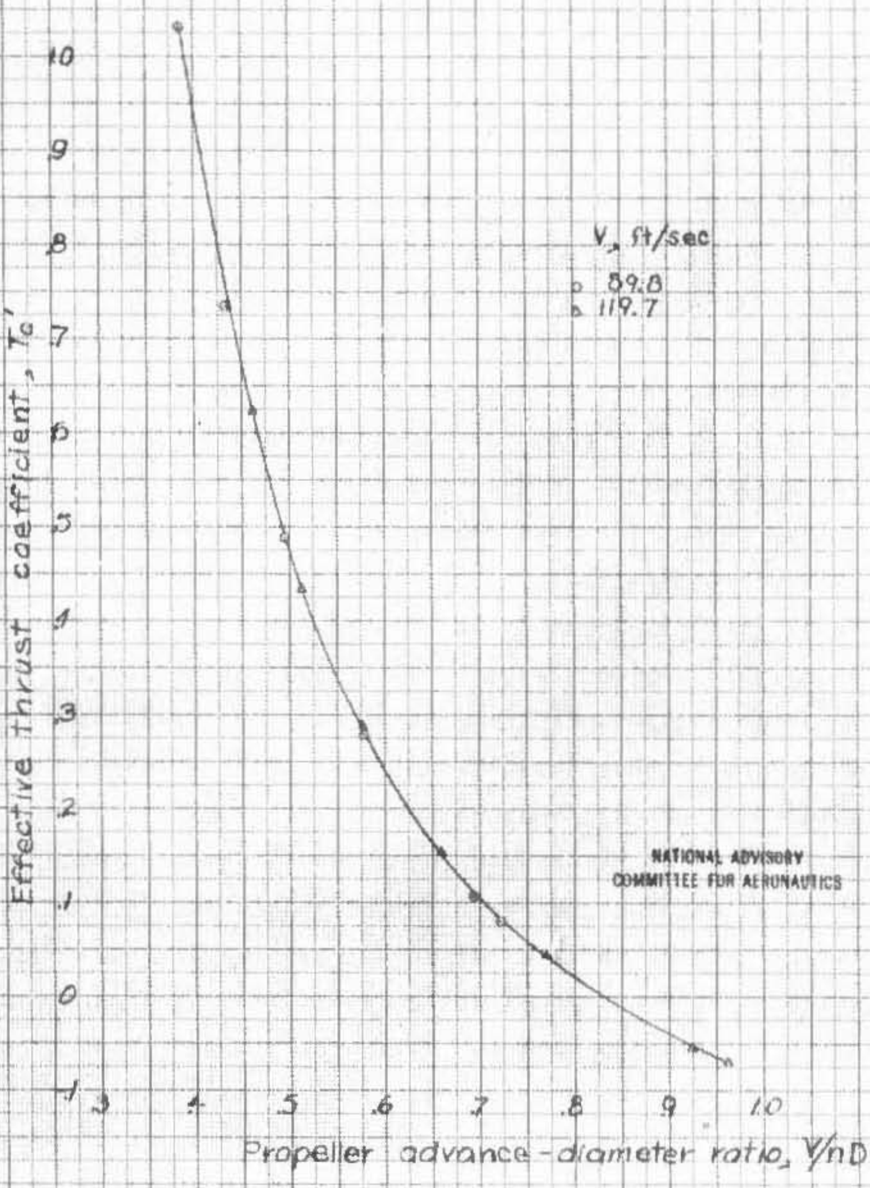

FIGURE 19.– Effective thrust coefficient as a function of propeller advance-diameter ratio for the 1/9 scale model of the XP-62 airplane. $\alpha = \delta_f = 0$, $D = 1.555'$, $\beta_F = \beta_R = 15°$

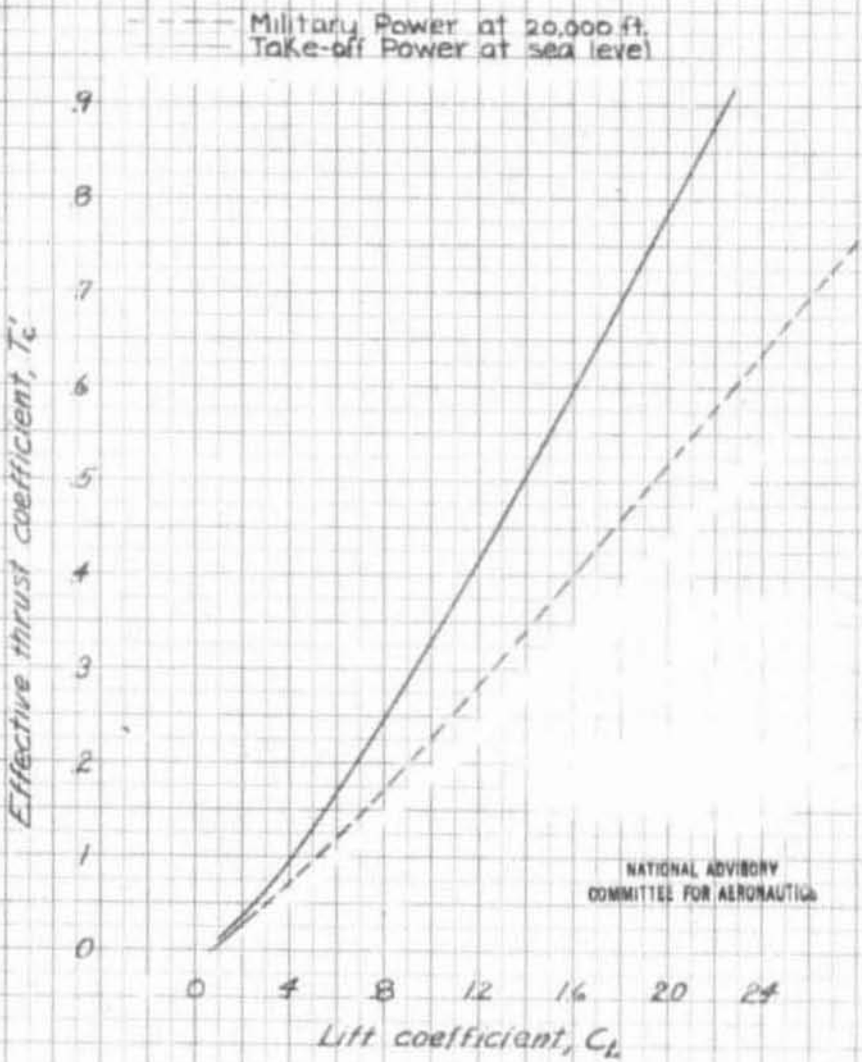

Figure 20.- Thrust coefficient available at any lift coefficient for the XP-62 airplane.

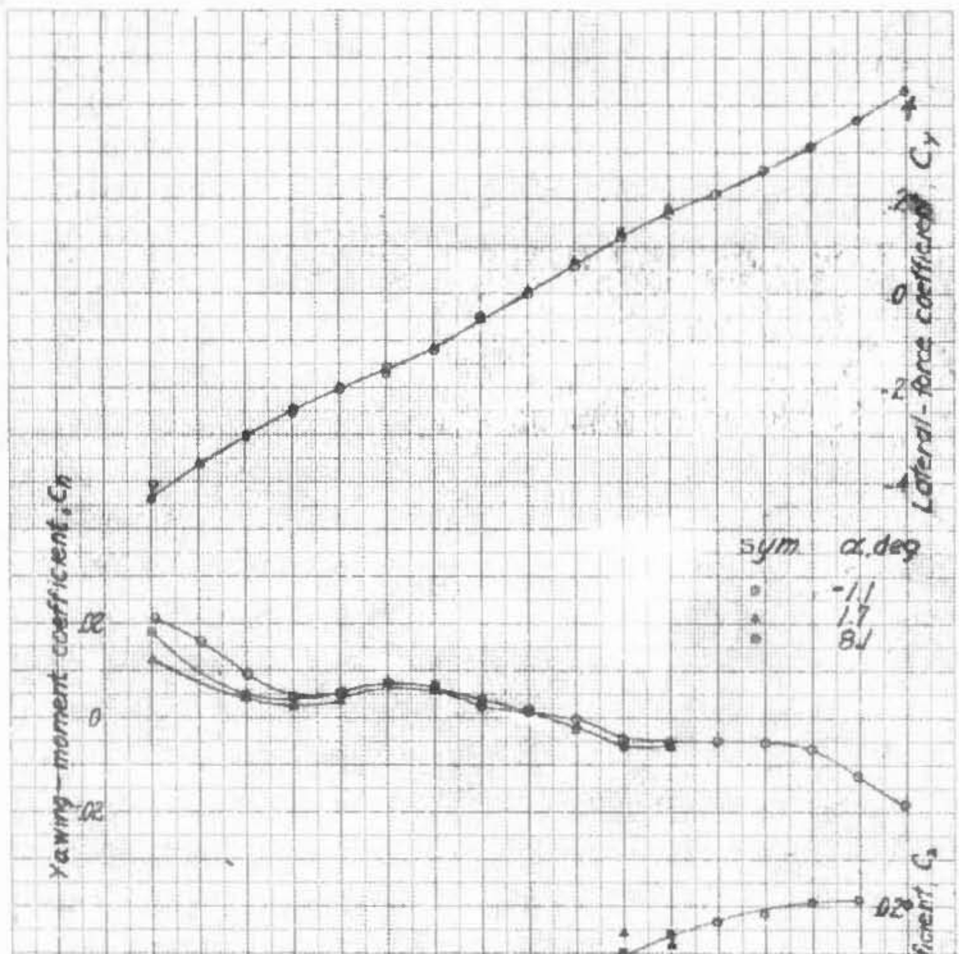

(a) Propeller windmilling

Figure 21.- Effect of angle of attack on the aerodynamic characteristics in yaw of the XP-62 model (1/9-scale) with rudder free. δ_t = 45°. Vertical tail VR, q = 9.21 lbs/sq.ft.

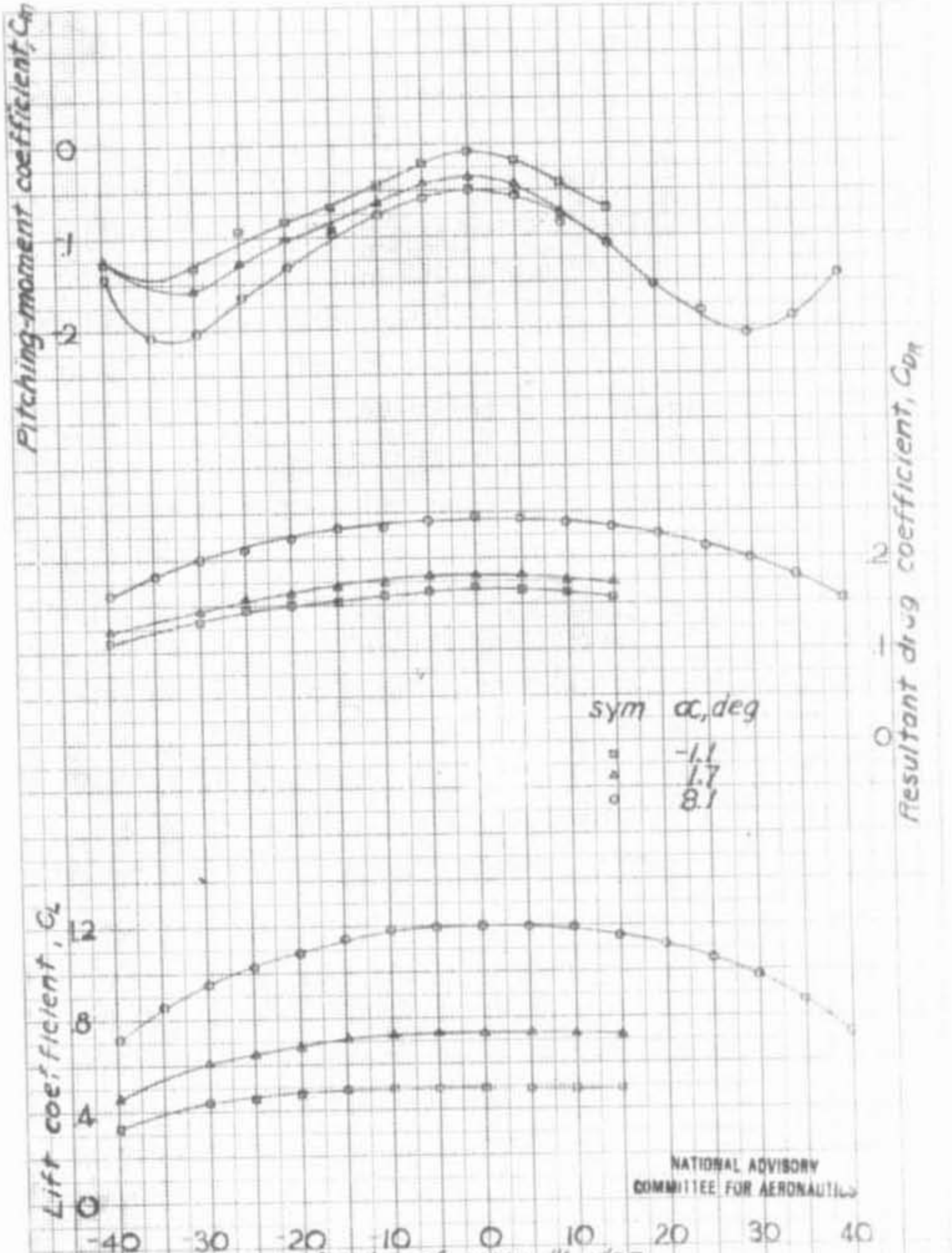

(a) Concluded

Figure 21.- Continued.

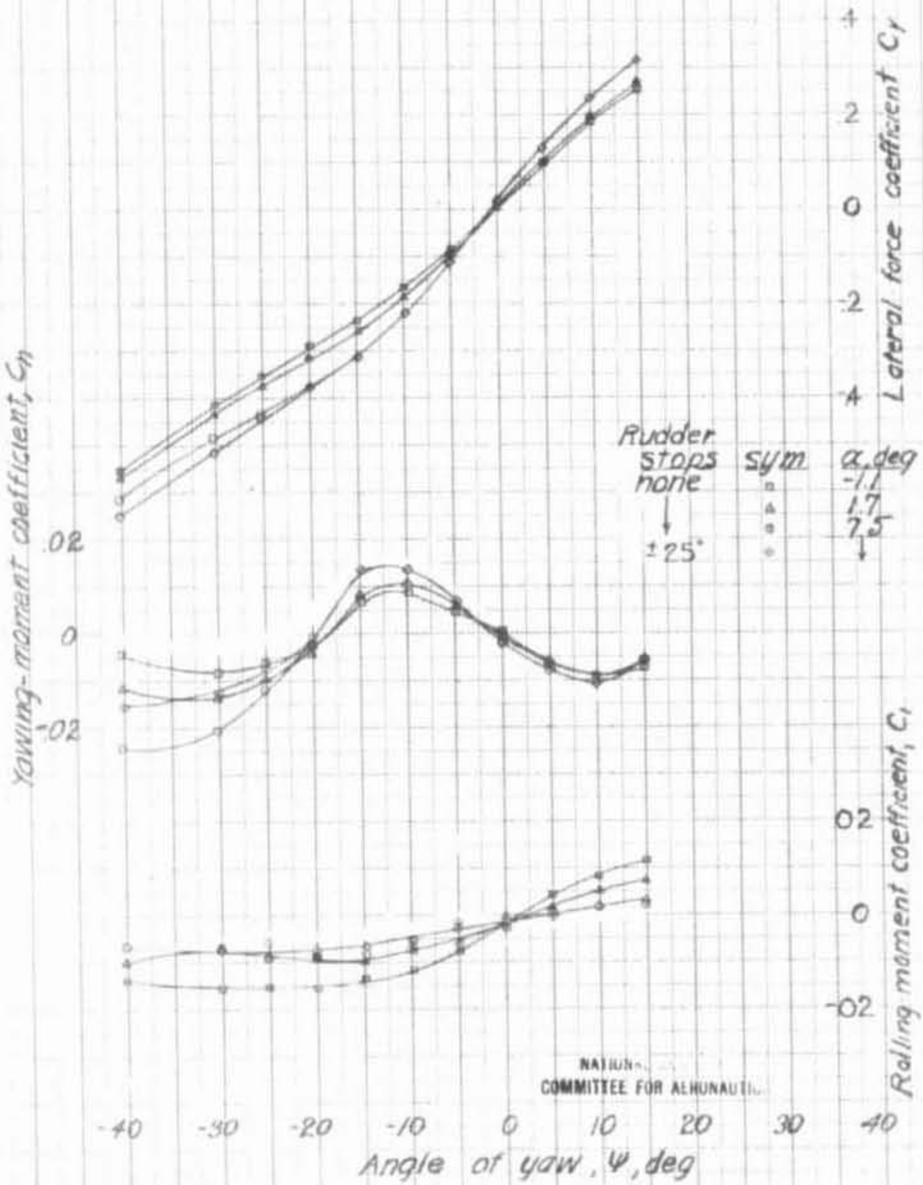

(b) Take off power.
Figure 21. continued.

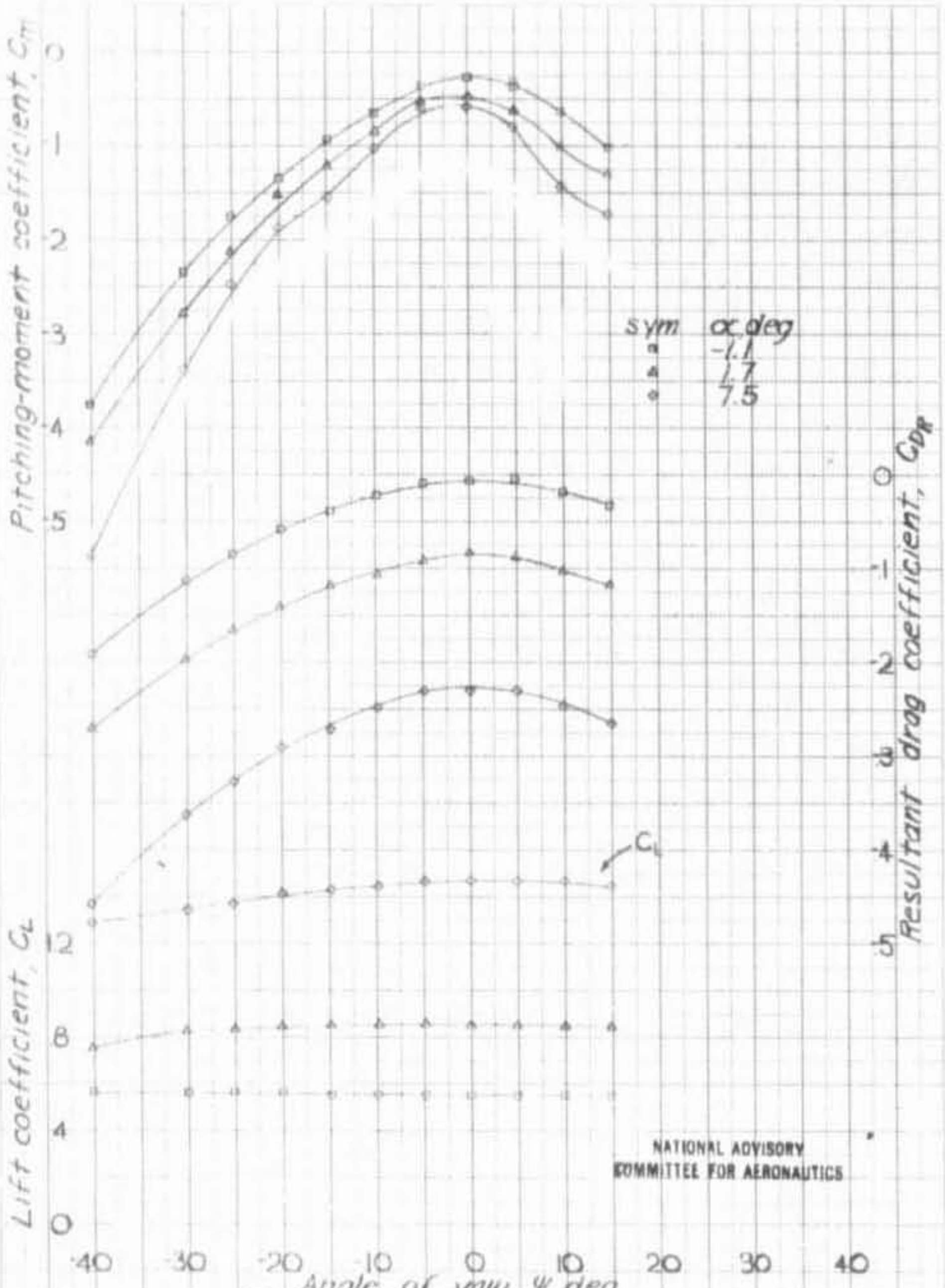

Angle of yaw, ψ, deg

(b) Concluded.

Figure 21.-Concluded.

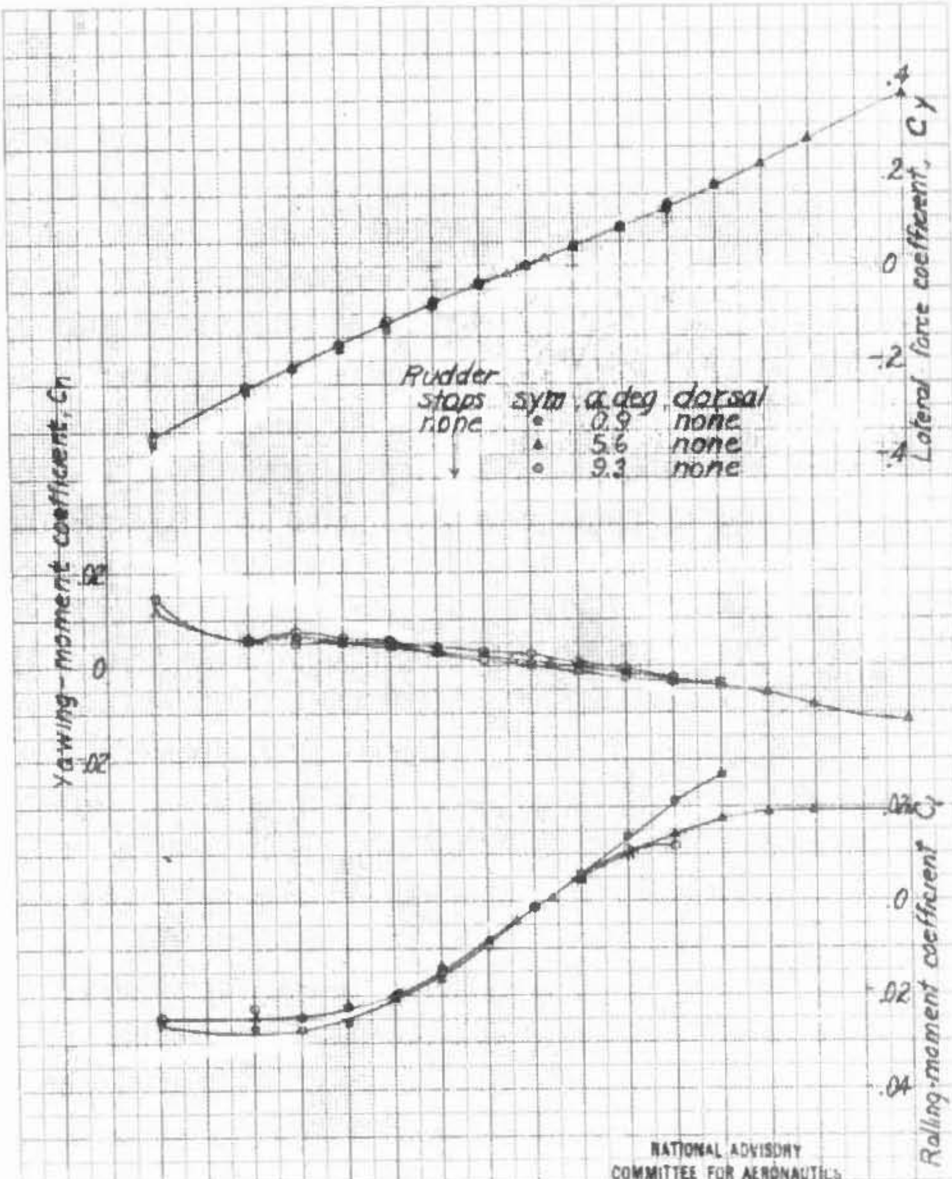

(a) Propeller windmilling.

Figure 22.-Effect of angle of attack on the aerodynamic characteristics in yaw of the XP-62 model (1/8 scale) with rudder free $\delta_f = 0$, vertical VR. $q = 9.21$ lbs/sq ft.

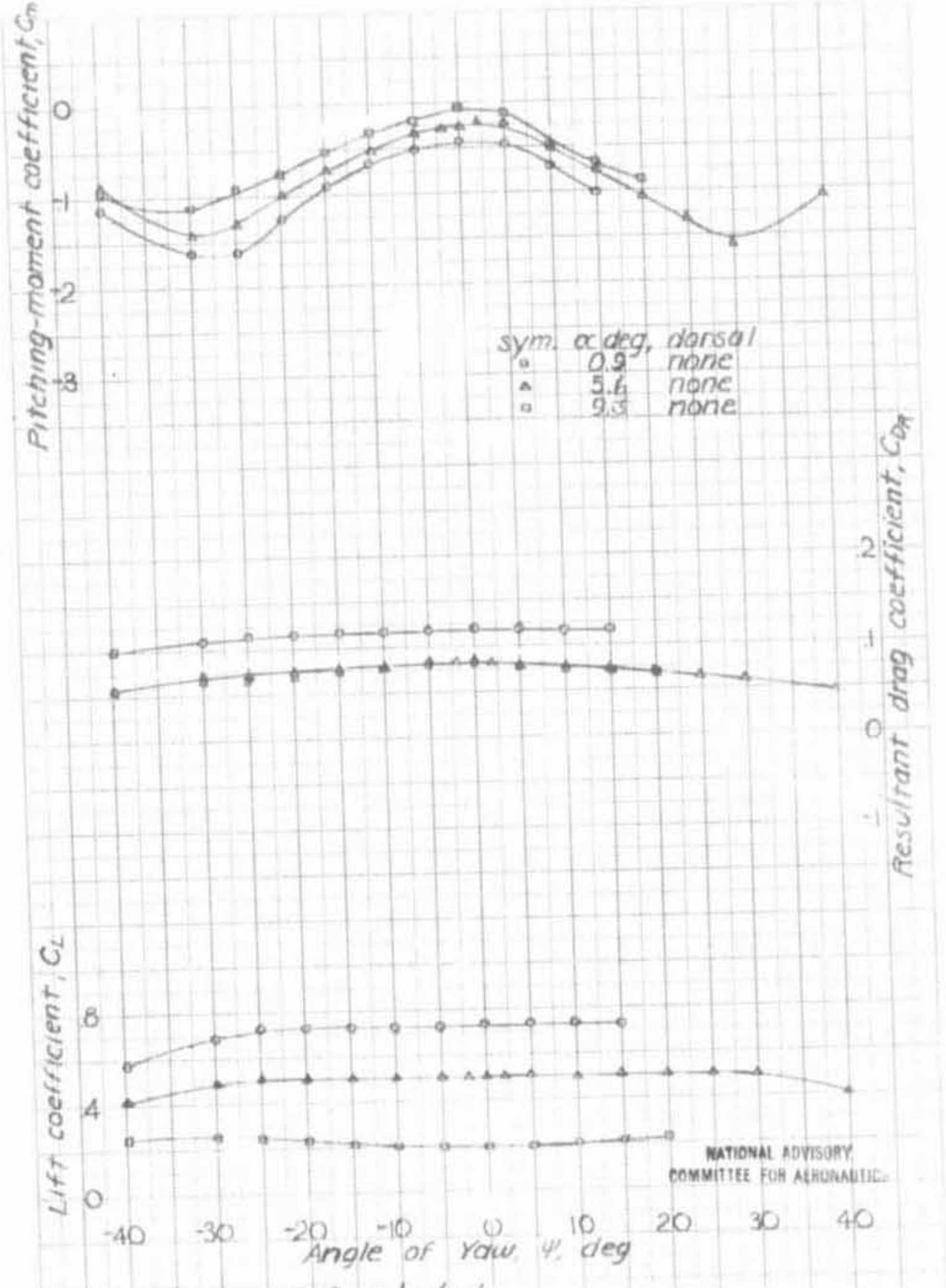

(a) Concluded

Figure 22. Continued

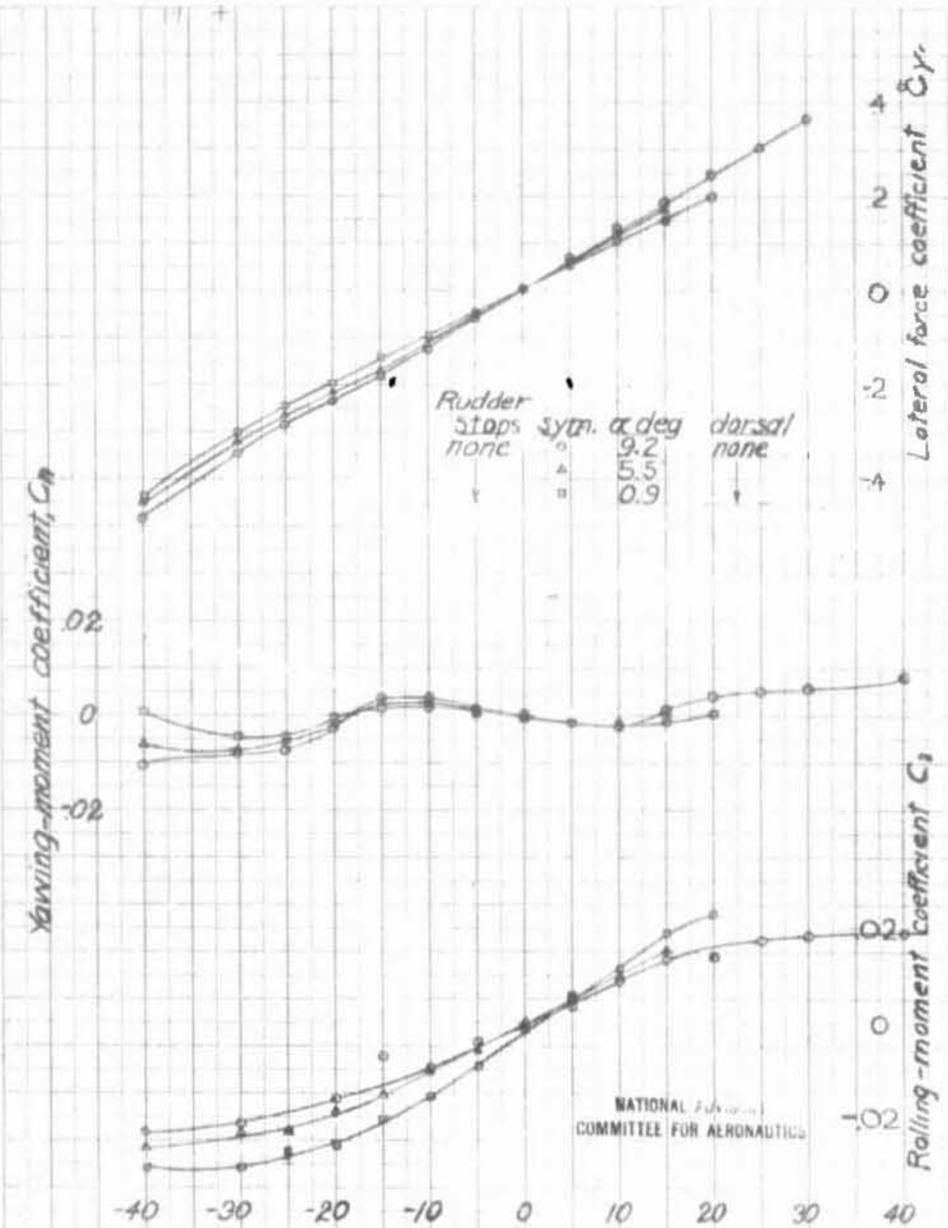

(b) Take-off power
Figure 22.- Continued.

L-779

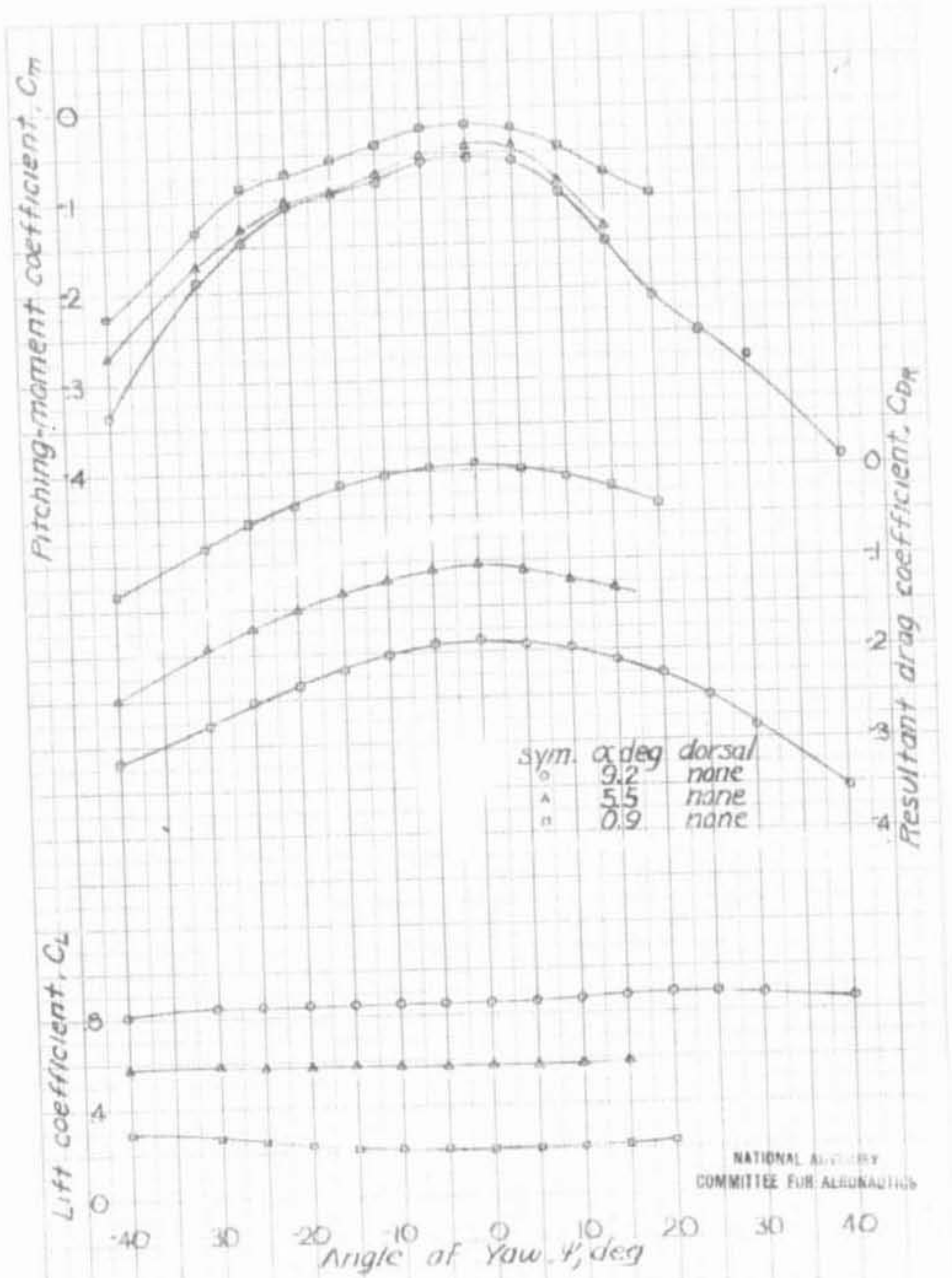

(b) Concluded.

Figure 22. Concluded.

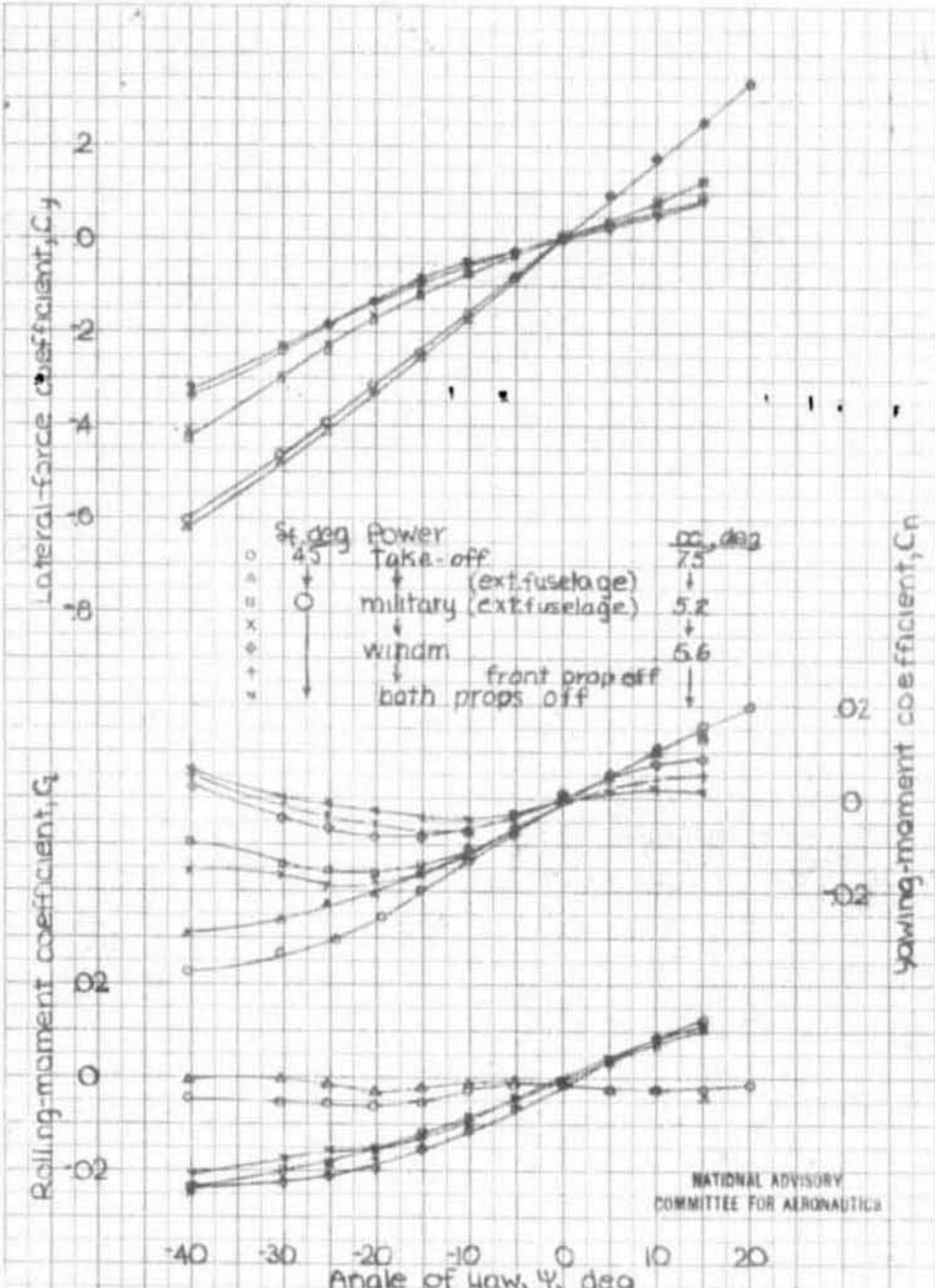

Figure 23.- Effect of yaw on the aerodynamic characteristics of the XP-62 model (1/4 scale) with tail surfaces removed. (Normal fuselage except as noted)

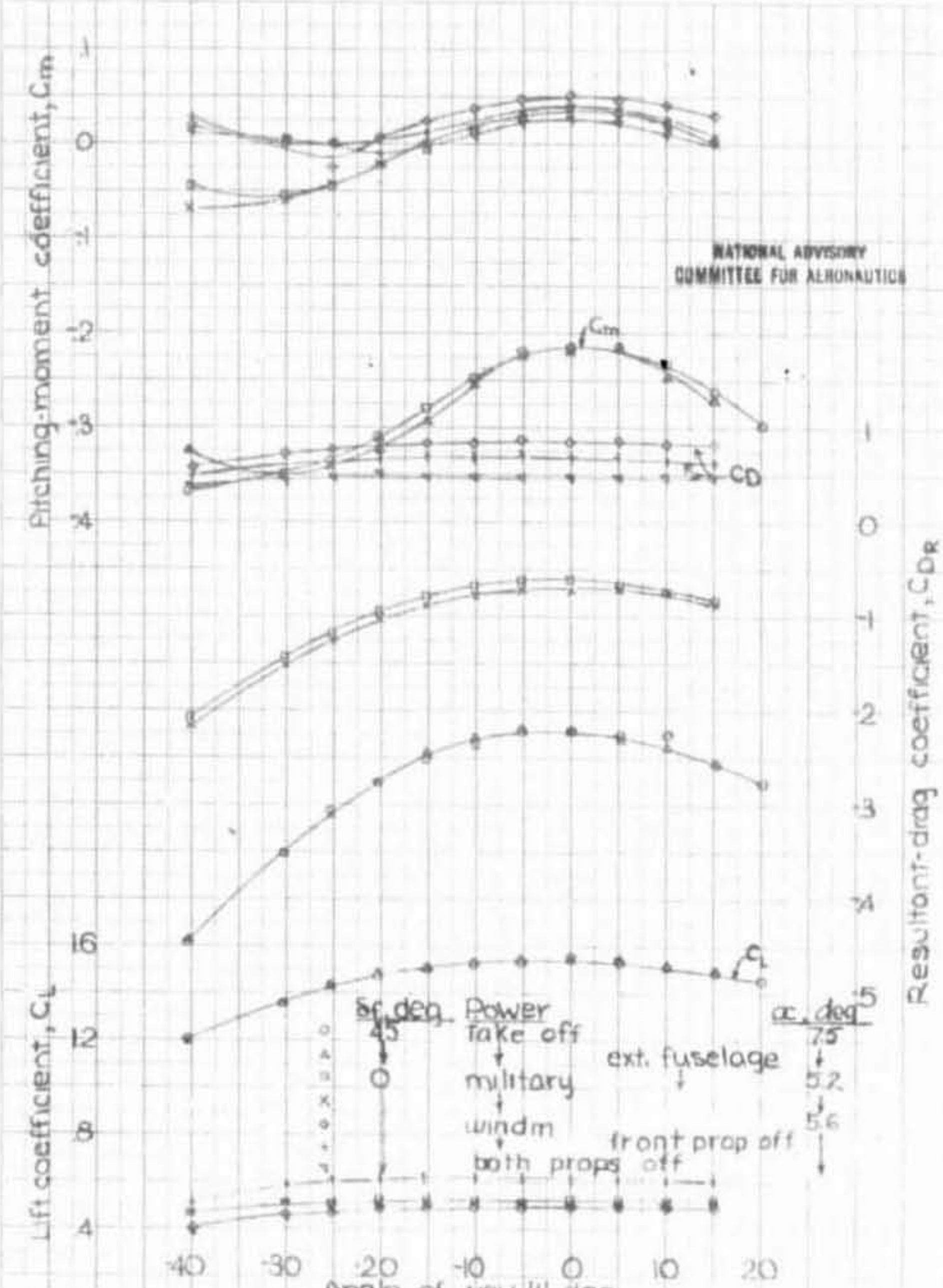

Figure 23.- Concluded.

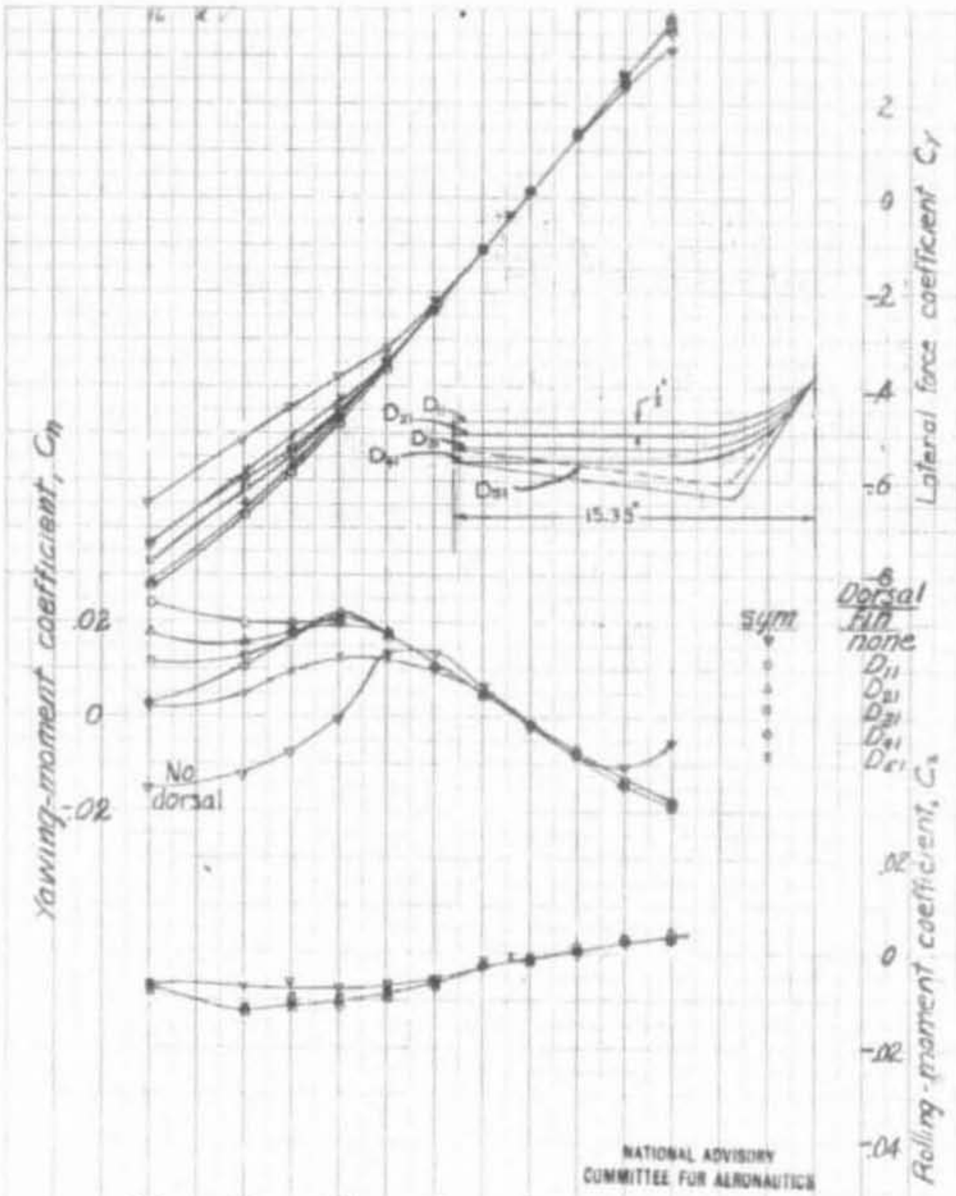

(a) Length #1

Figure 24.- Effect of various dorsal fins on the aerodynamic characteristics in yaw of the XP-62 model (1/4-scale) with rudder free. Stops ±25°; δ_f-45°, α-7.5° take off power, Tail VR

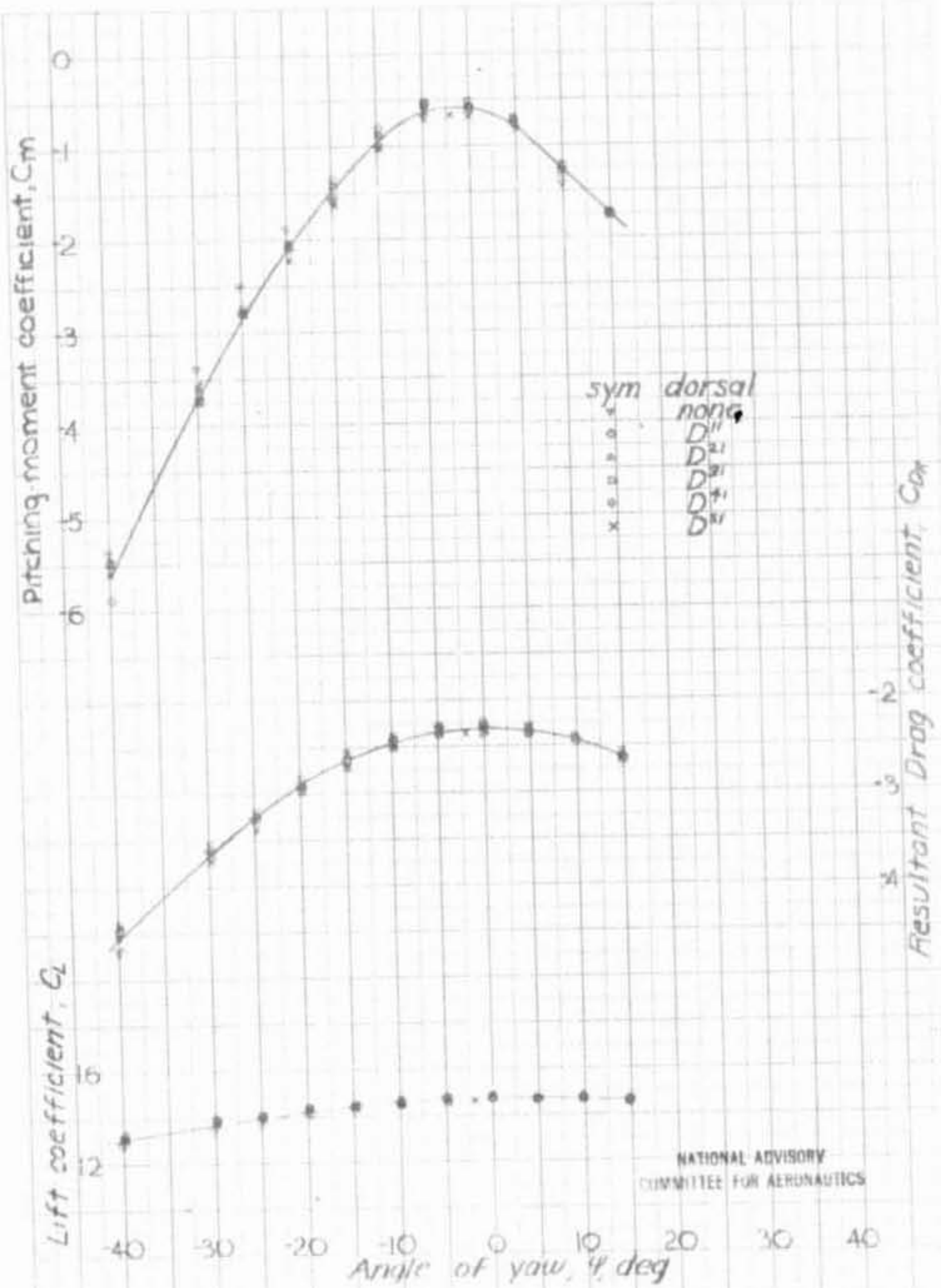

(a) Concluded
Figure 24. Continued.

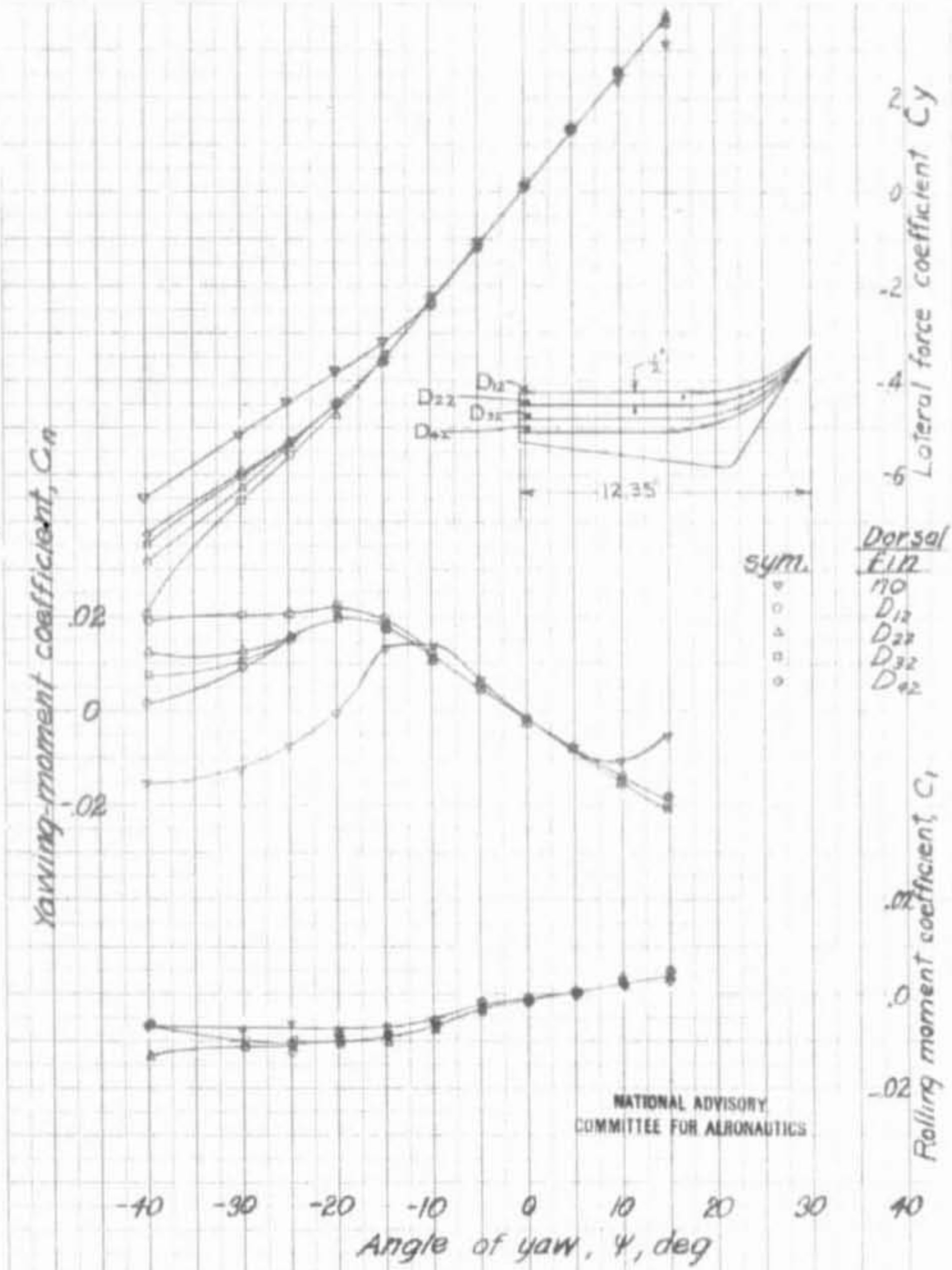

(b) Length #2

Figure 24- continued.

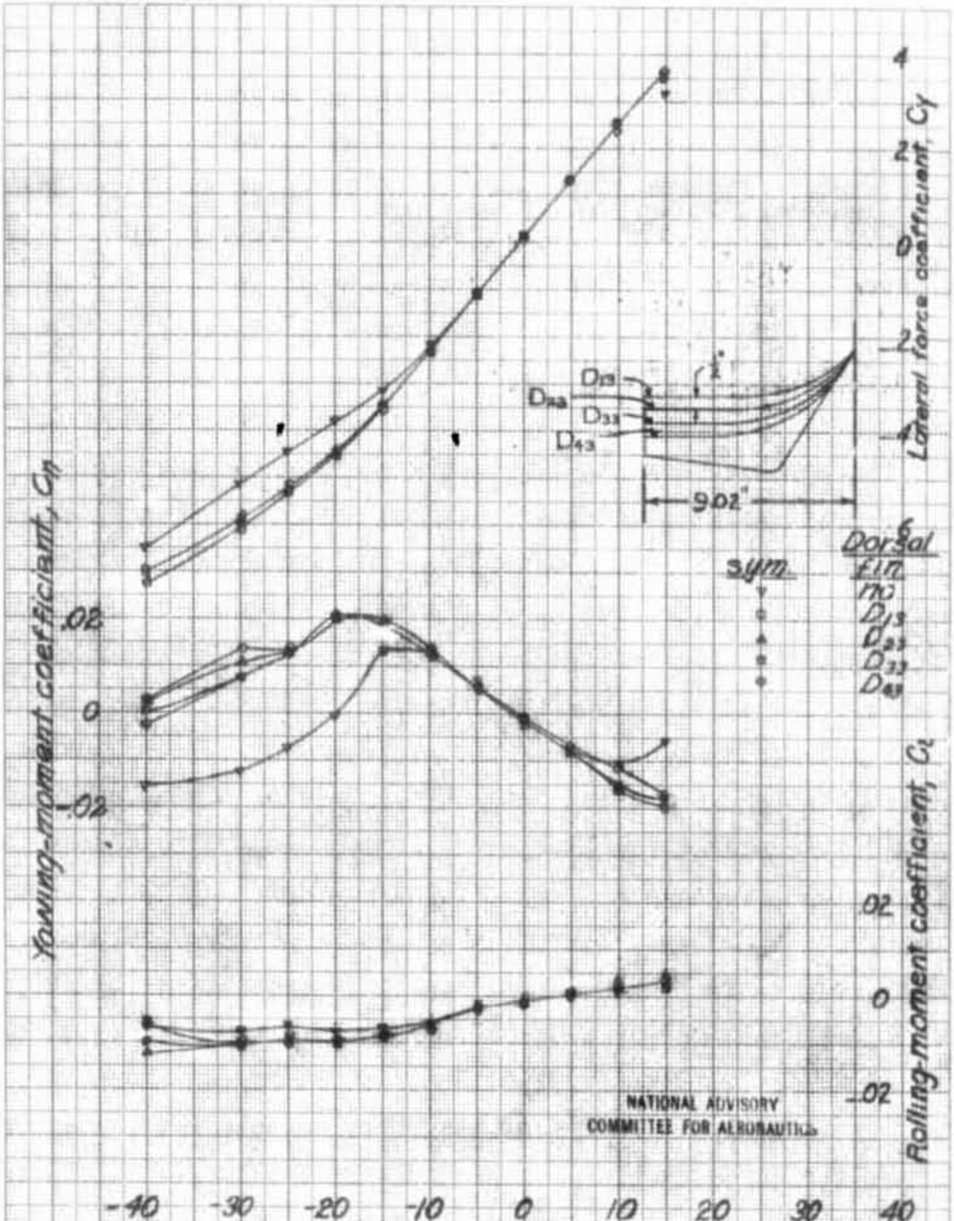

(c) Length #3

Figure 24.- concluded.

L-779

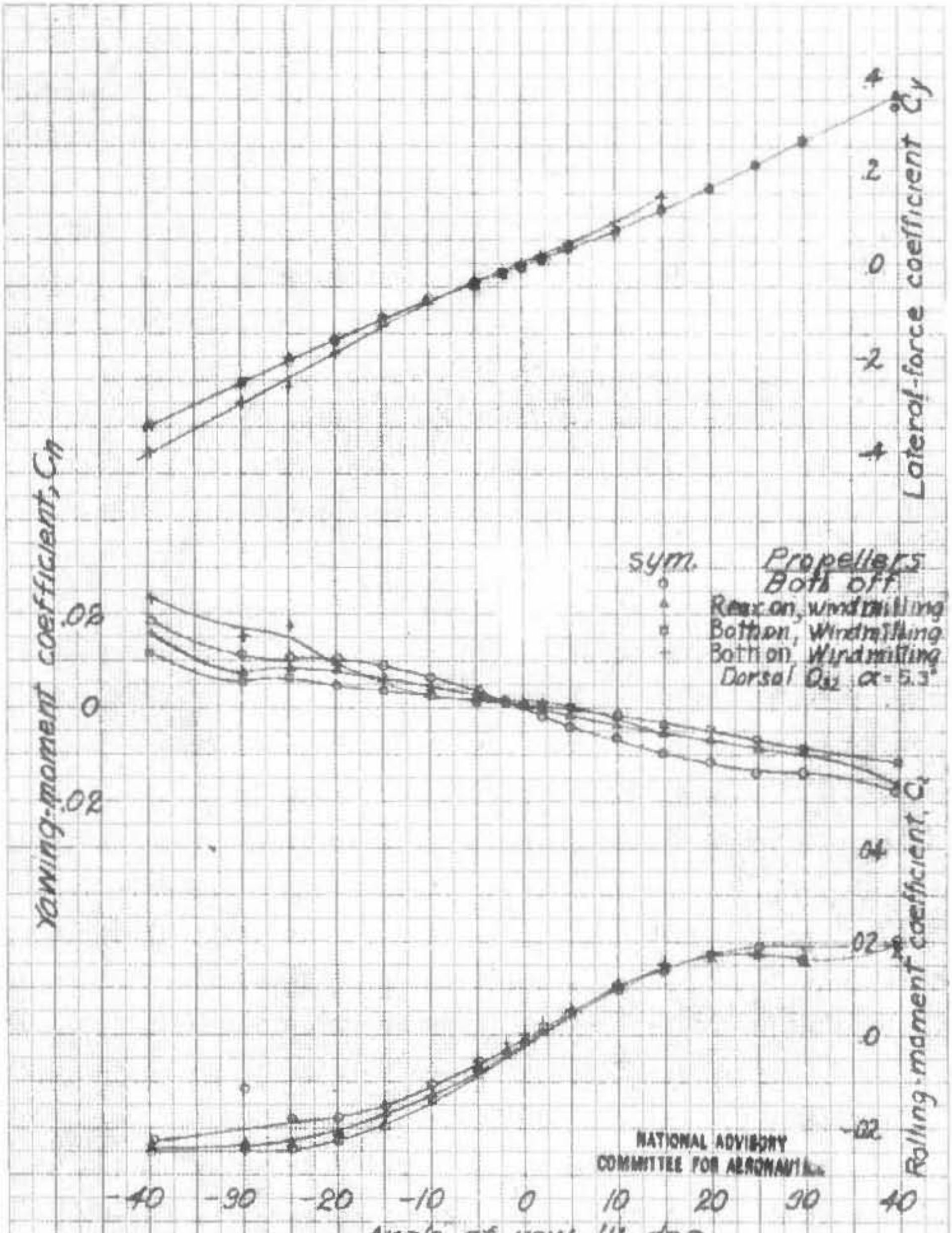

Figure 25.– Effect of propeller on the aerodynamic characteristics in yaw of the XP-62 model (1/4-scale) with rudder free. $\delta_r = 0$, $q = 16.37$ lbs sq ft, $\alpha = 5.5°$ Tail VR

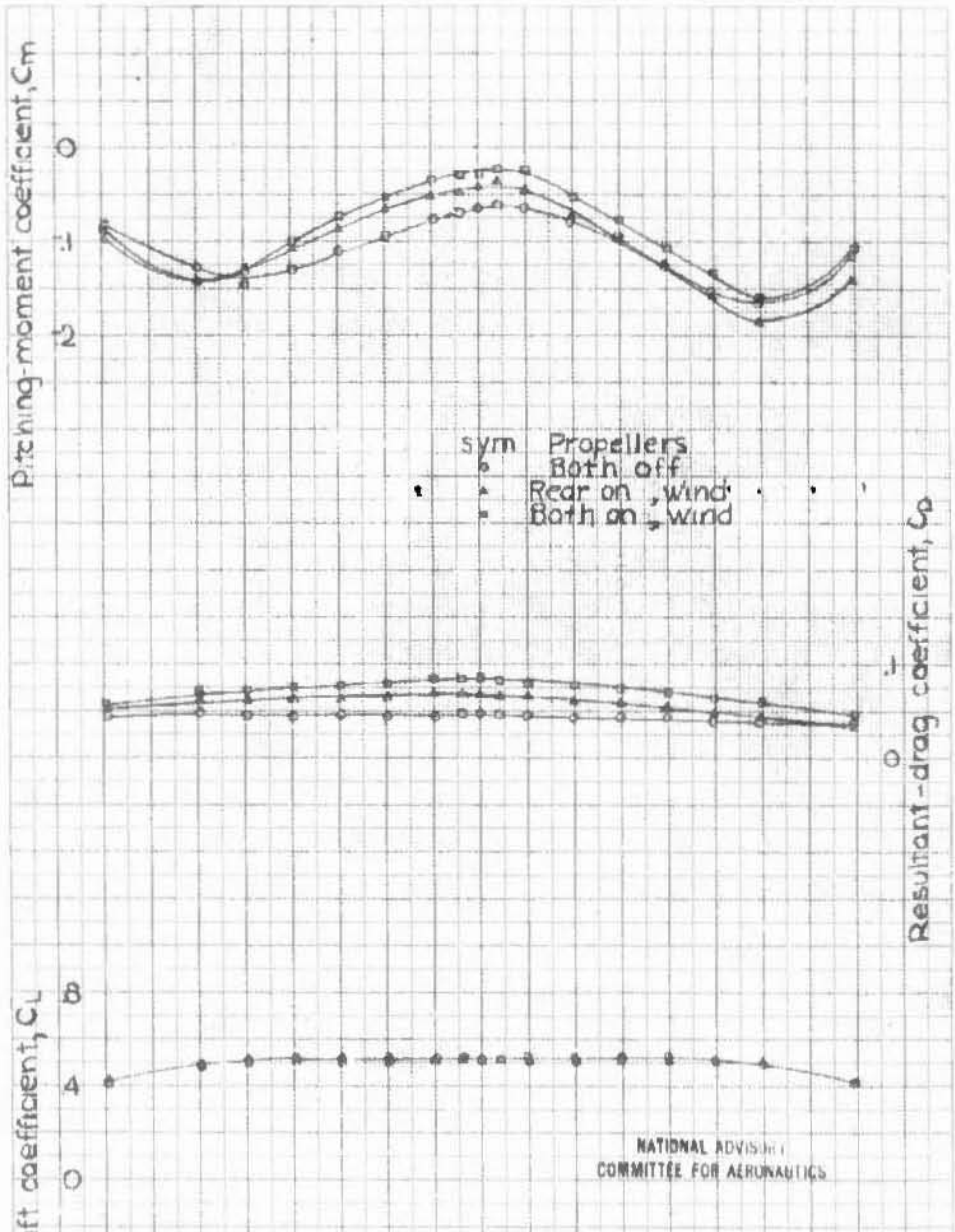

Figure 25.- Concluded.

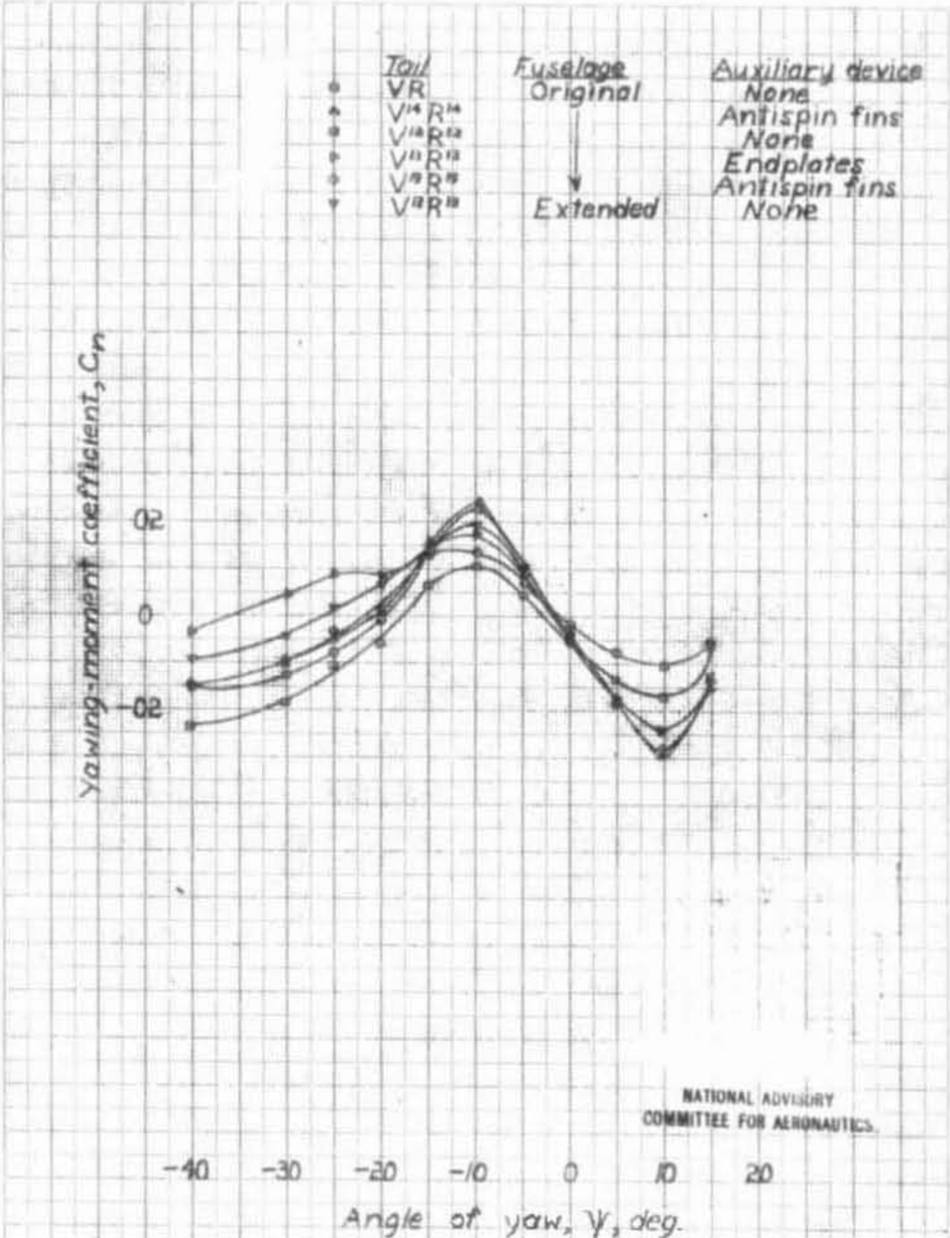

Figure 26.-Comparison of rudder-free characteristics of the 1/9-scale model of XP-62 airplane with various vertical tail arrangements. $\delta_f = 45°$, $\alpha = 7.5°$, take-off power, $q = 9.21$ lbs/ft^2.

L-779

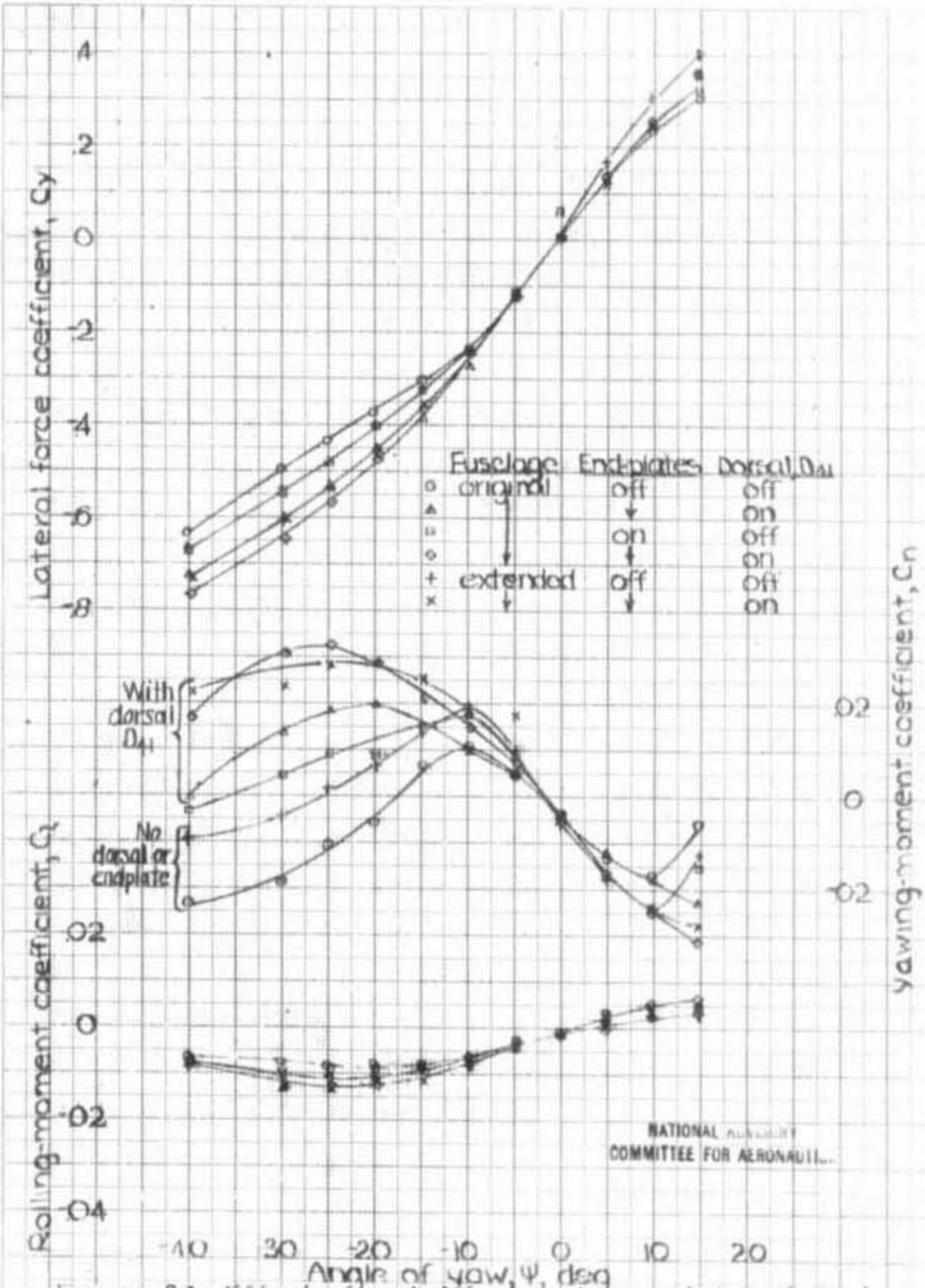

Figure 27.- Effect of endplates on horizontal tail and fuselage extension on the aerodynamic characteristics of the XP-62 model (1/4-scale) with vertical tail $V^{13}R^{13}$ and $V^{13}R^{13}E$. Rudder free. Take-off power, α = -15°, q = 9.21 lb/sq ft, δf = 45°.

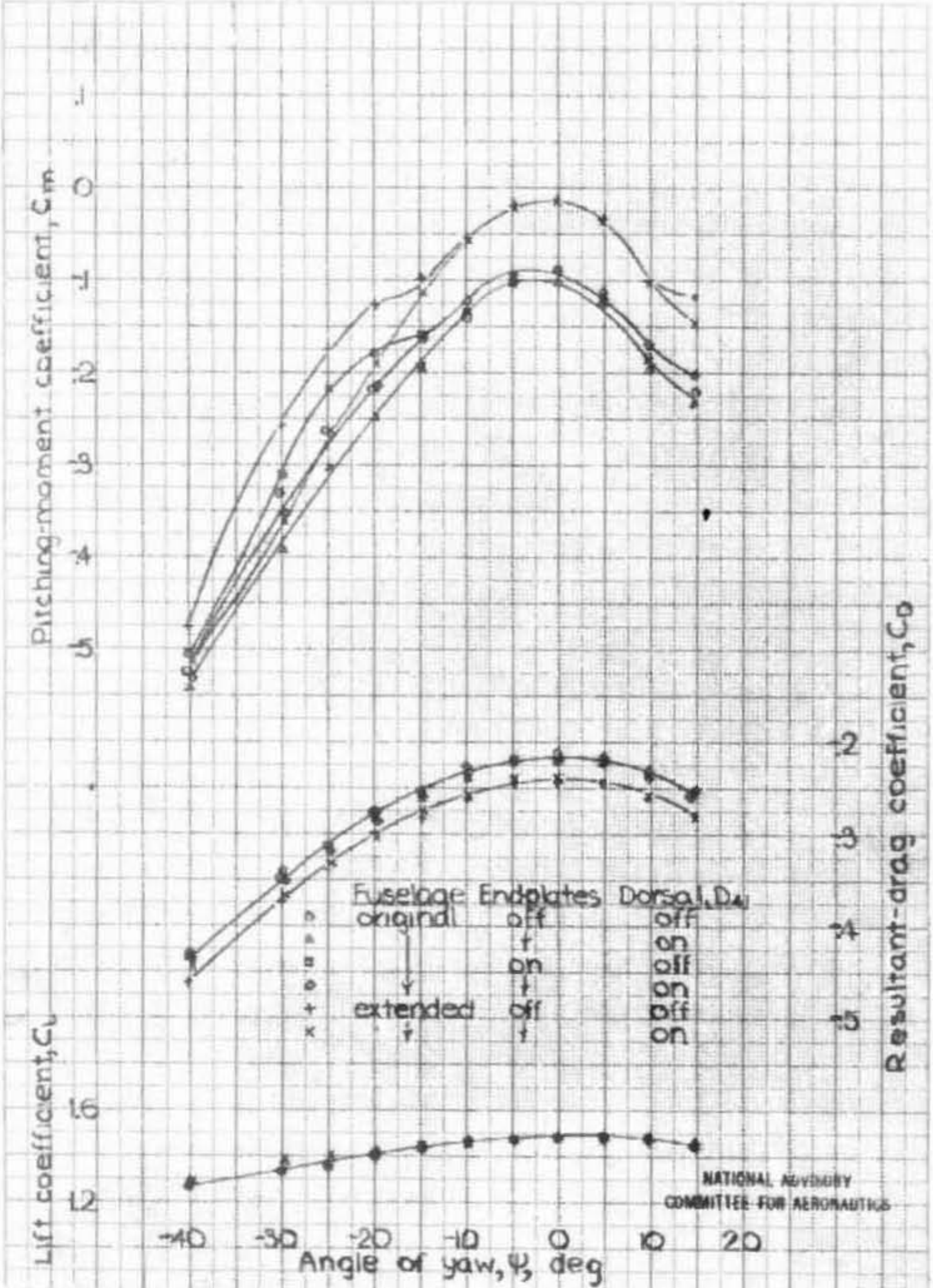

Figure 27.- Concluded.

L-779

L-779

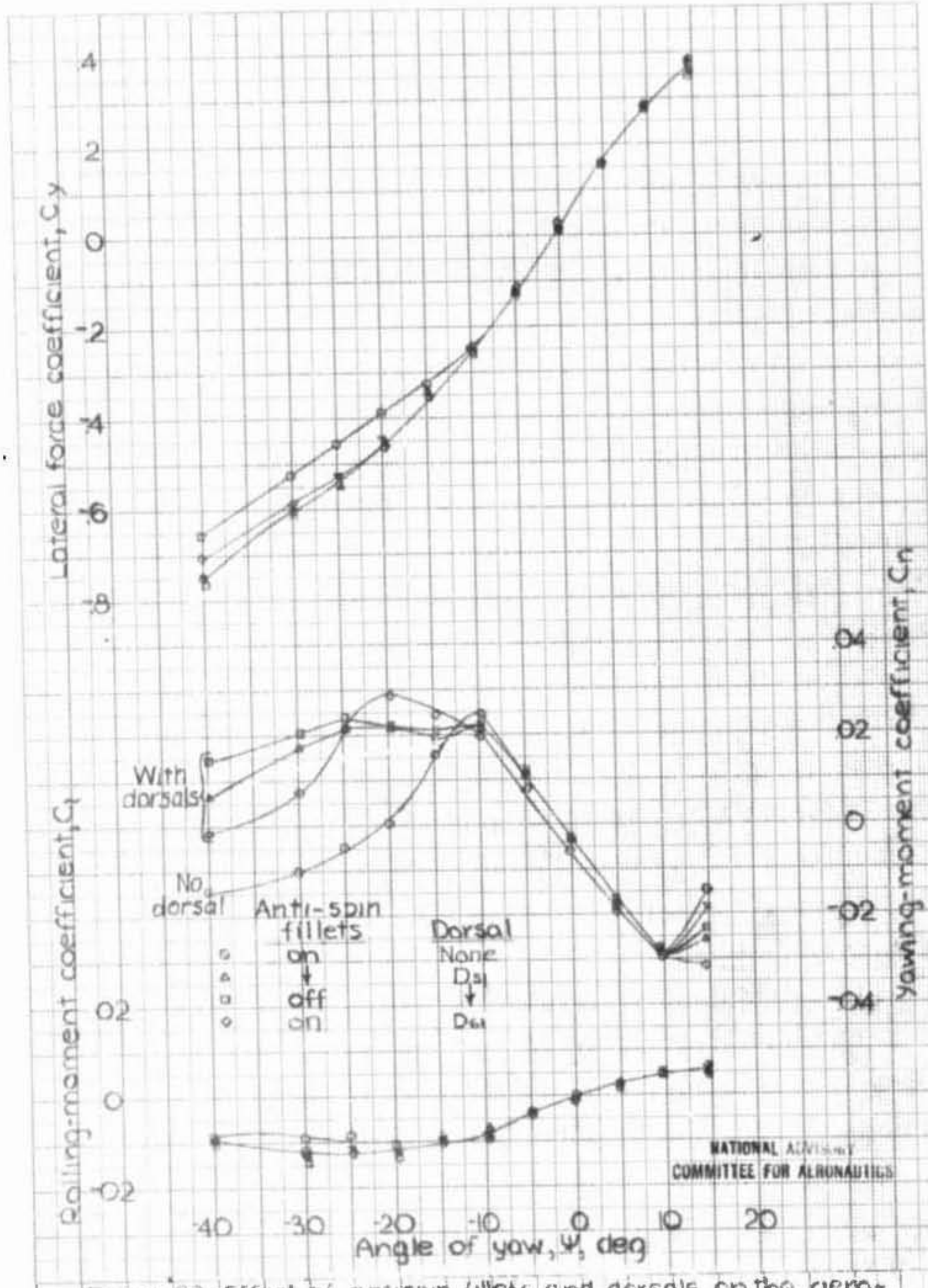

Figure 28.-Effect of antispin fillets and dorsals on the aerodynamic characteristics of the XP-62 model (1/8 scale) with vertical tail V"B". Rudder free, δ_f 45°, Take-off power, α=15°, Rudder stops ± 25°.

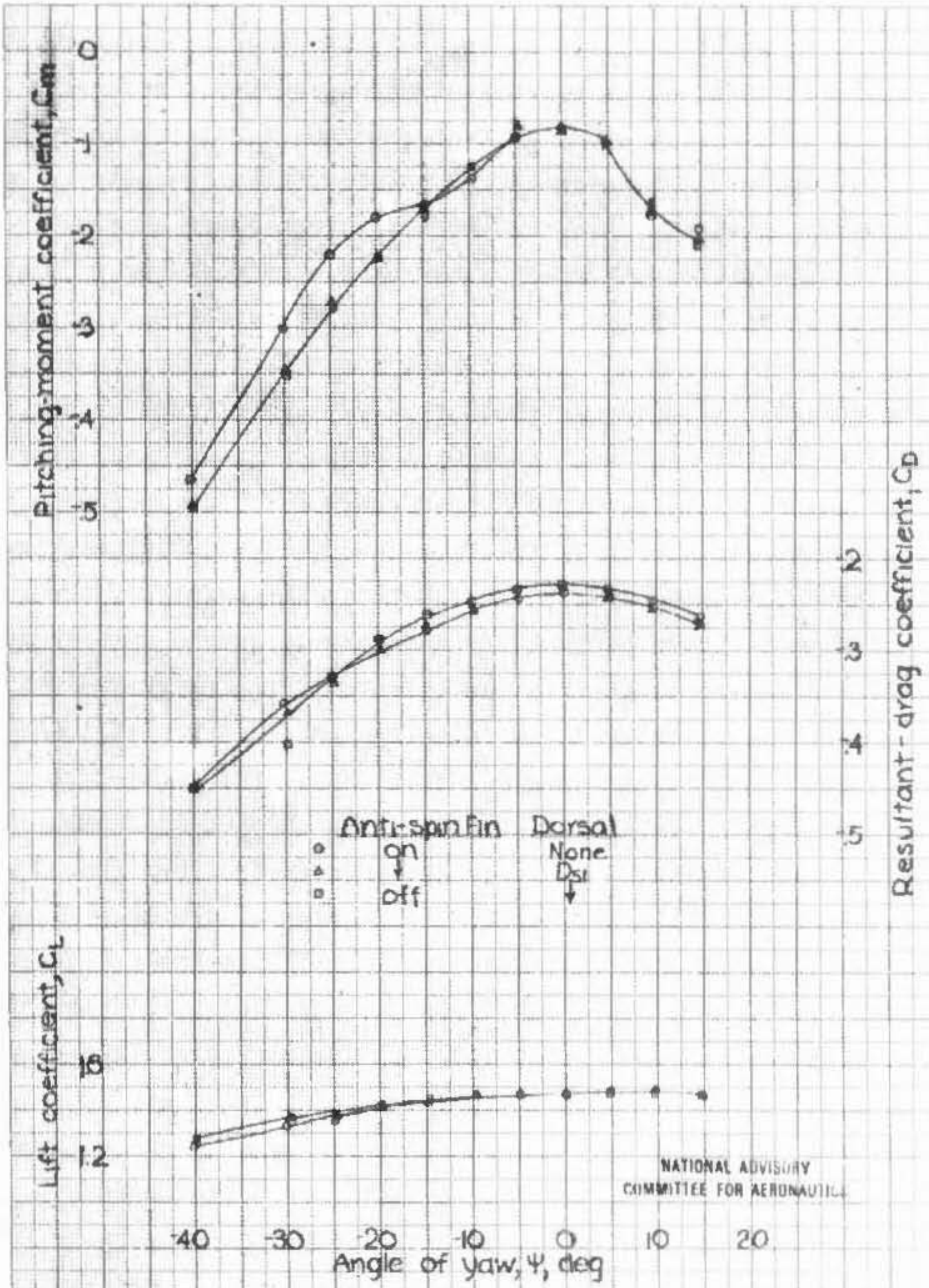

Figure 28.- concluded.

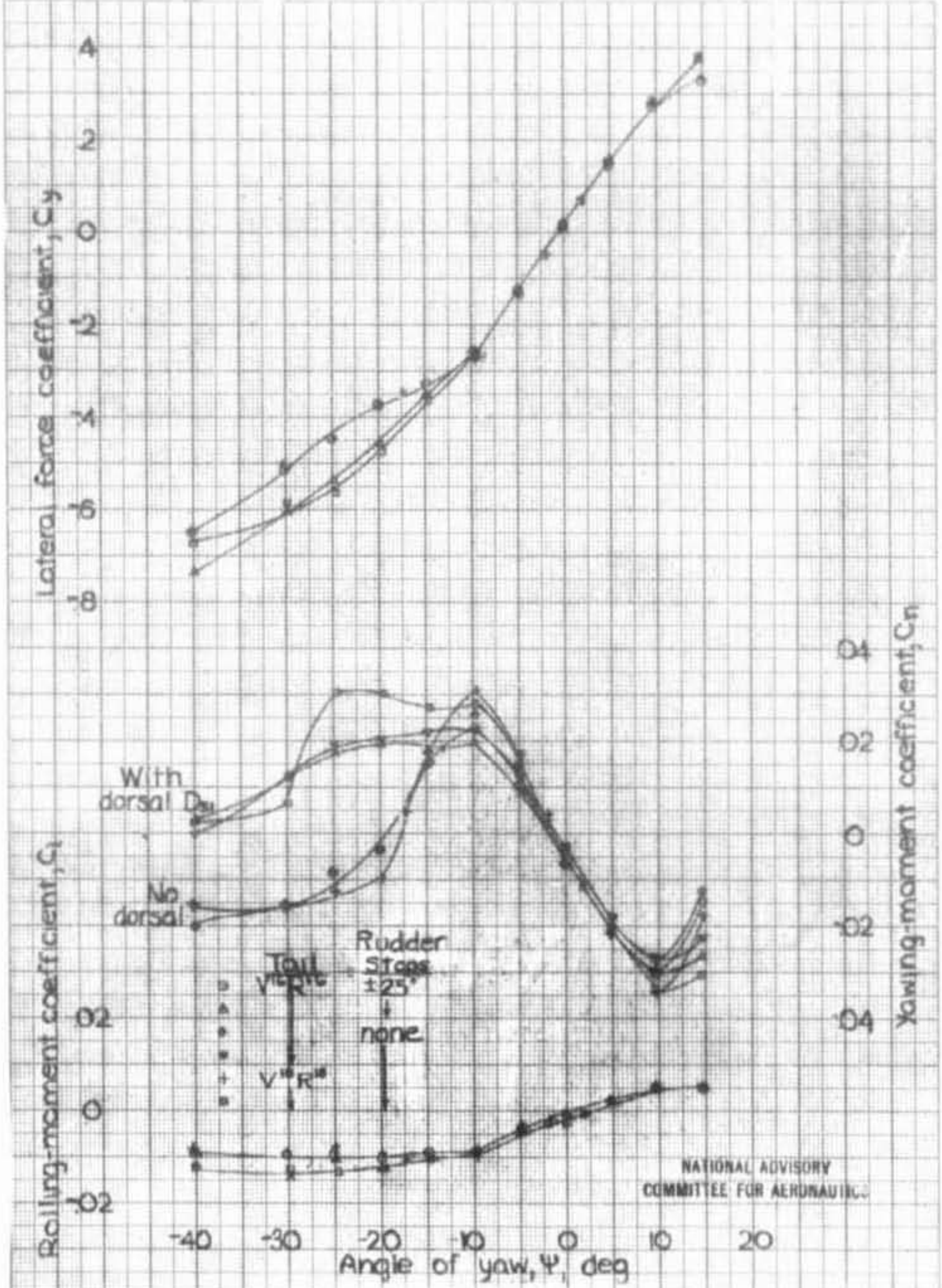

Figure 29.- Effect of a dorsal fin and rudder balance on the aerodynamic characteristics of the XP-62 model (⅛ scale) with vertical tails $V^{16}R^{16}$ and $V^{8}R^{18}$. Rudder free, $S_f = 45°$, Take-off power, $\alpha_t = 7.5°$, Antispin fillets on.

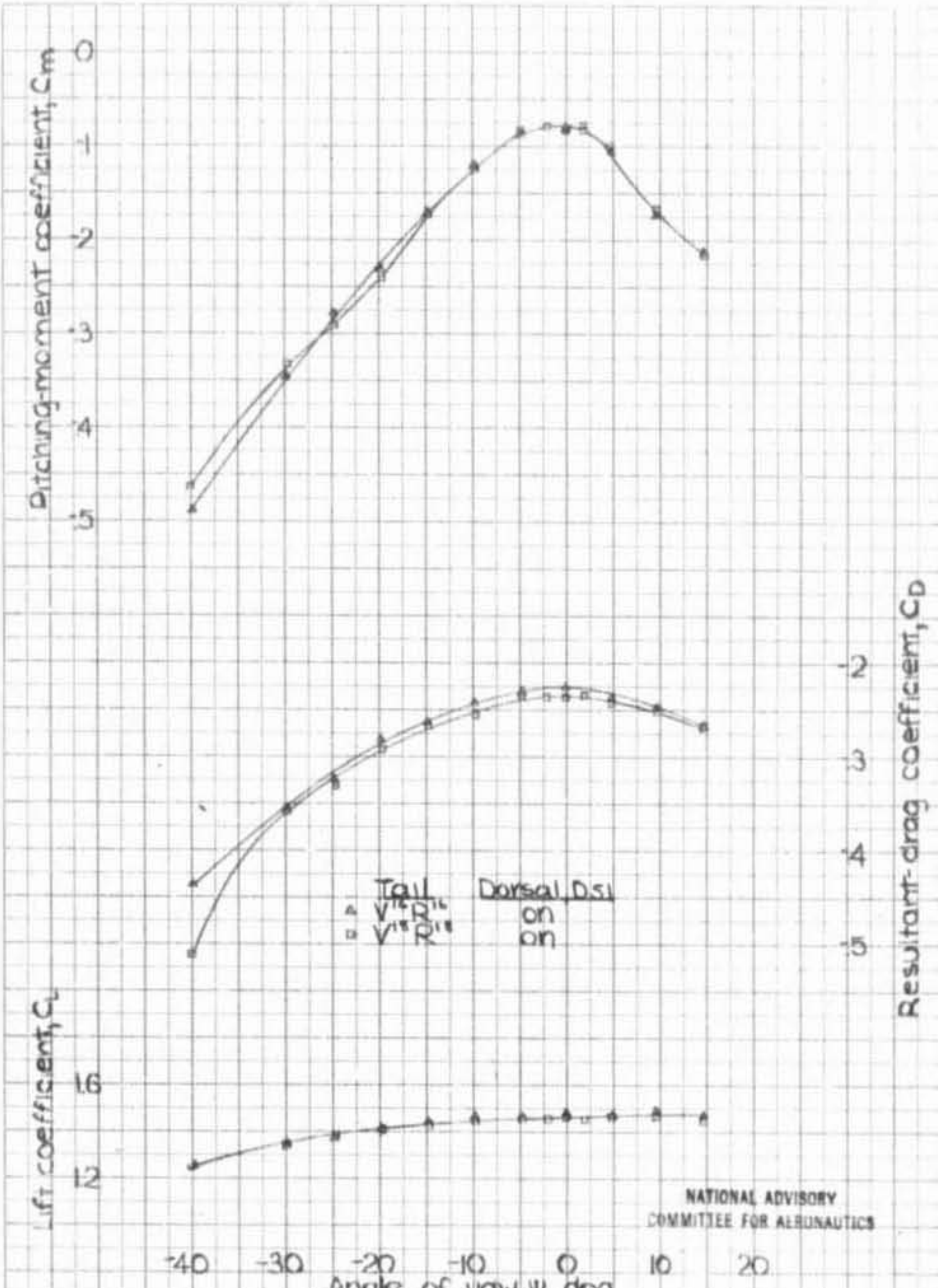

Figure 24.- concluded.

L-779

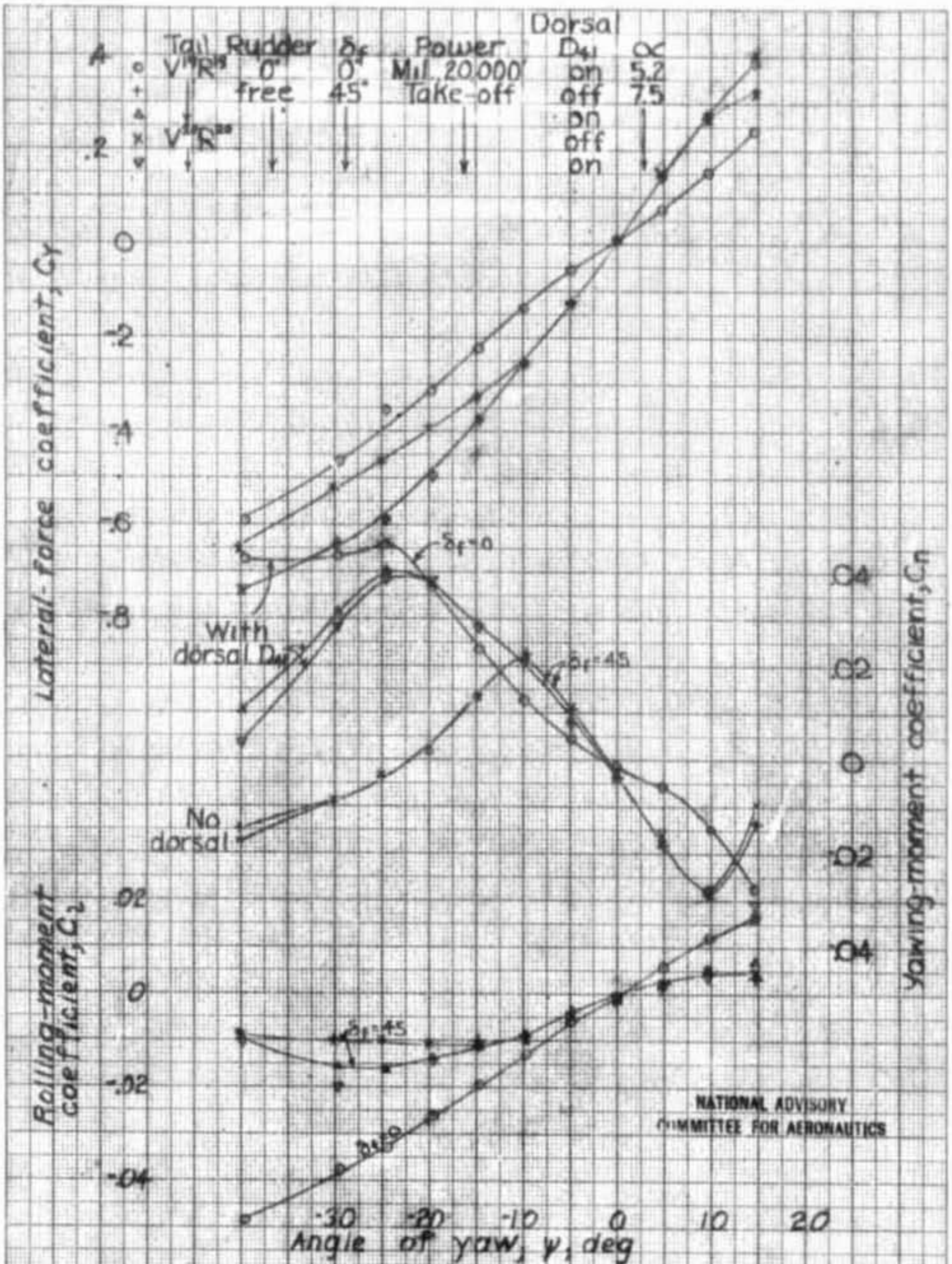

Figure 30-Effect of yaw on the aerodynamic characteristics of the XP-62 model (1/4 scale) with vertical tail $V^{19}R^{19}$ and $V^{20}R^{20}$

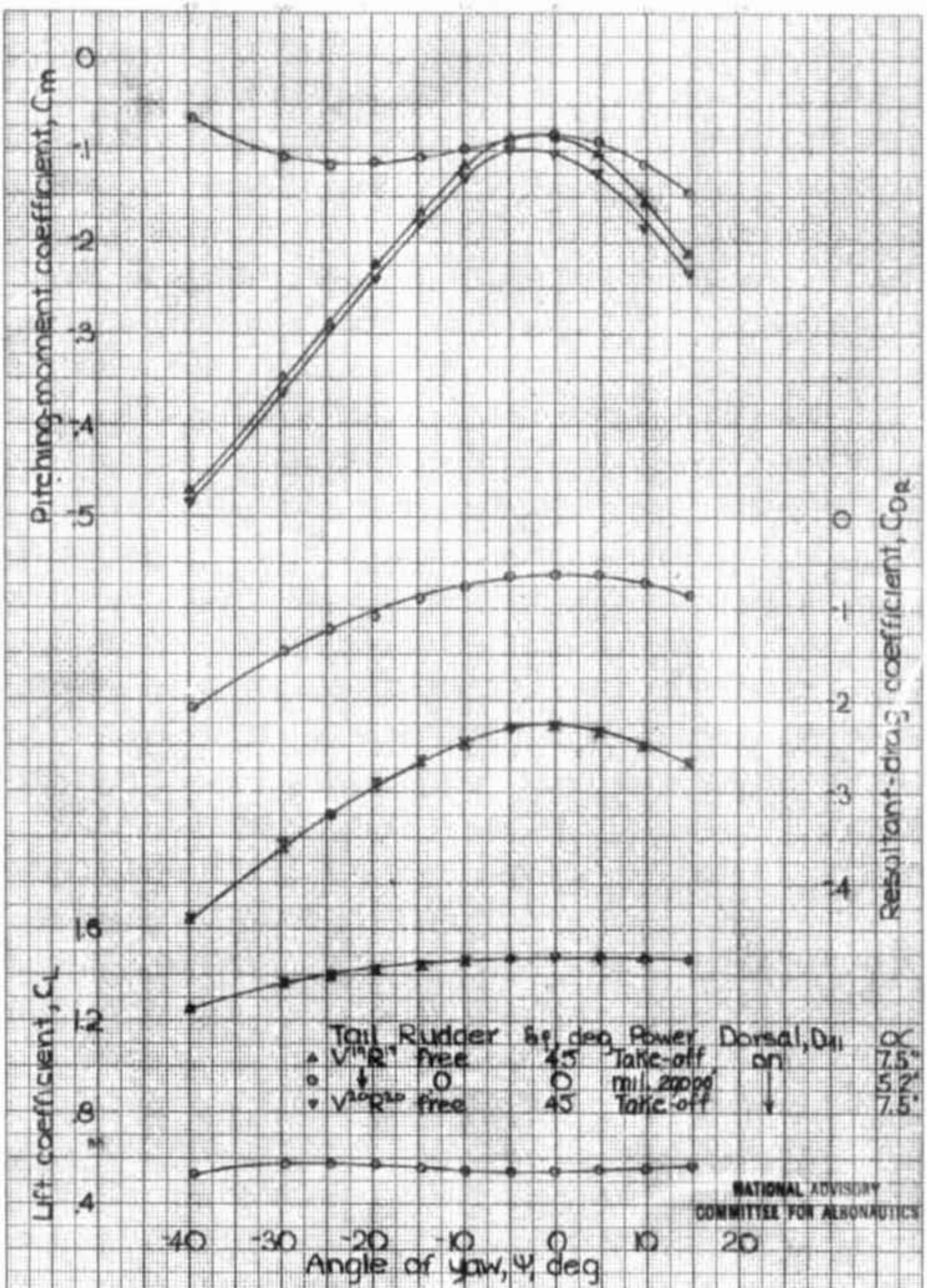

Figure 30.-concluded.

L-779

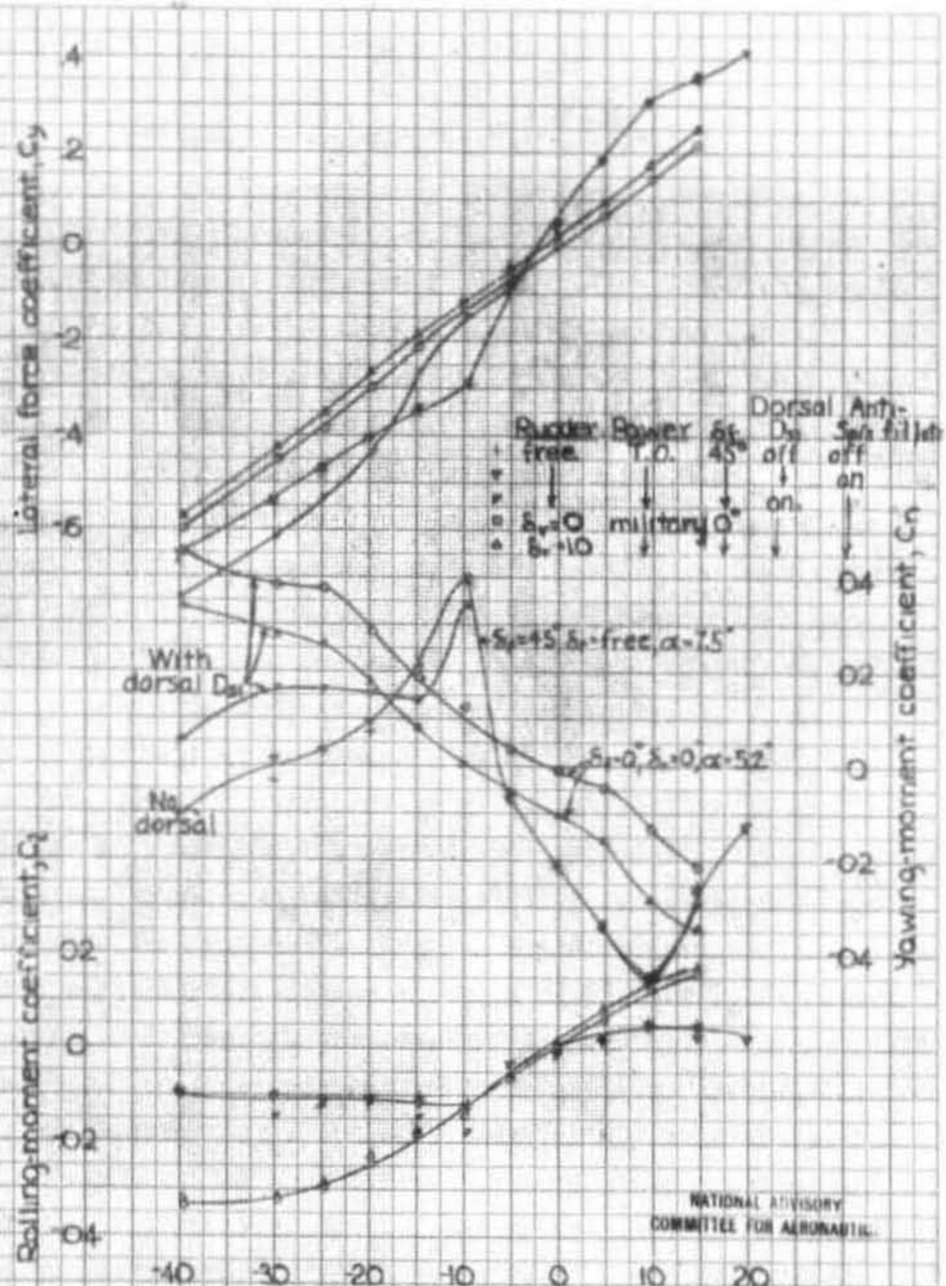

Figure 36.-Effect of yaw on the aerodynamic characteristics of the XP 62 model (1/4 scale) with vertical tail $V^{14}R^{14}$ (Bevel trailing edge).

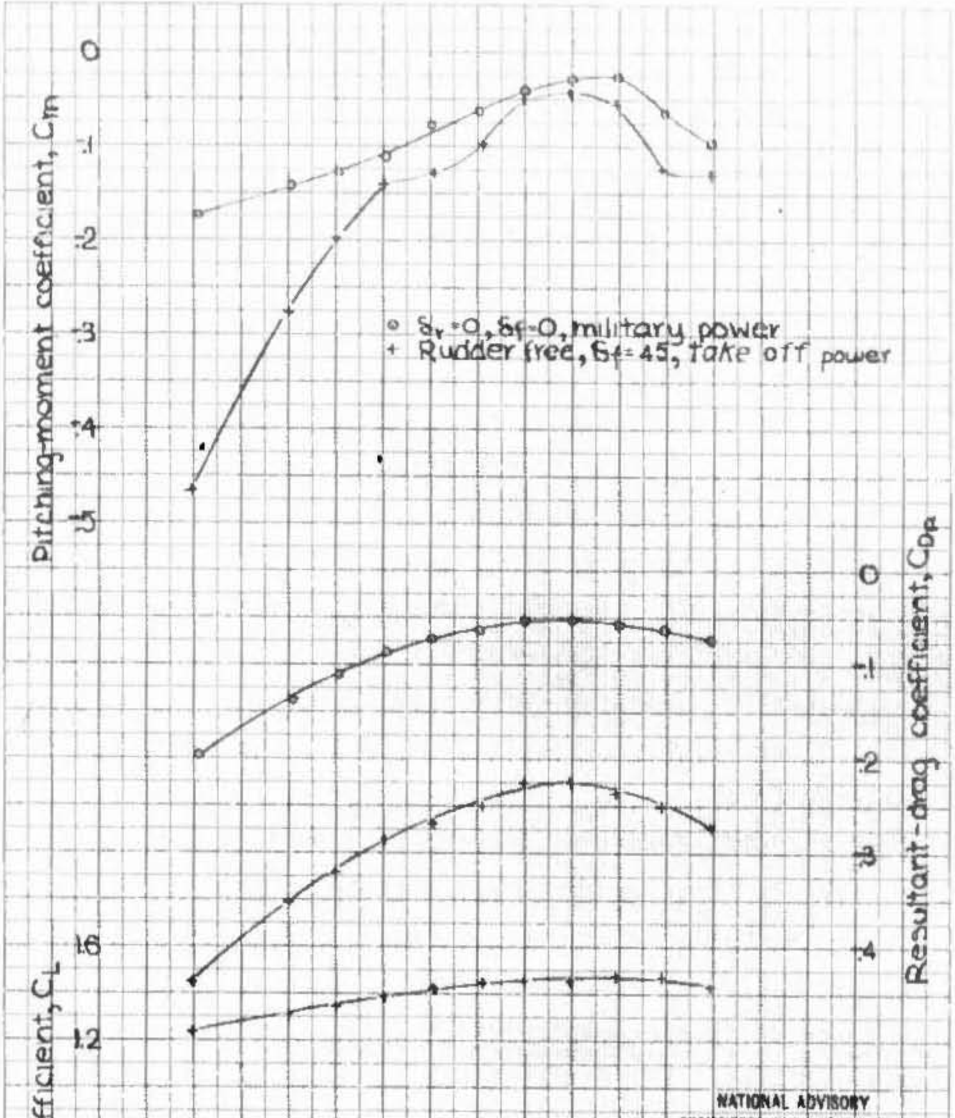

Figure 31.-concluded.-

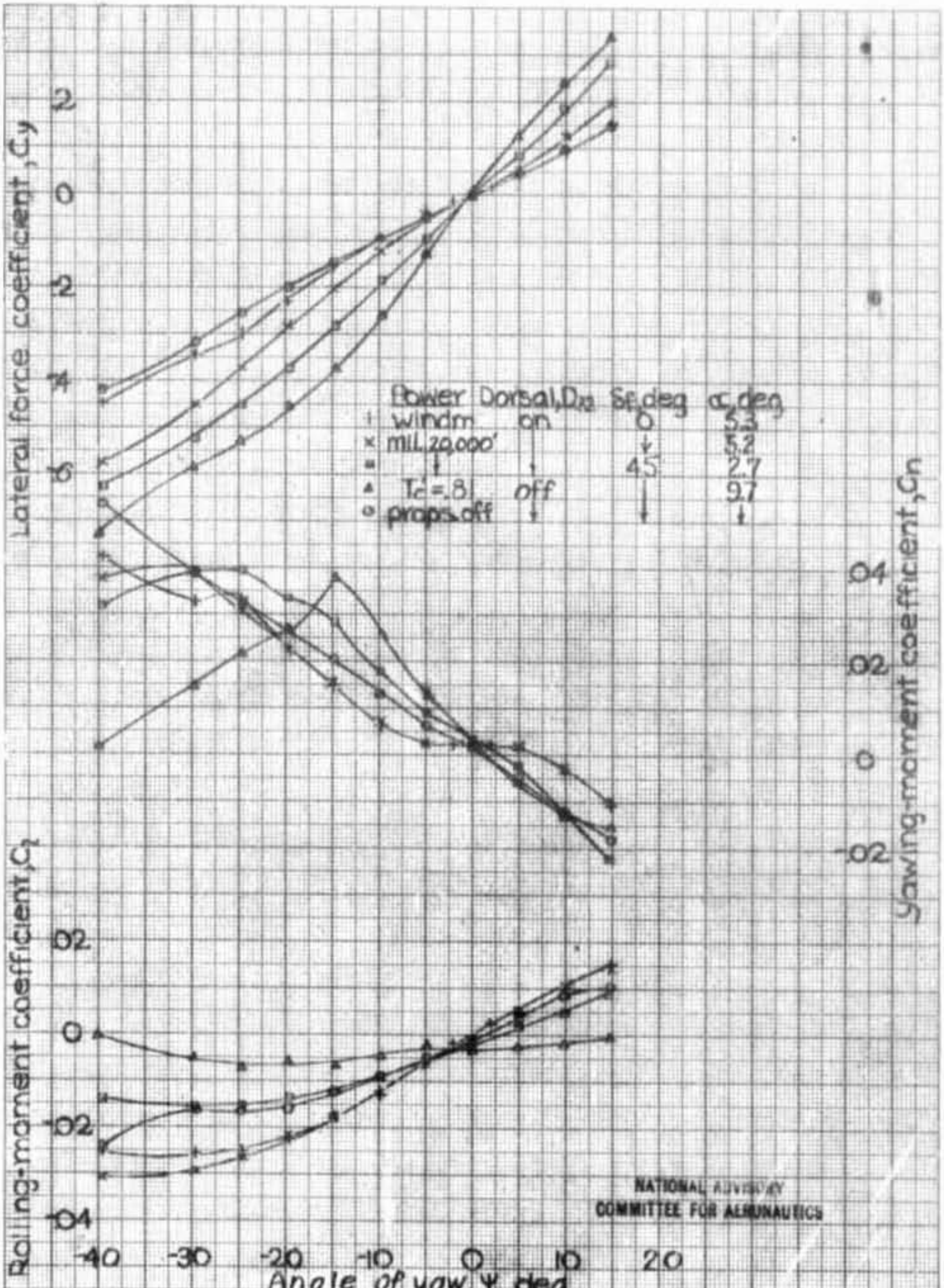

Figure 32-Effect of yaw on the aerodynamic characteristics of the XP-62 model (¼ scale) with vertical tail VR. $\delta_r = 0$.

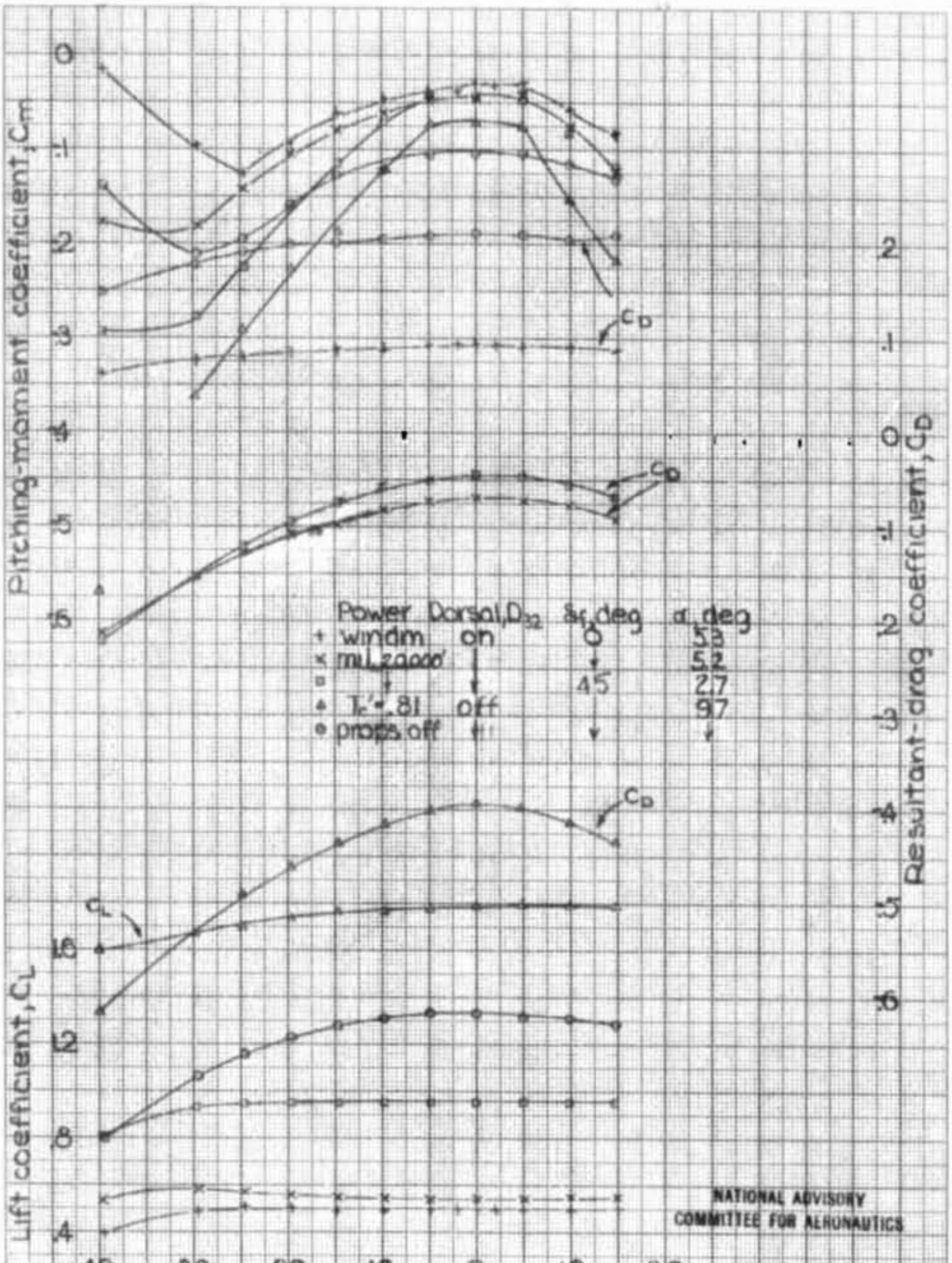

Figure 32.-concluded.

L-779

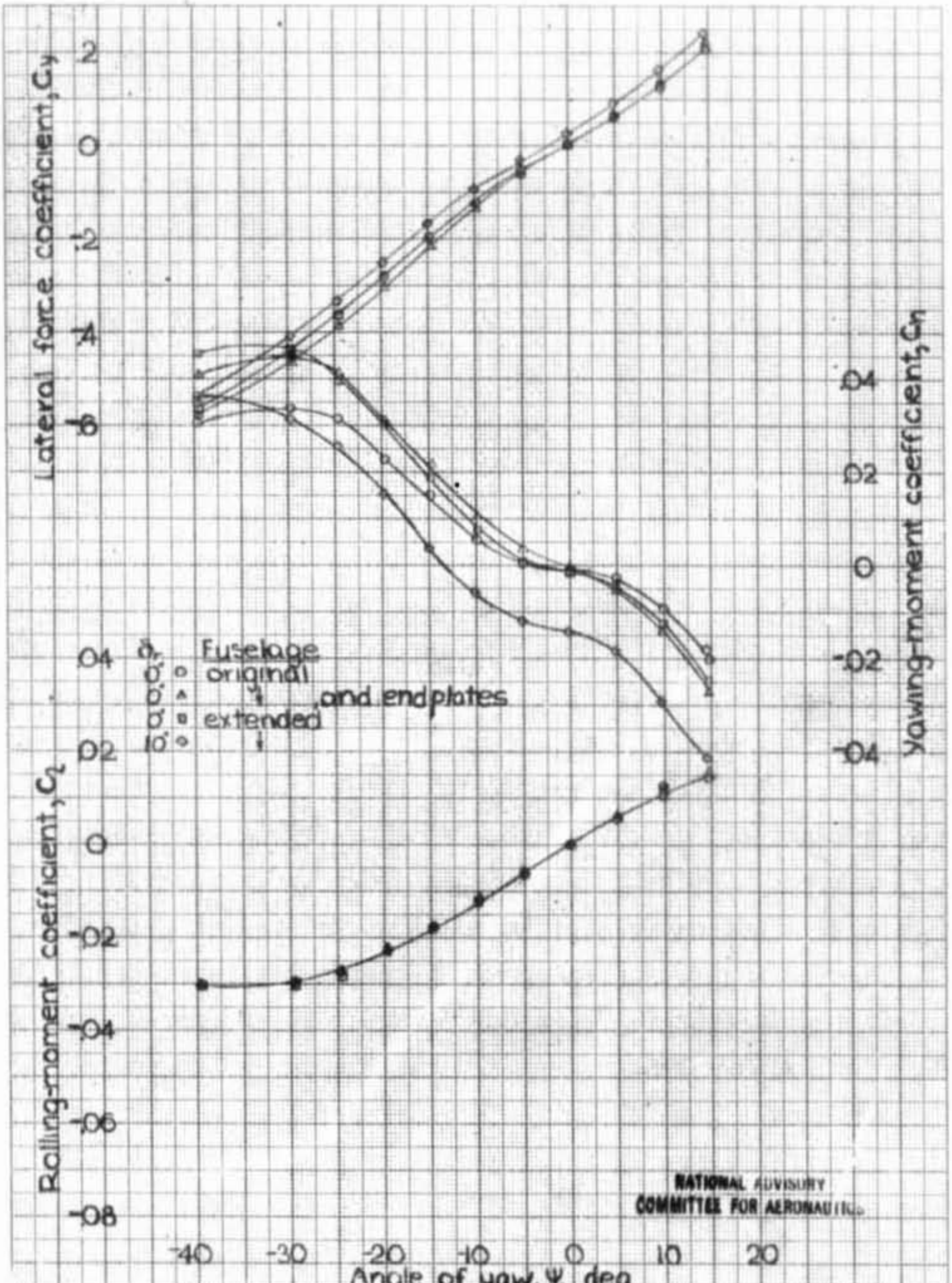

(a) $\delta_a = 0$, Mil. power 20,000, $\alpha = 5.2°$

Figure 33.-Effect of yaw on the aerodynamic characteristics of the XP-62 model (1/5 scale) with vertical tail $V^{11}R^{5}$ and $V^{8}R^{5}t$, Dorsal D_{41}.

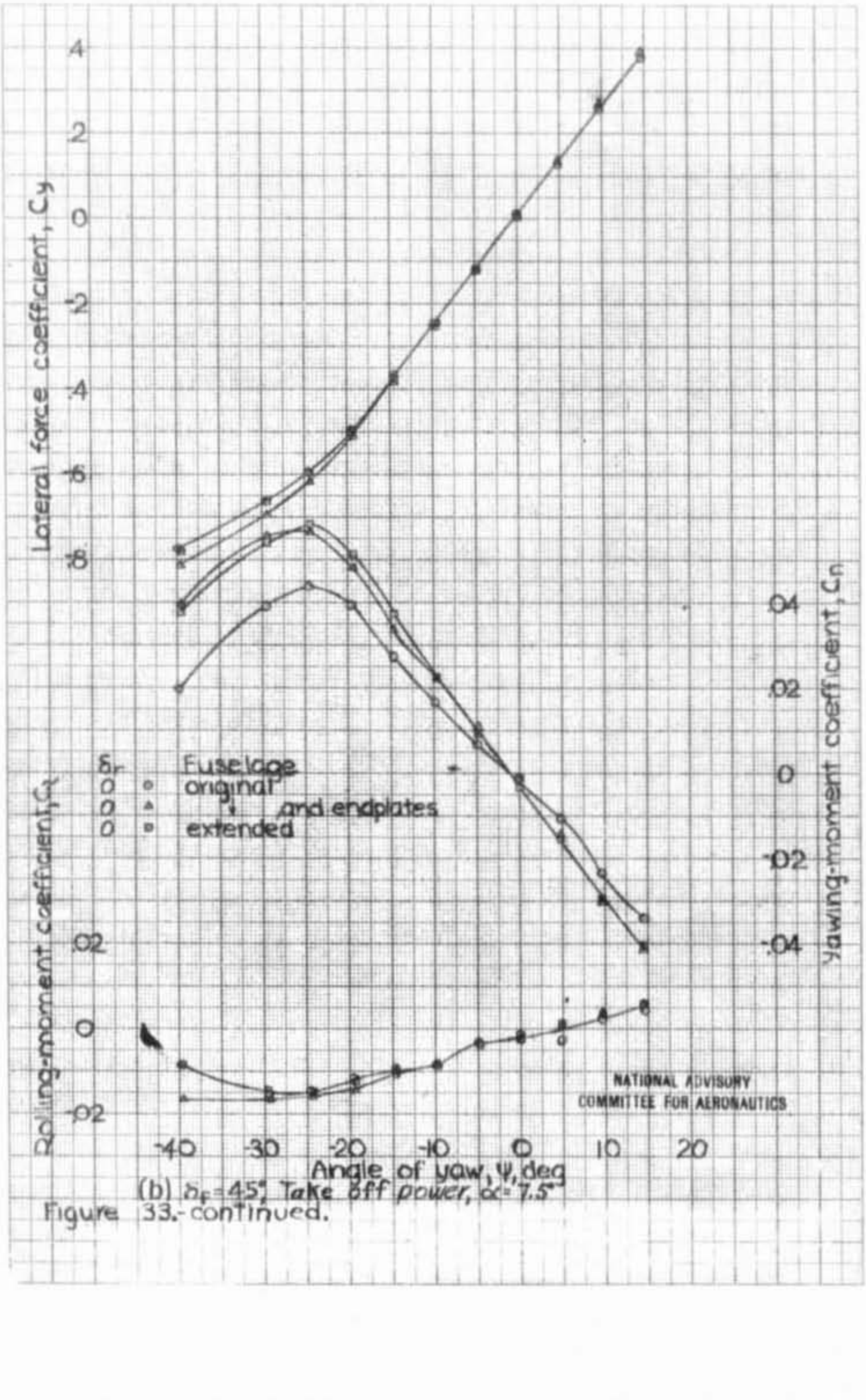

(b) $\delta_f = 45°$, Take off power, $\alpha = 7.5°$

Figure 33.- continued.

L-779

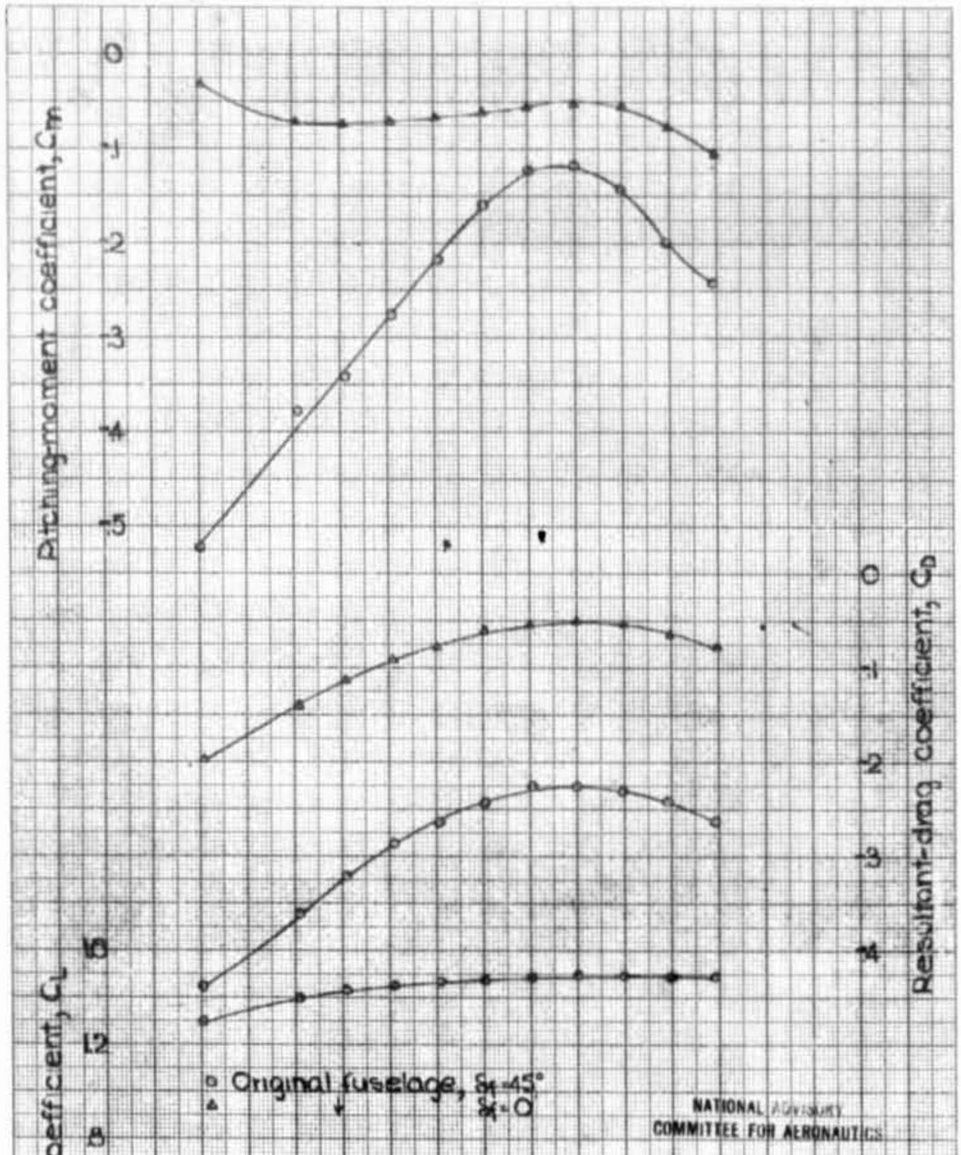

Figure 33.- concluded.

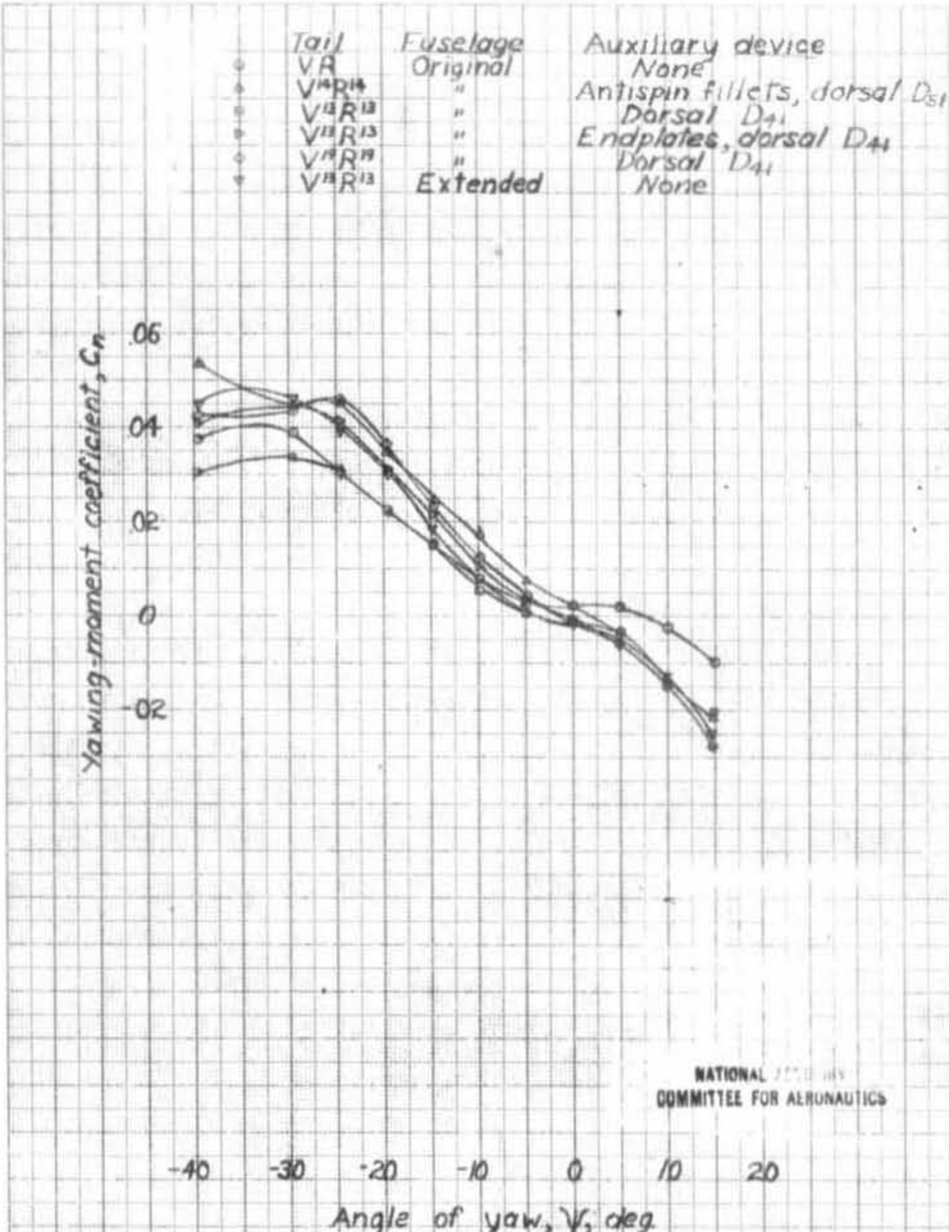

Figure 34.- Comparison of rudder-fixed characteristics of the 1/9-scale model of XP-62 airplane with various vertical tail arrangements $\delta_f = 0°$, $\alpha = 3.2°$, military power at 20,000 ft, $q = 9.21\#/ft^2$, $\delta_r = 0°$.

L-779

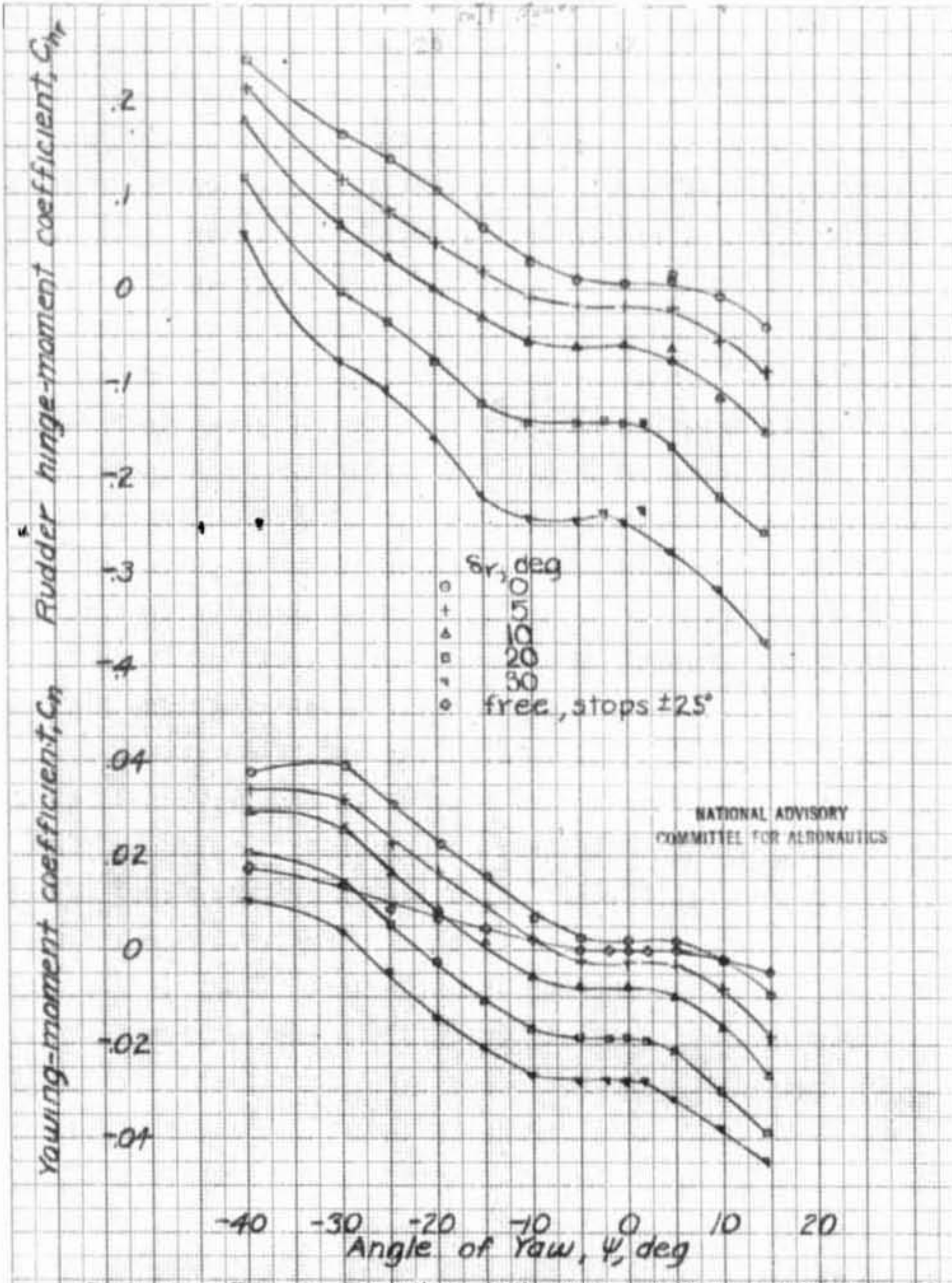

Figure 35-Effect of rudder deflection on the aerodynamic characteristics in yaw of the XP-62 1/8-scale model with vertical tail VR. δ_f=0, military power, α=5.24°, dorsal D_{32}, q=8.21 lbs/sq ft.

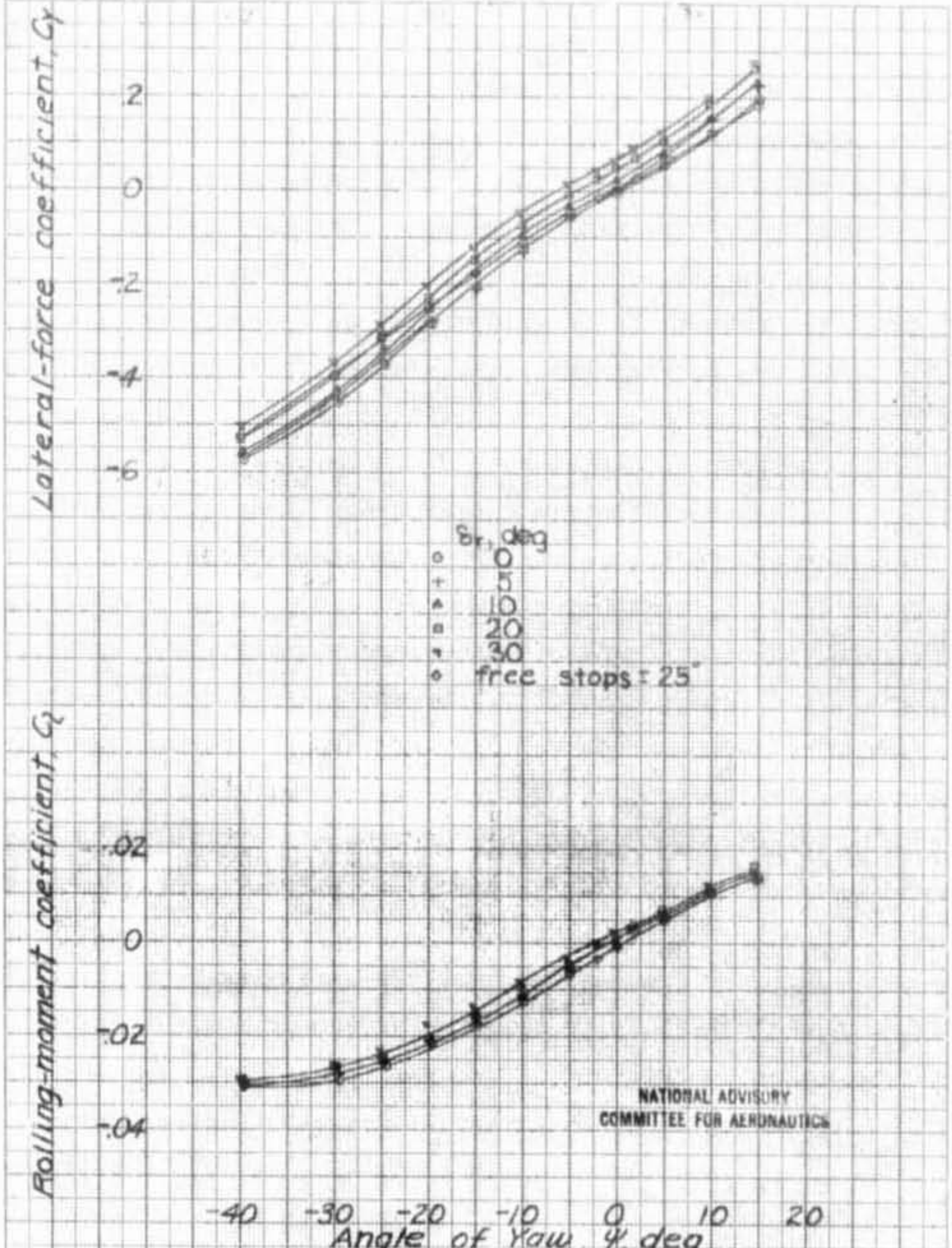

Figure 35.-Continued

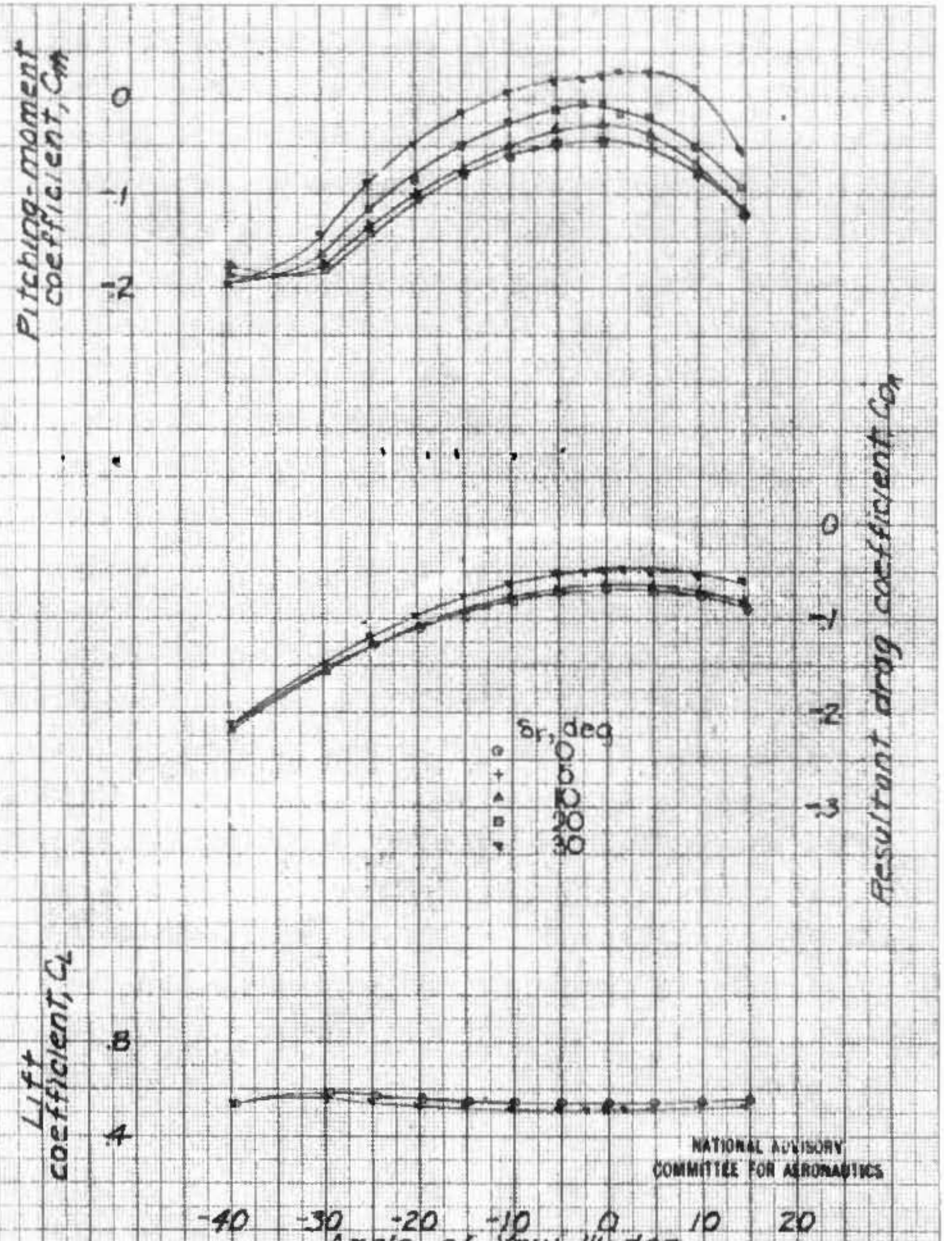

Figure 35. - Concluded.

L-779

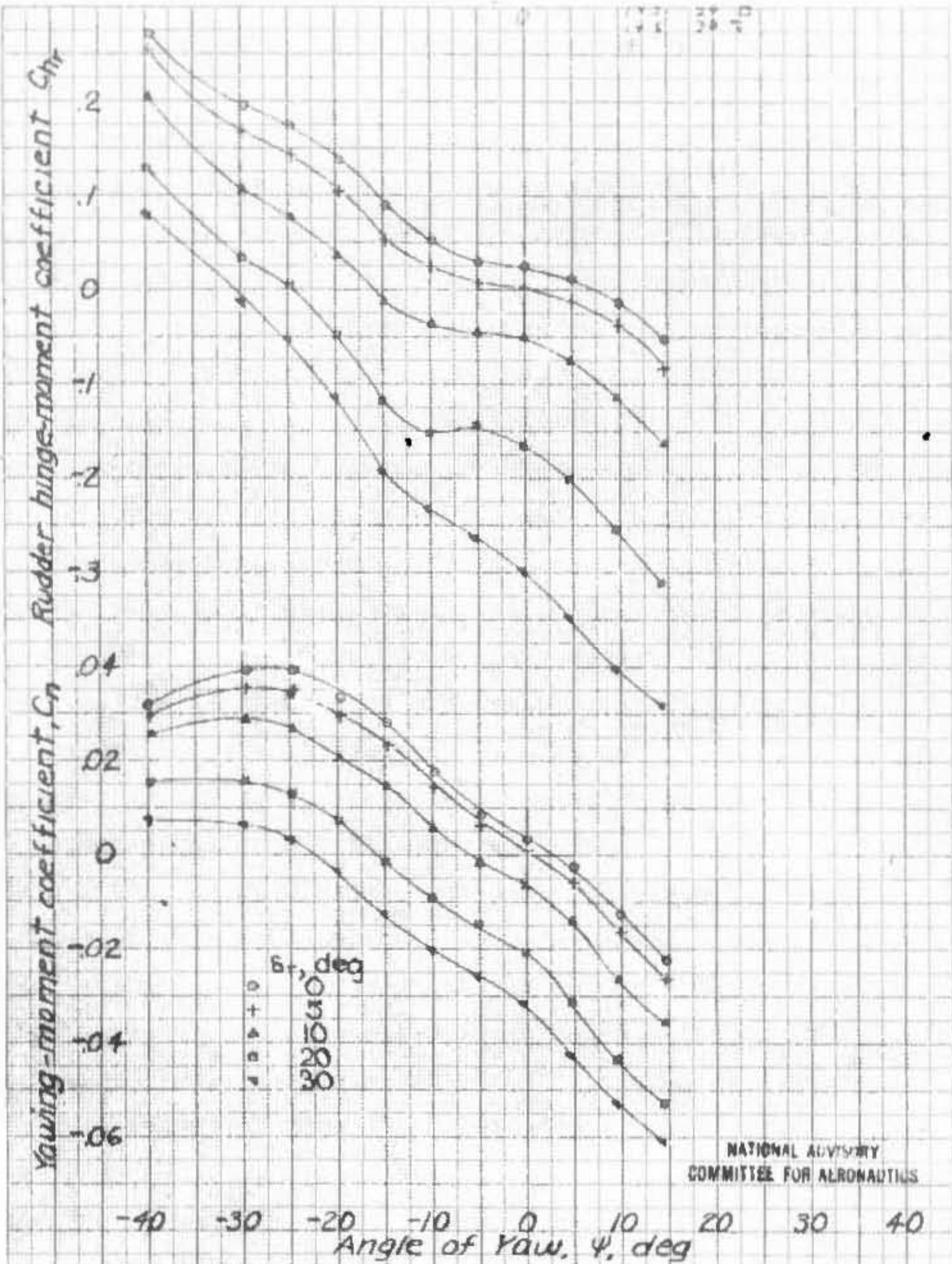

Figure 36.-Effect of rudder deflection on the aerodynamic characteristics in yaw of the XP-62 1/8-scale model with vertical tail VR. δ_f -45°, military power, α = 2.7°, dorsal D32, L.G. up, q = 9.21 lbs/sq ft,

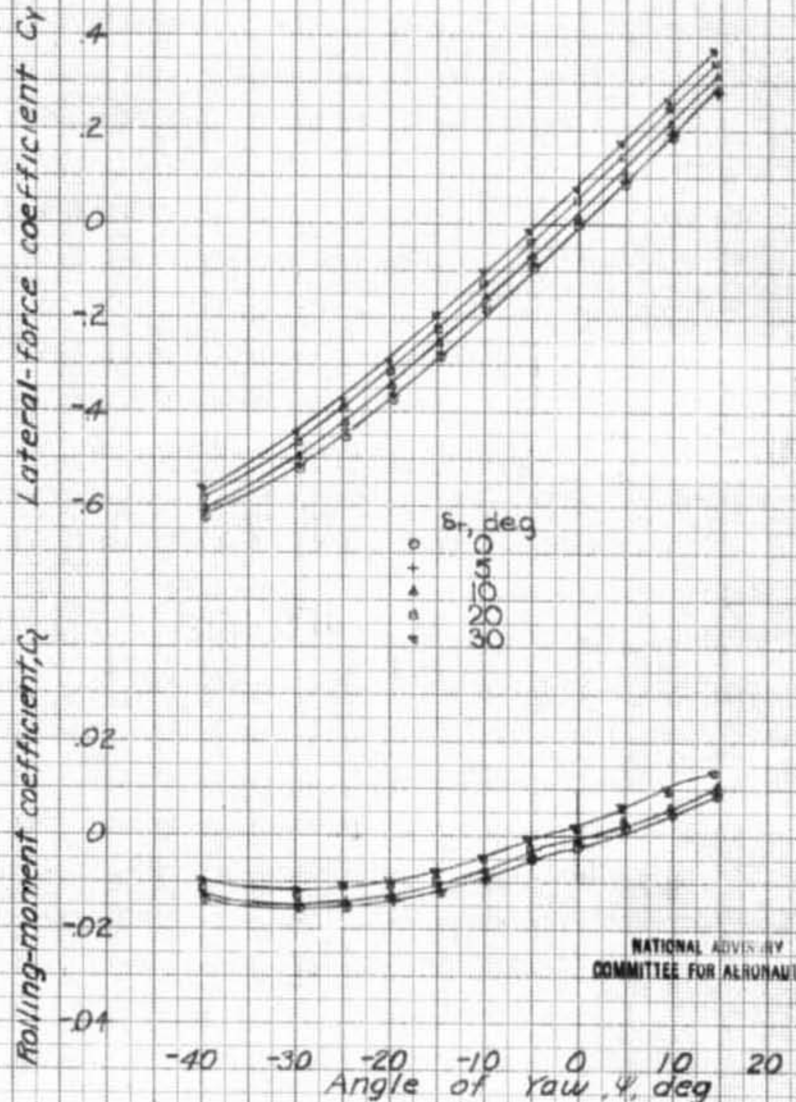

Figure 36.-Continued.

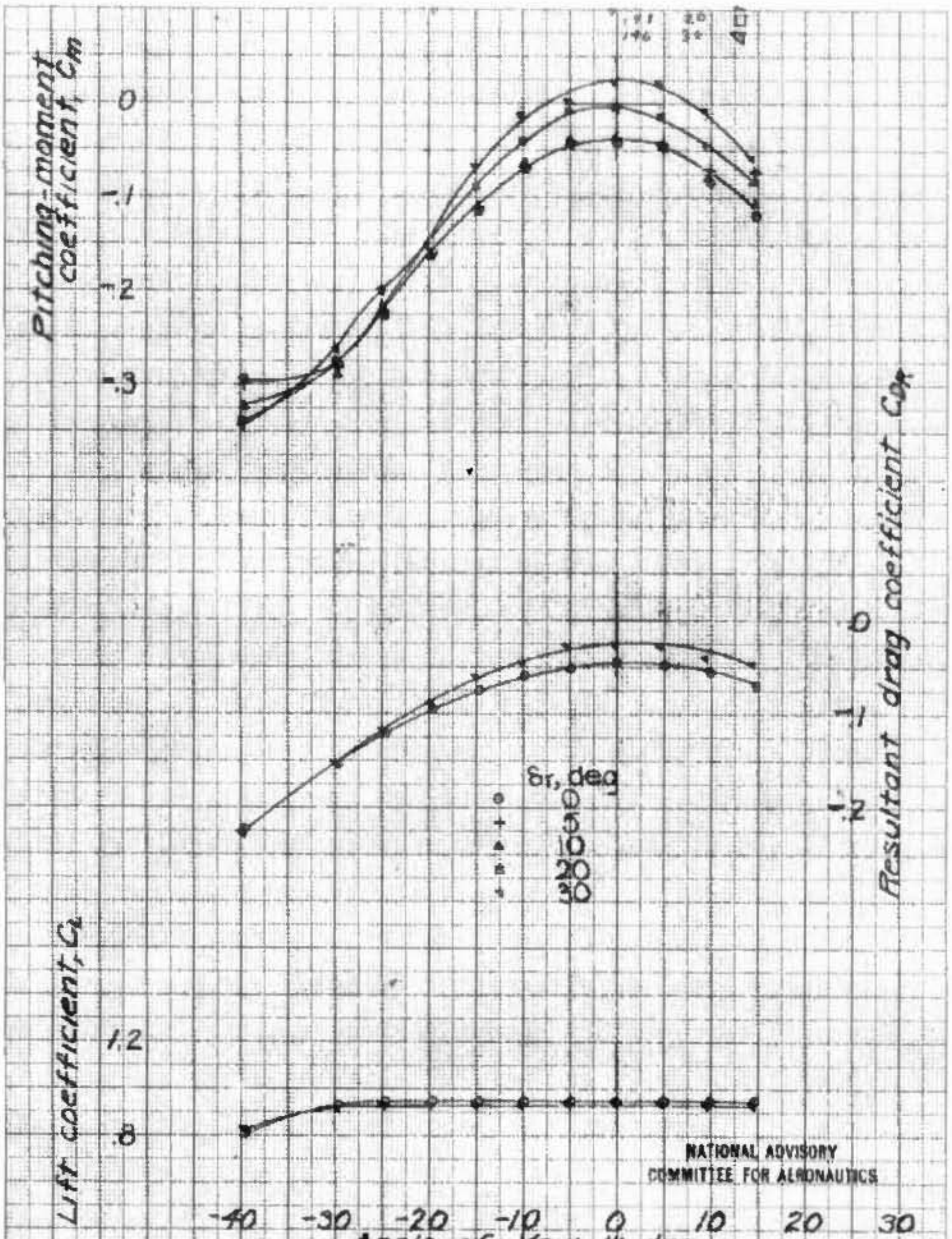

Figure 36.-Concluded

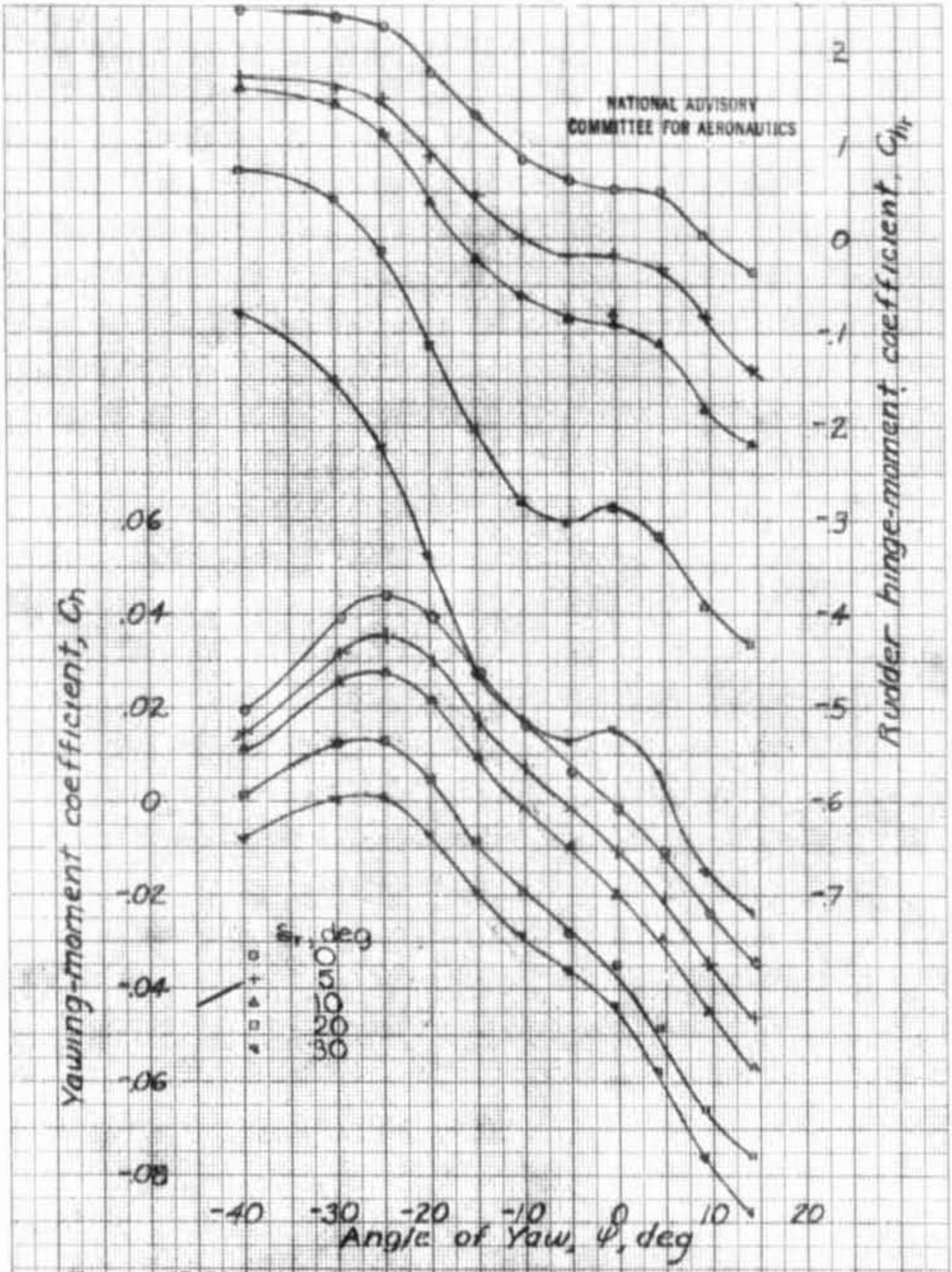

Figure 37.-Effect of rudder deflection on the aerodynamic characteristics in yaw of the XP-62 model ($\frac{1}{4}$-scale) with vertical tall $V^{15}R^{15}$ δ_f=45°, Take off power, Dorsal D_{11}, α=1.5°.

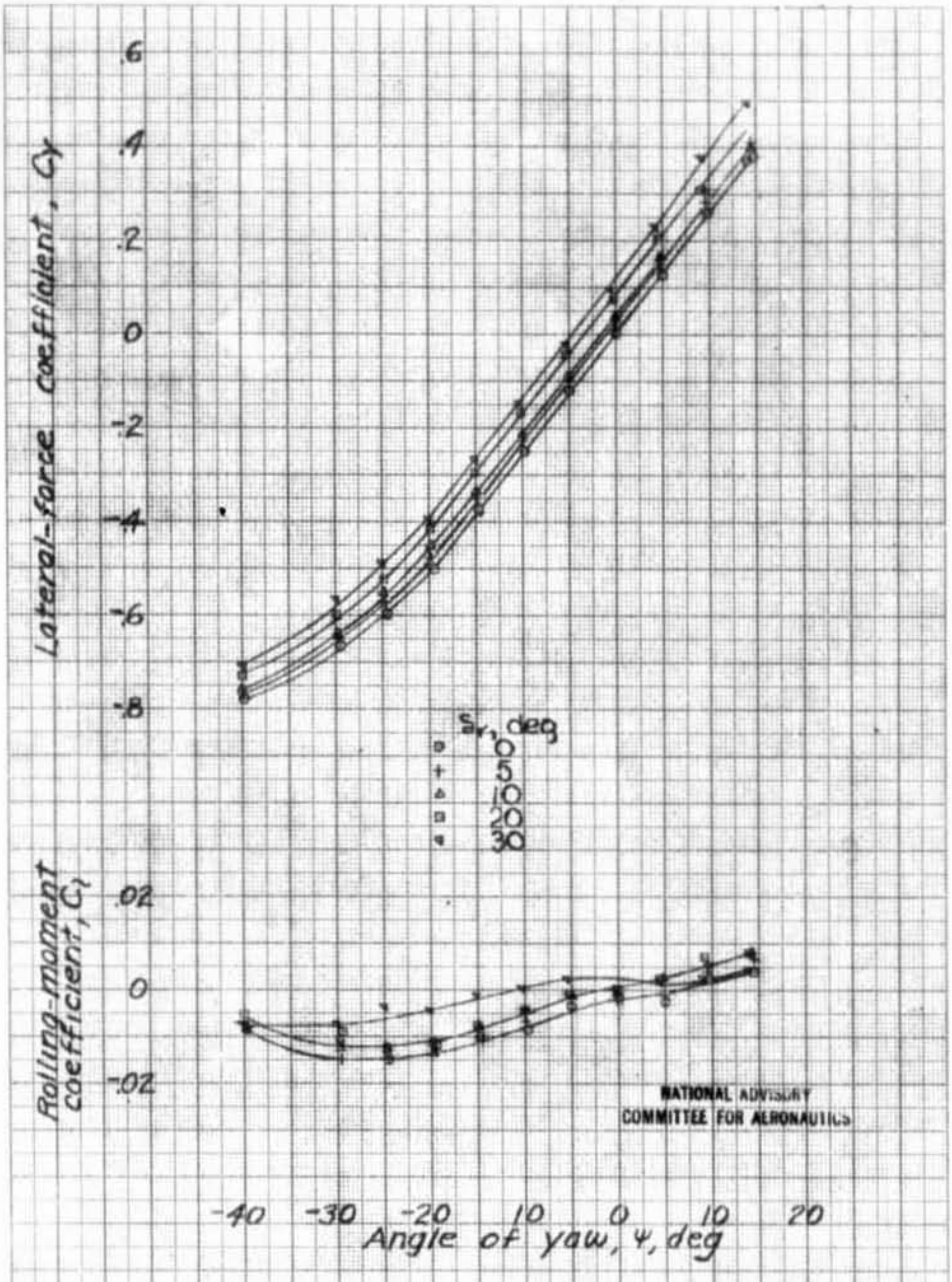

Figure 37.- Continued.

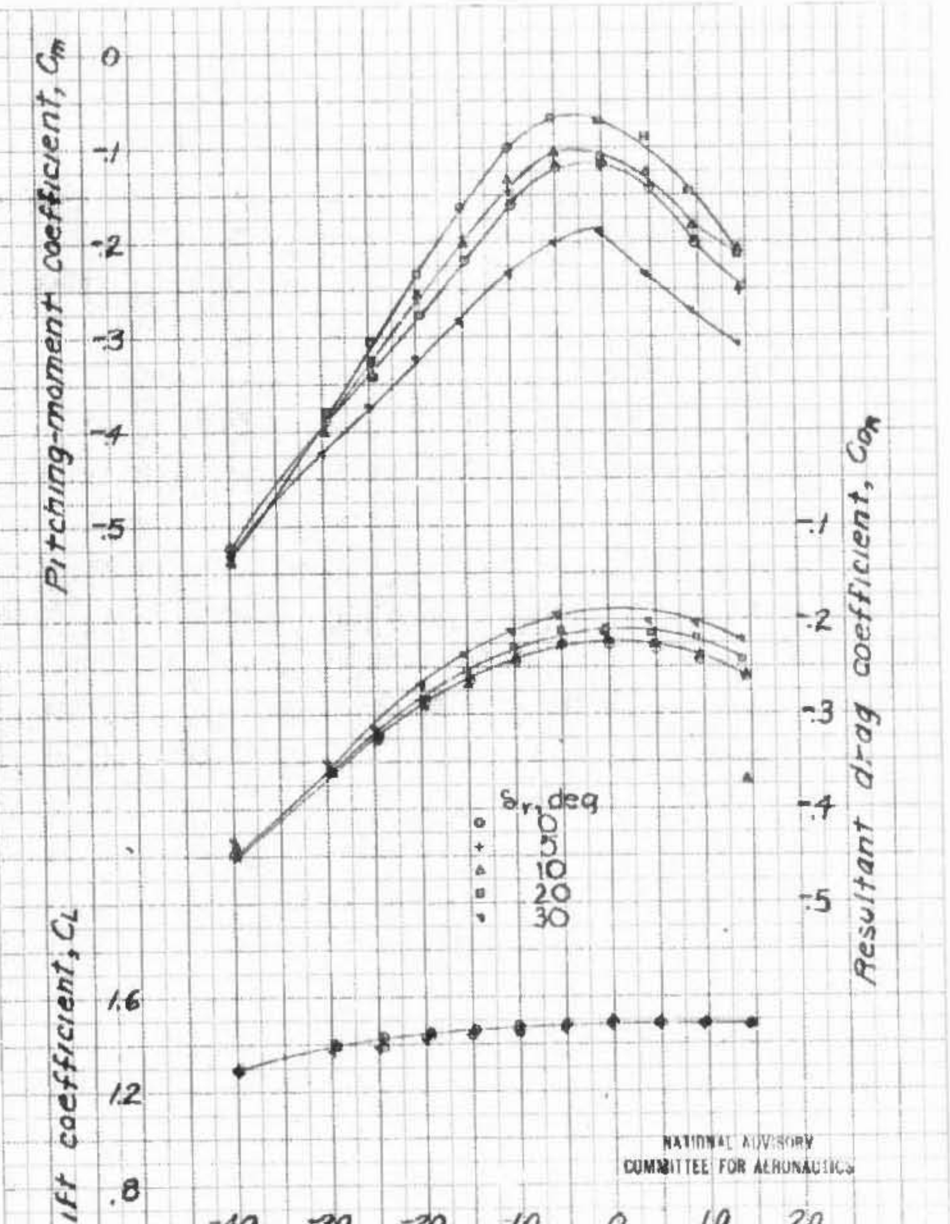

Figure 37.- concluded.

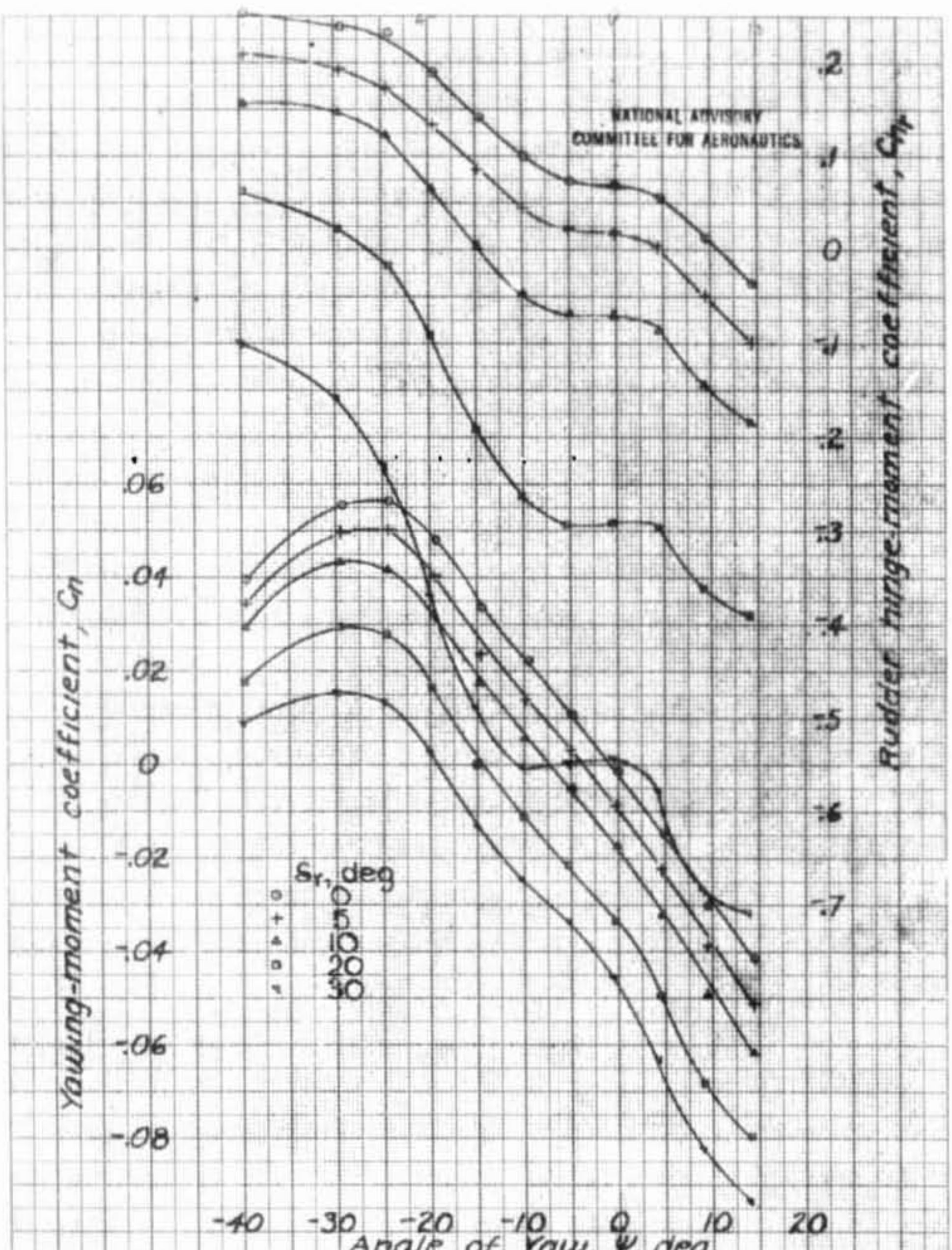

Figure 38-Effect of rudder deflection on the aerodynamic characteristics in yaw of the XP-62 model (1/4 scale) with vertical tail V''R'' and endplates on horizontal tail. δf=45, Take-off power, Dorsal D11, α=7.5°.

L-779

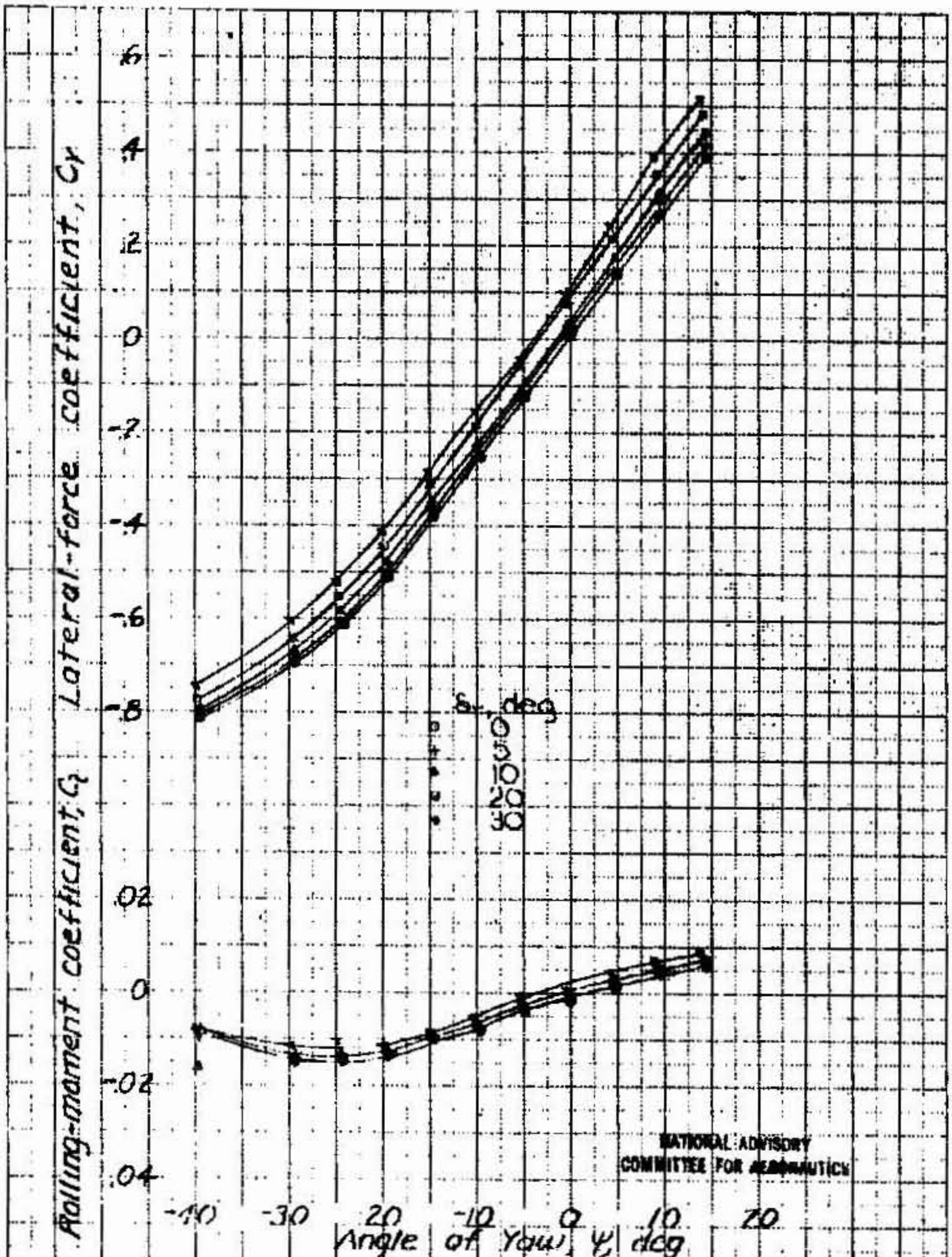

Figure 28. continued.

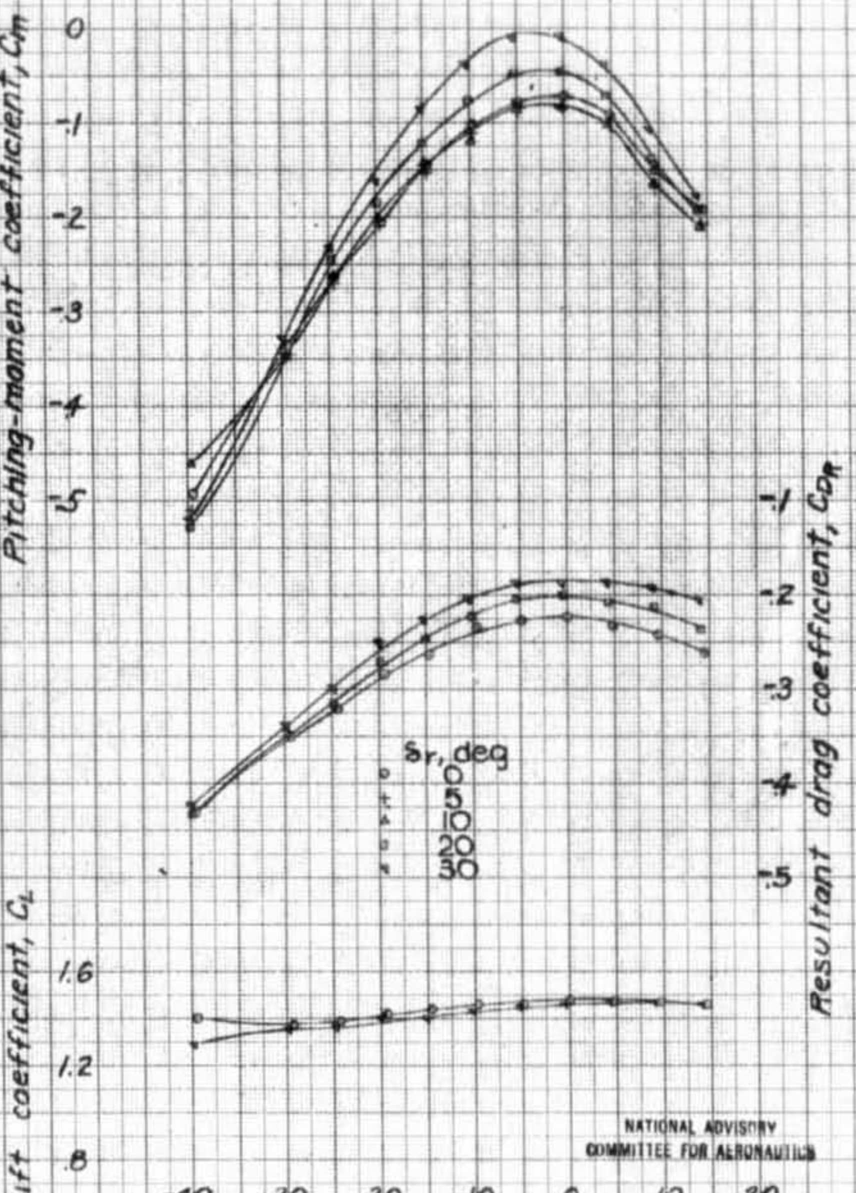

Figure 38.- concluded.

L-779

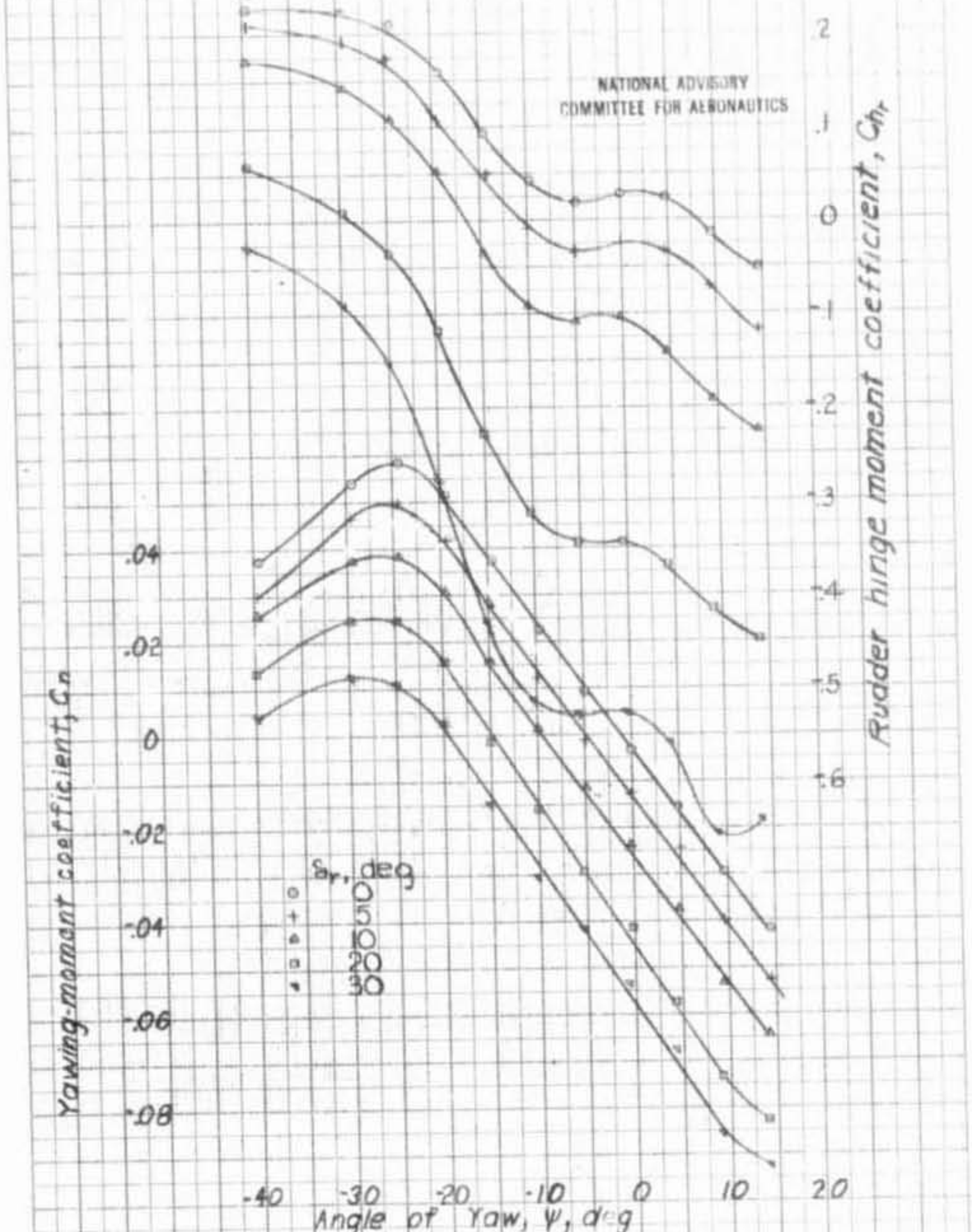

Figure 39.-Effect of rudder deflection on the aerodynamic characteristics in yaw of the XP-62 model (1/4 scale) with vertical tail $V^{13}R^{13}E$ (fuselage extended 4"). $\delta_f = 45°$, take off power, Dorsal D_{41}, $\alpha = 7.5°$.

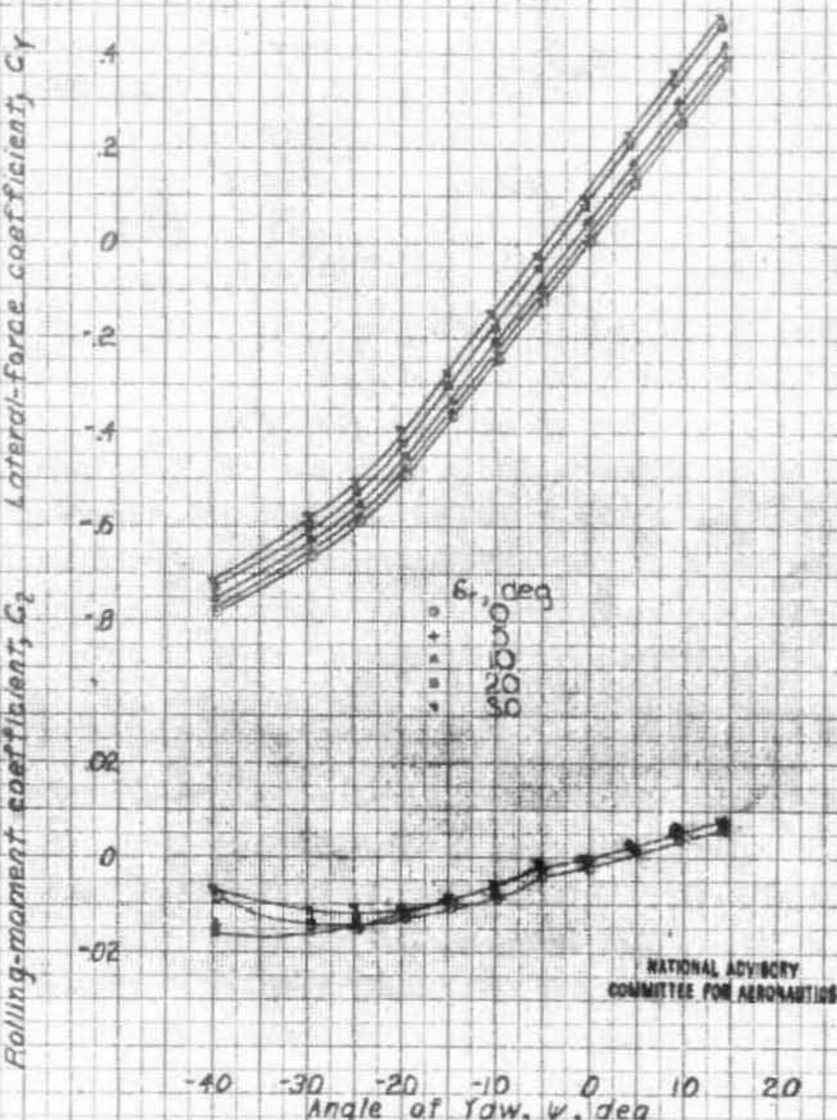

Figure 39.-continued.

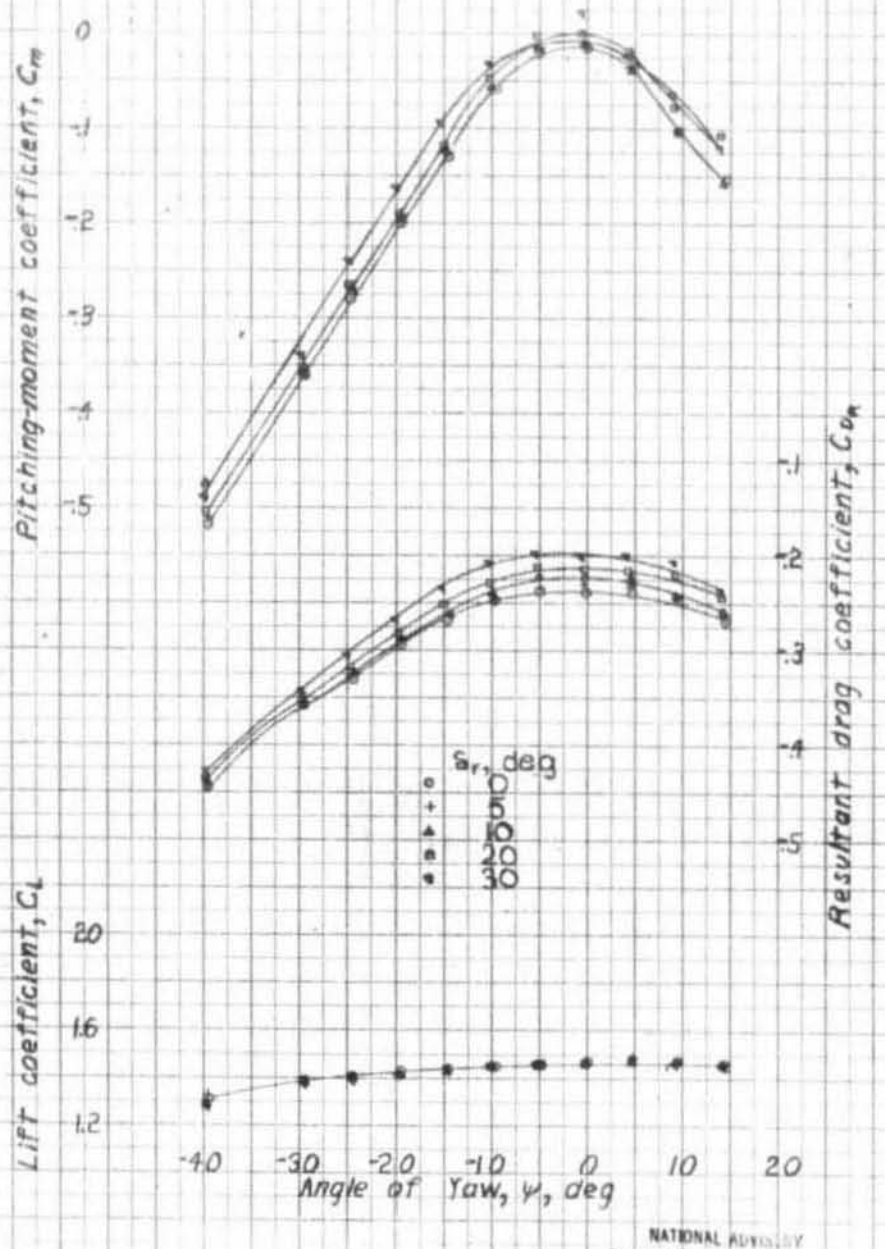

Figure 39.- concluded.

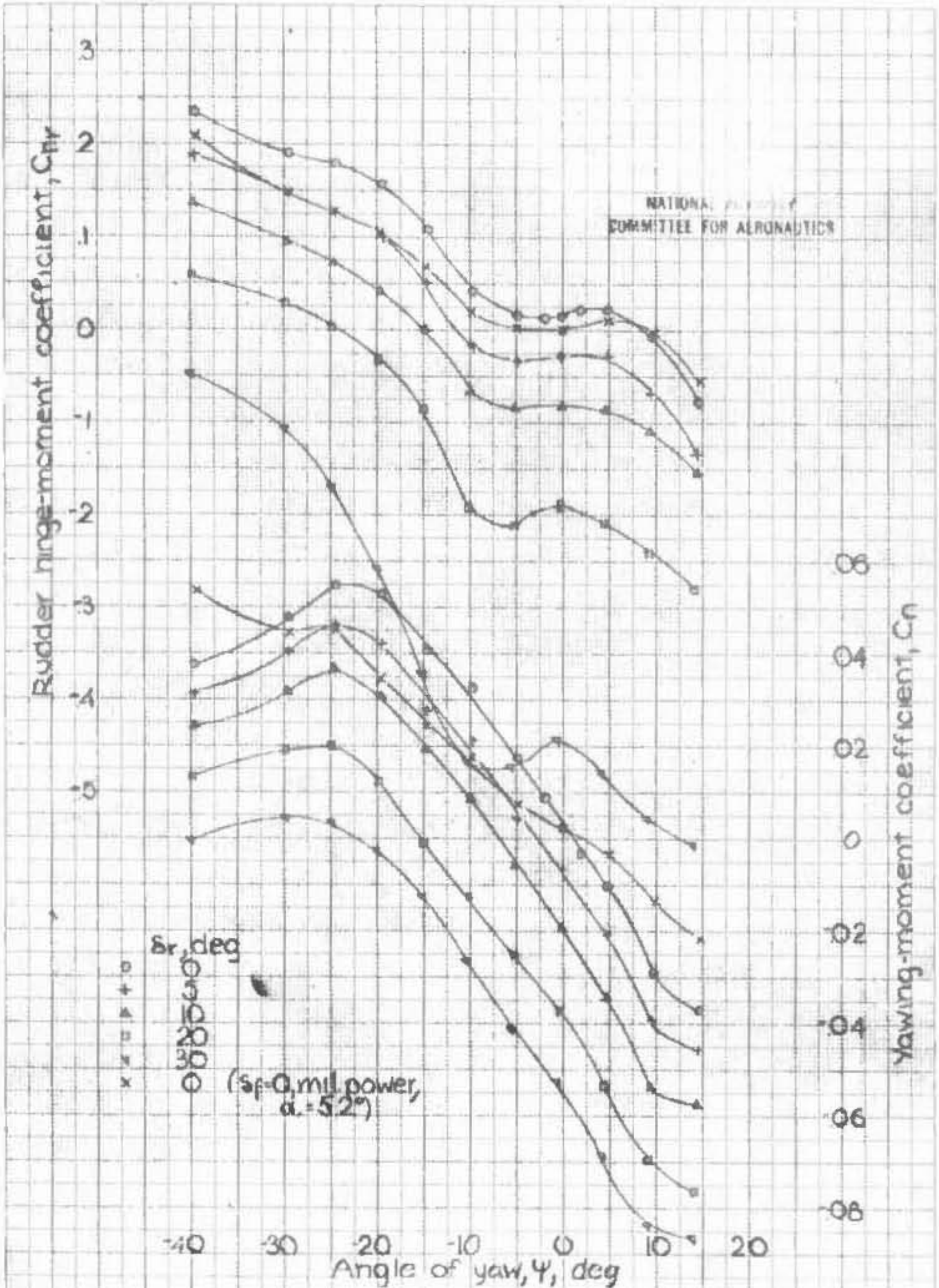

Figure 40.-Effect of rudder deflection on the aerodynamic characteristics in yaw of the XP-62 model (1/4 scale) with vertical tail $V^{14}R^{14}$. $\delta_f=45°$. Take-off power, Dorsal D_{5la}. Anti-spin fillets, α=7.5°.

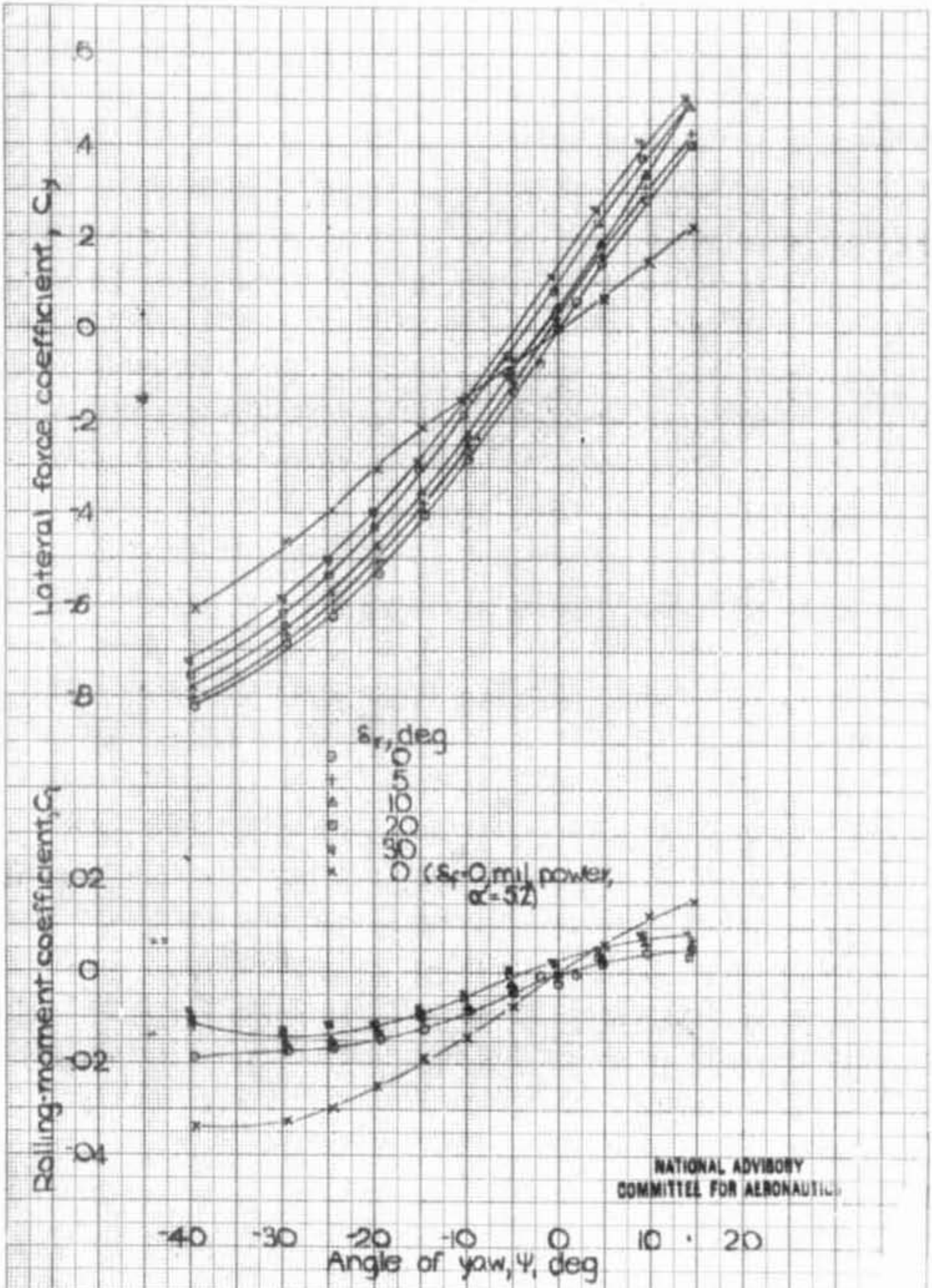

Figure 40.-continued

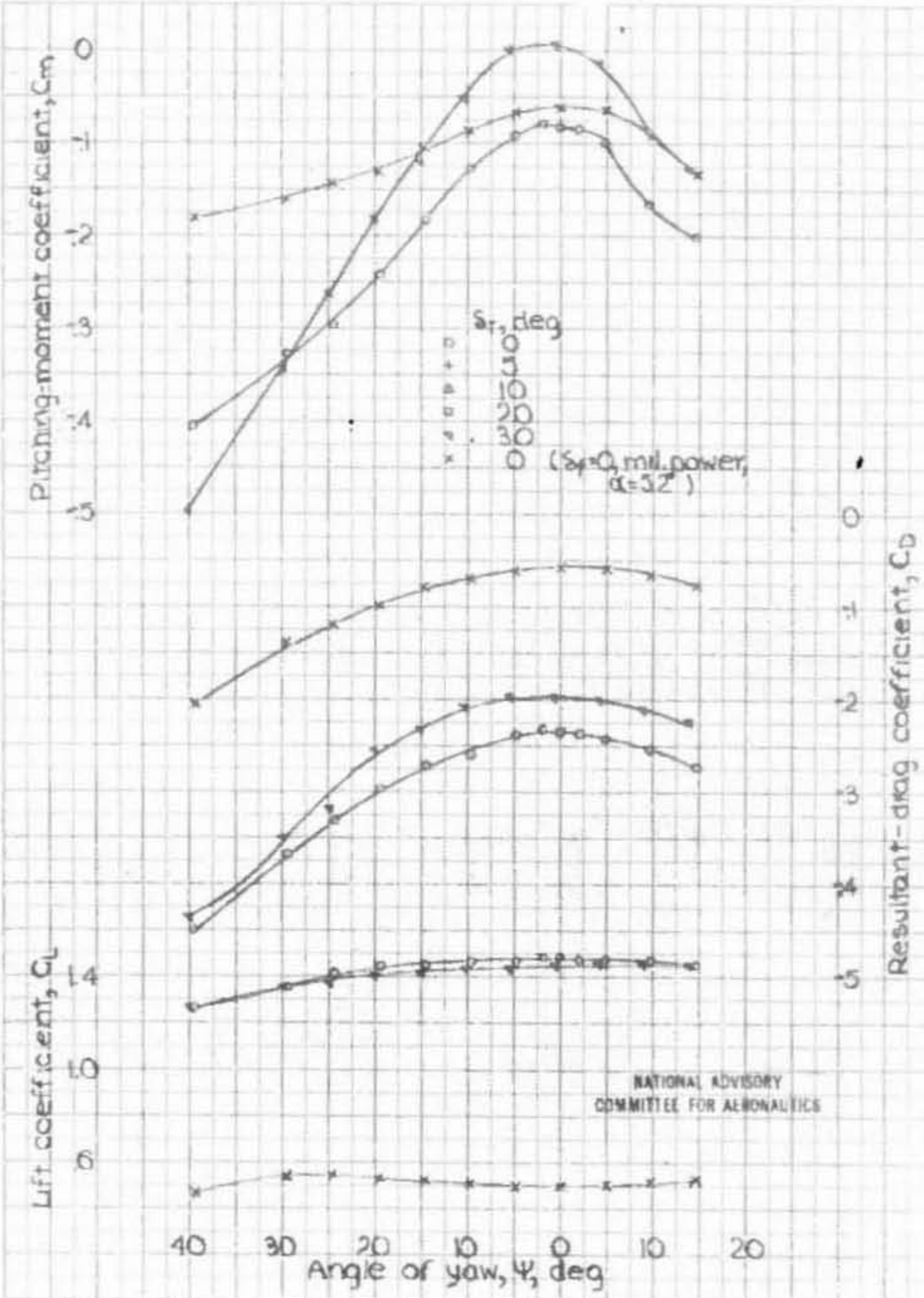

Figure 40.-concluded.

L-779

L-779

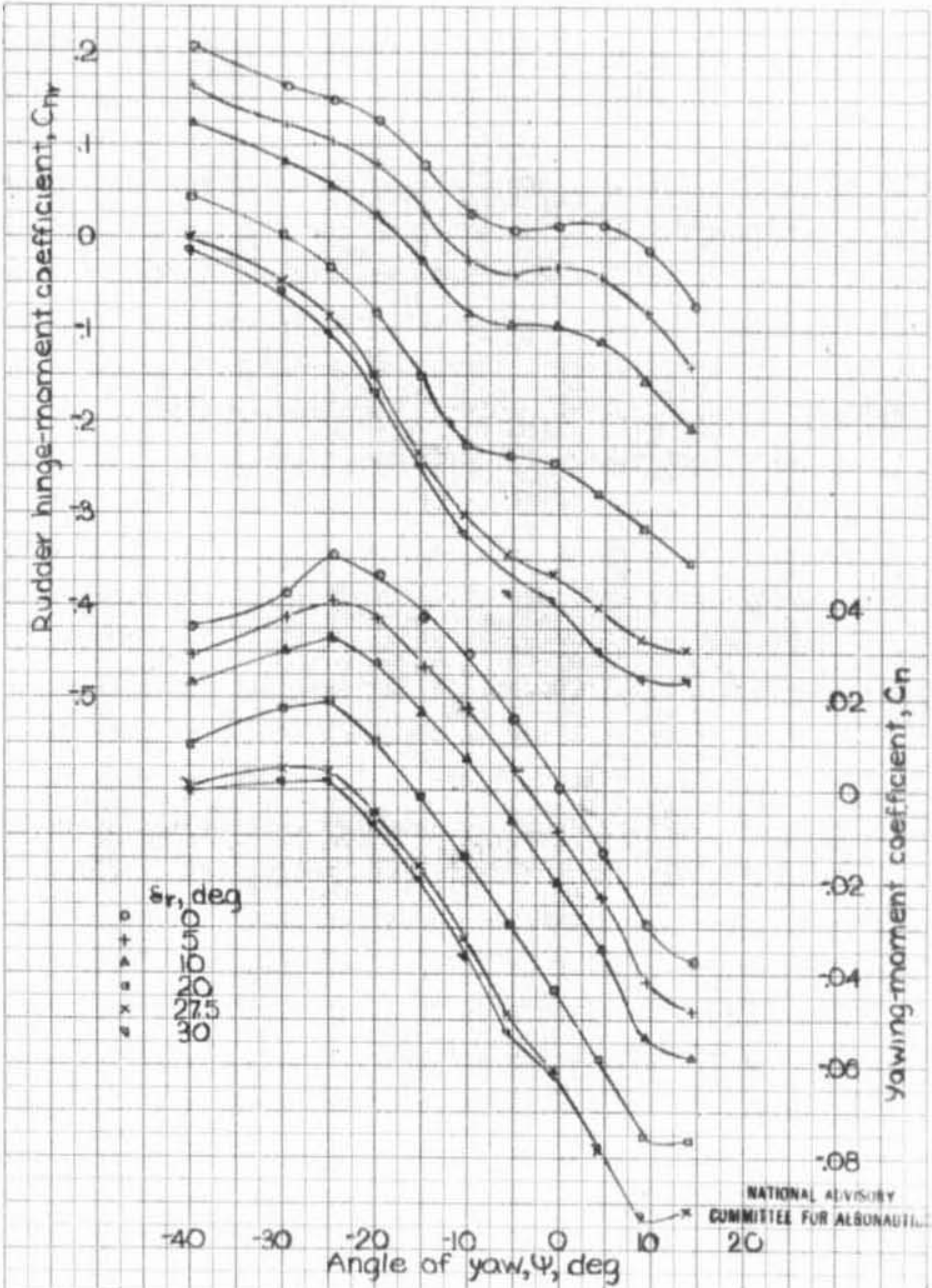

Figure 41.Effect of rudder deflection on the aerodynamic characteristics in yaw of the XP-62 model(1/4 scale) with vertical tail $V^{16}R^{16}$ δ_f = 45° Take-off power Dorsal 51a. Anti-spin fillets α = 2.5°.

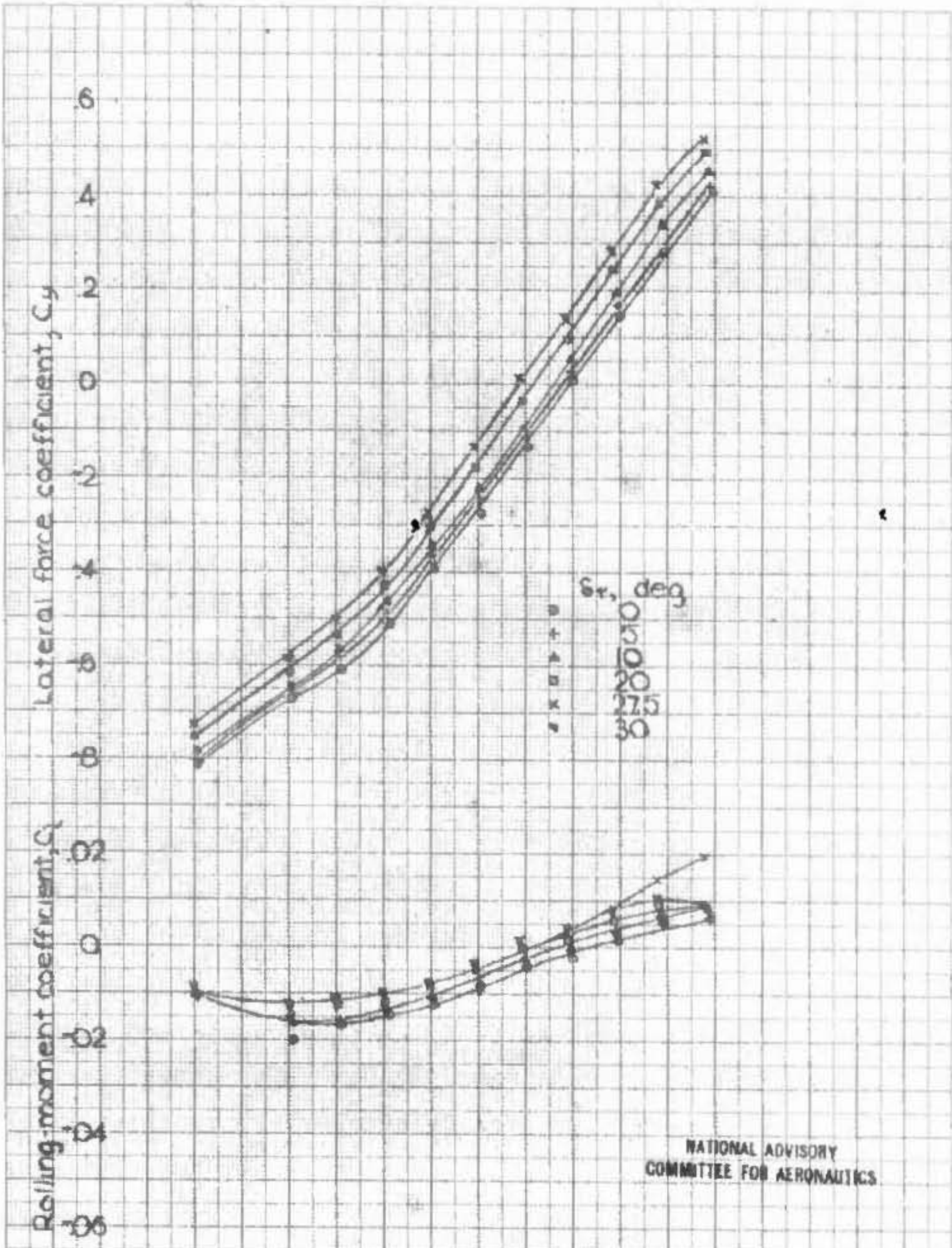

Figure 41.-continued

L-779

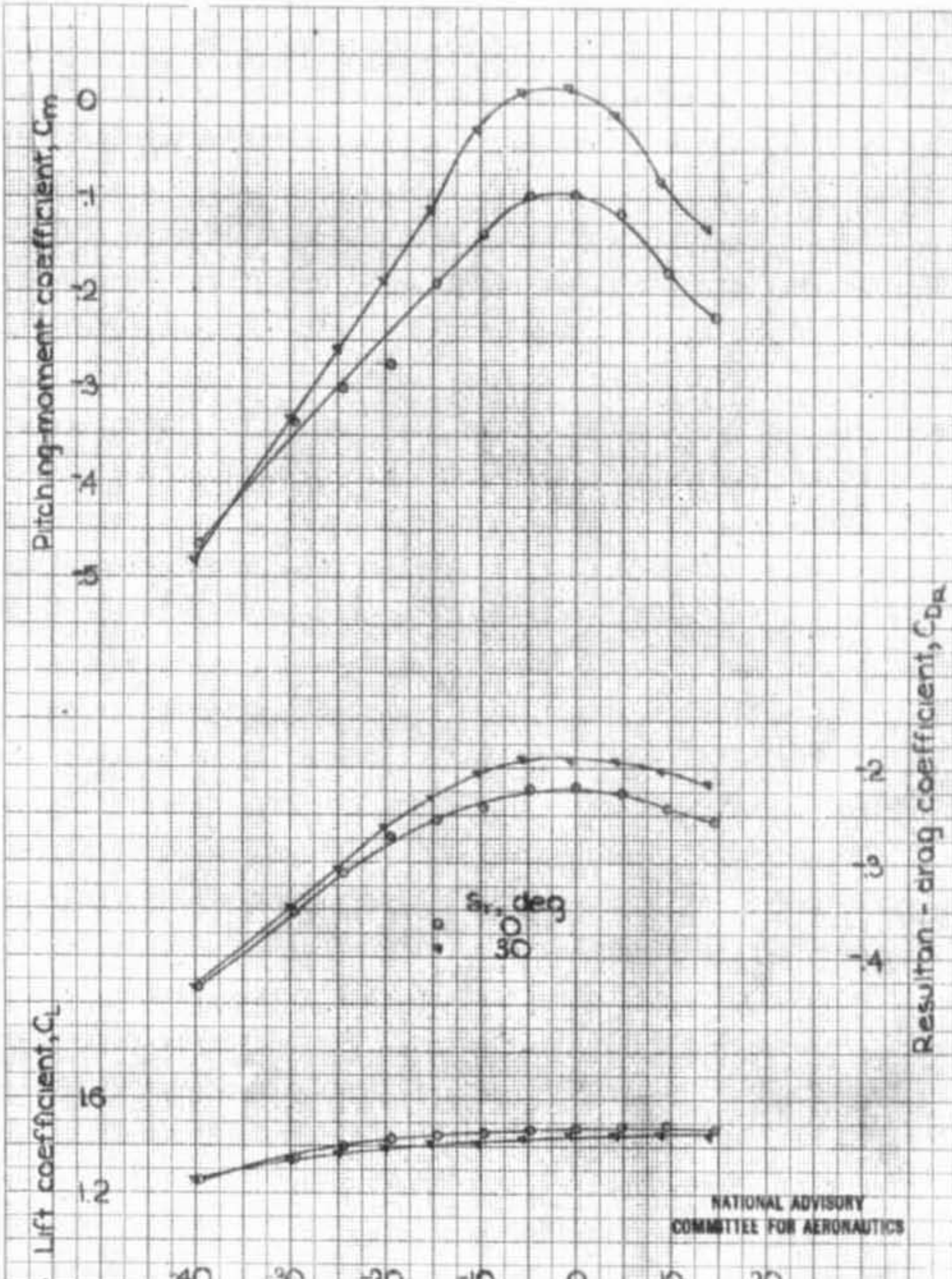

Figure 41-concluded

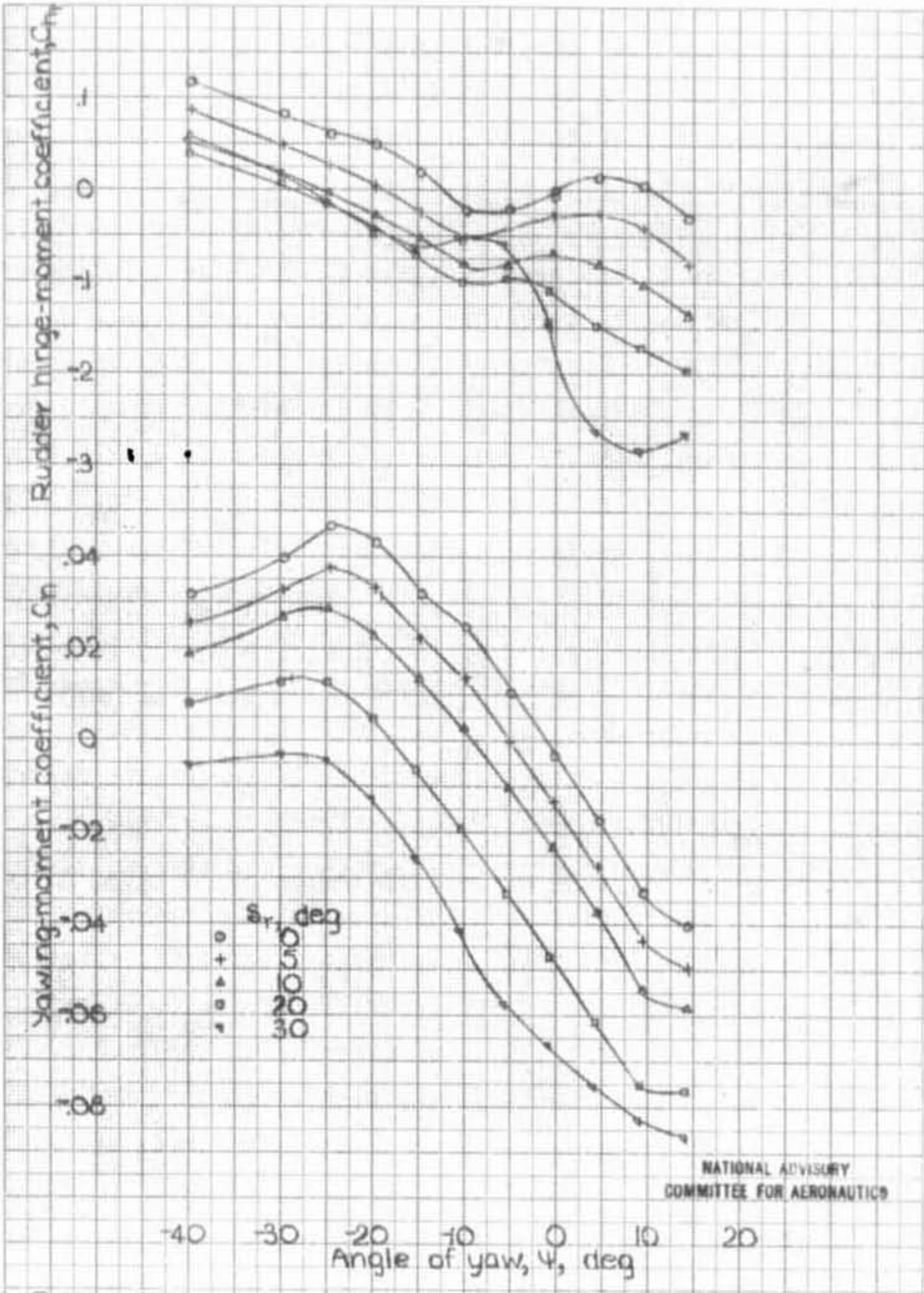

Figure 42.-Effect of rudder deflection on the aerodynamic characteristics in yaw of the XP-62 model (1/4 scale) with vertical tail $V^{18}R^{18}$. δ_f=45°, Take-off power, Dorsal 51a, Anti-spin fillets, α=7.5°.

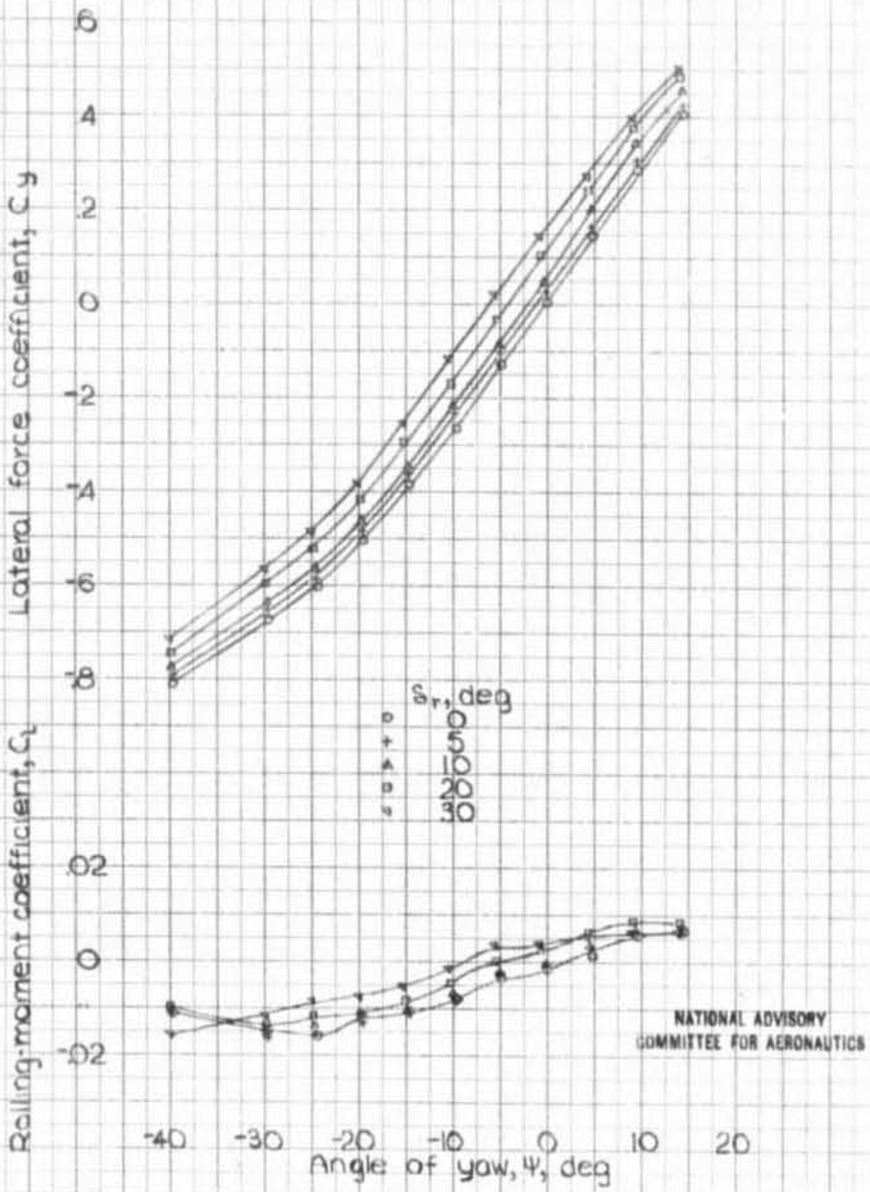

Figure 42 continued

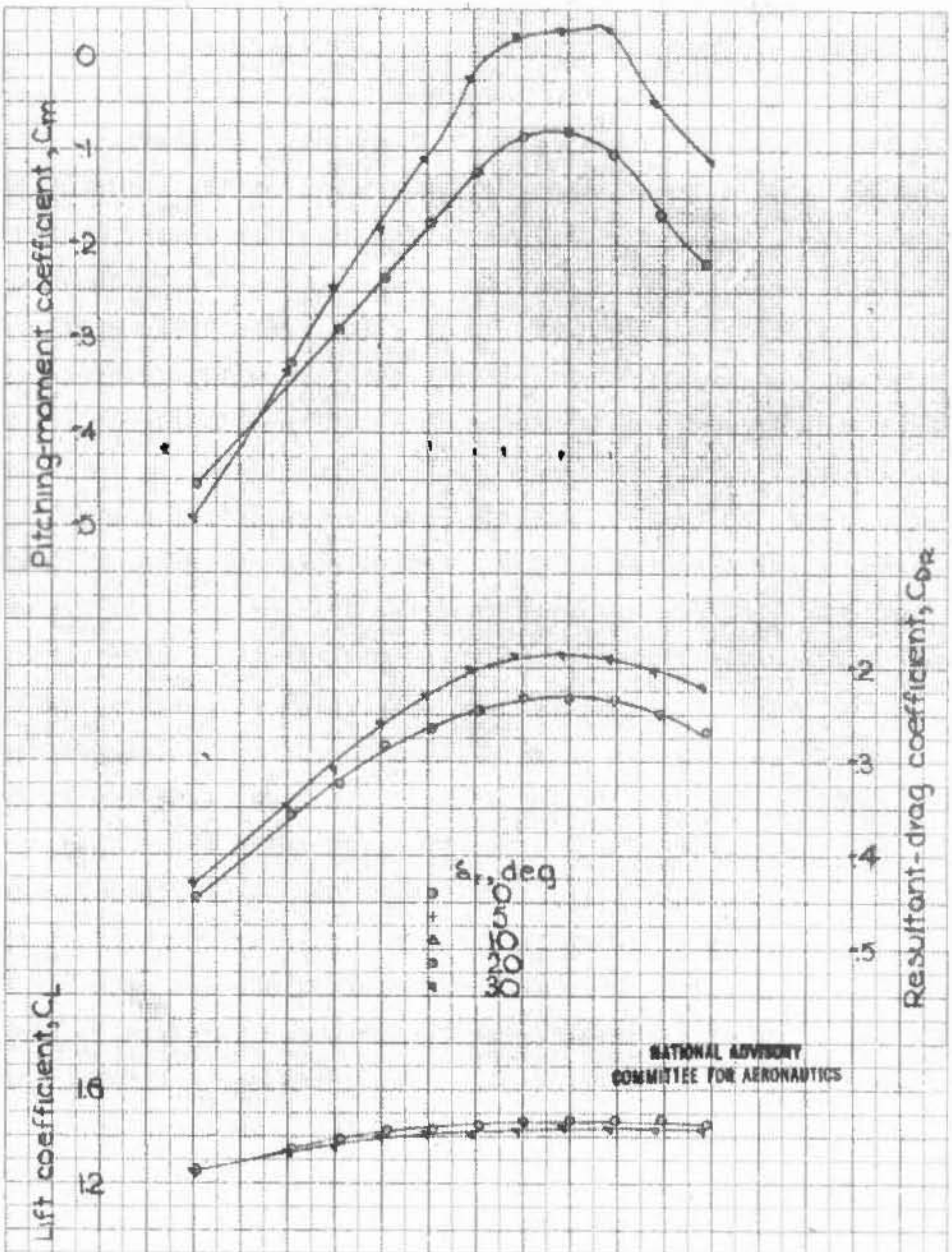

Figure 42.- Concluded.

L-779

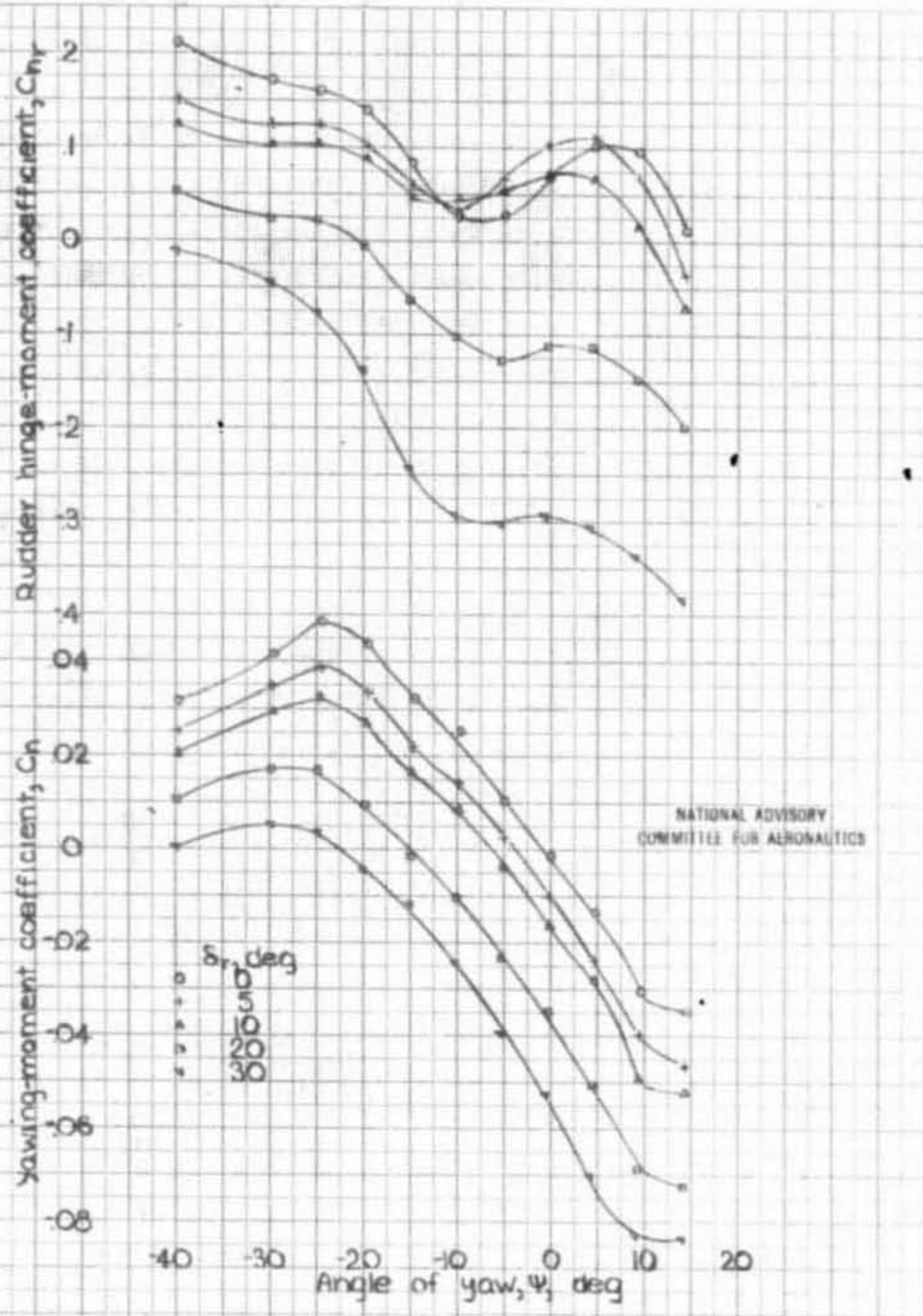

Figure 43.- Effect of rudder deflection on the aerodynamic characteristics in yaw of the XP-62 model (1/4 scale) with vertical tail $V^{14}R^{14}$ (bevel trailing edge). δ_f=45° Take-off power. α=7.5° Dorsal D_{5la}.

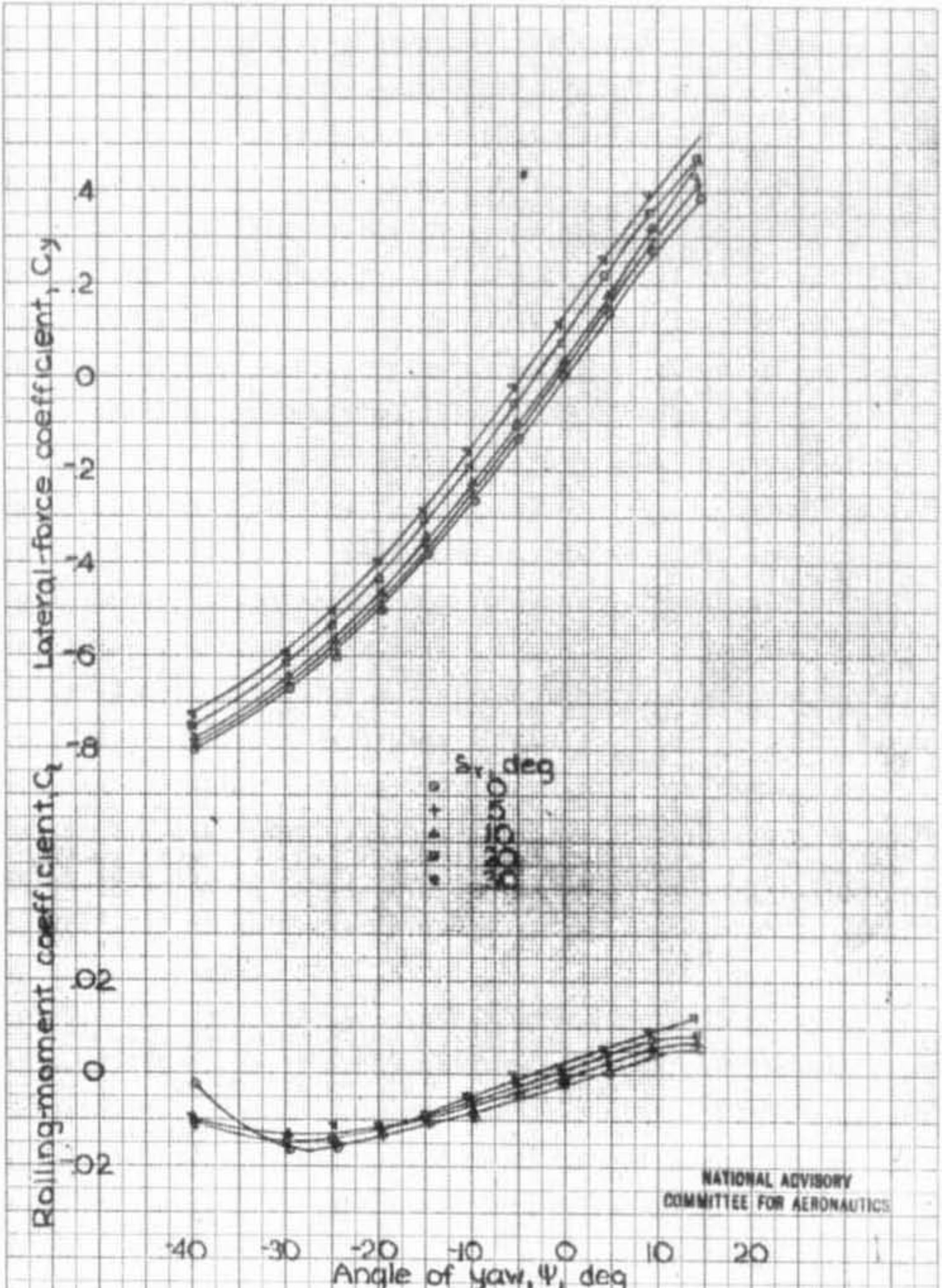

Figure 43.- continued.

L-779

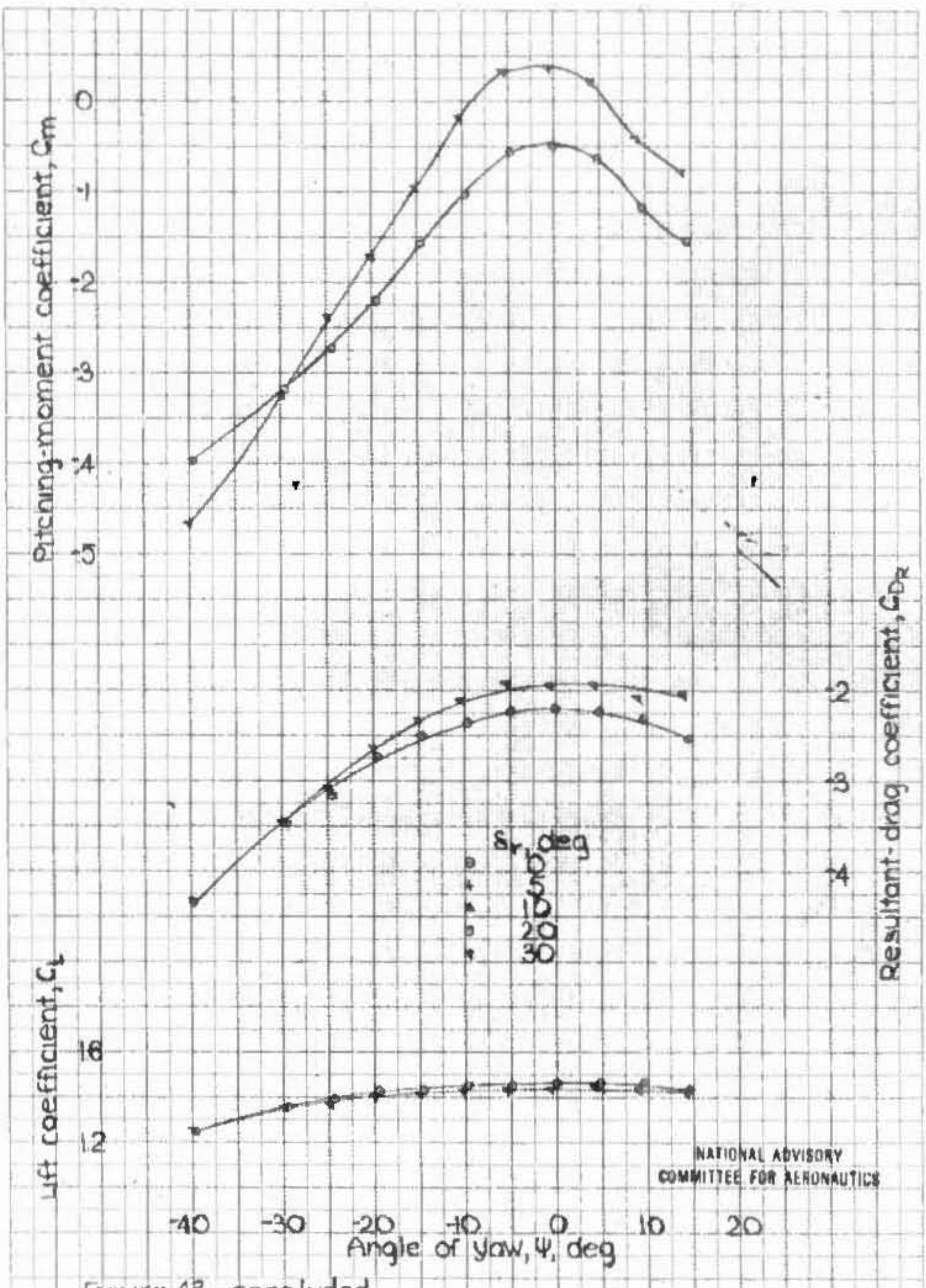

Figure 43.- concluded.

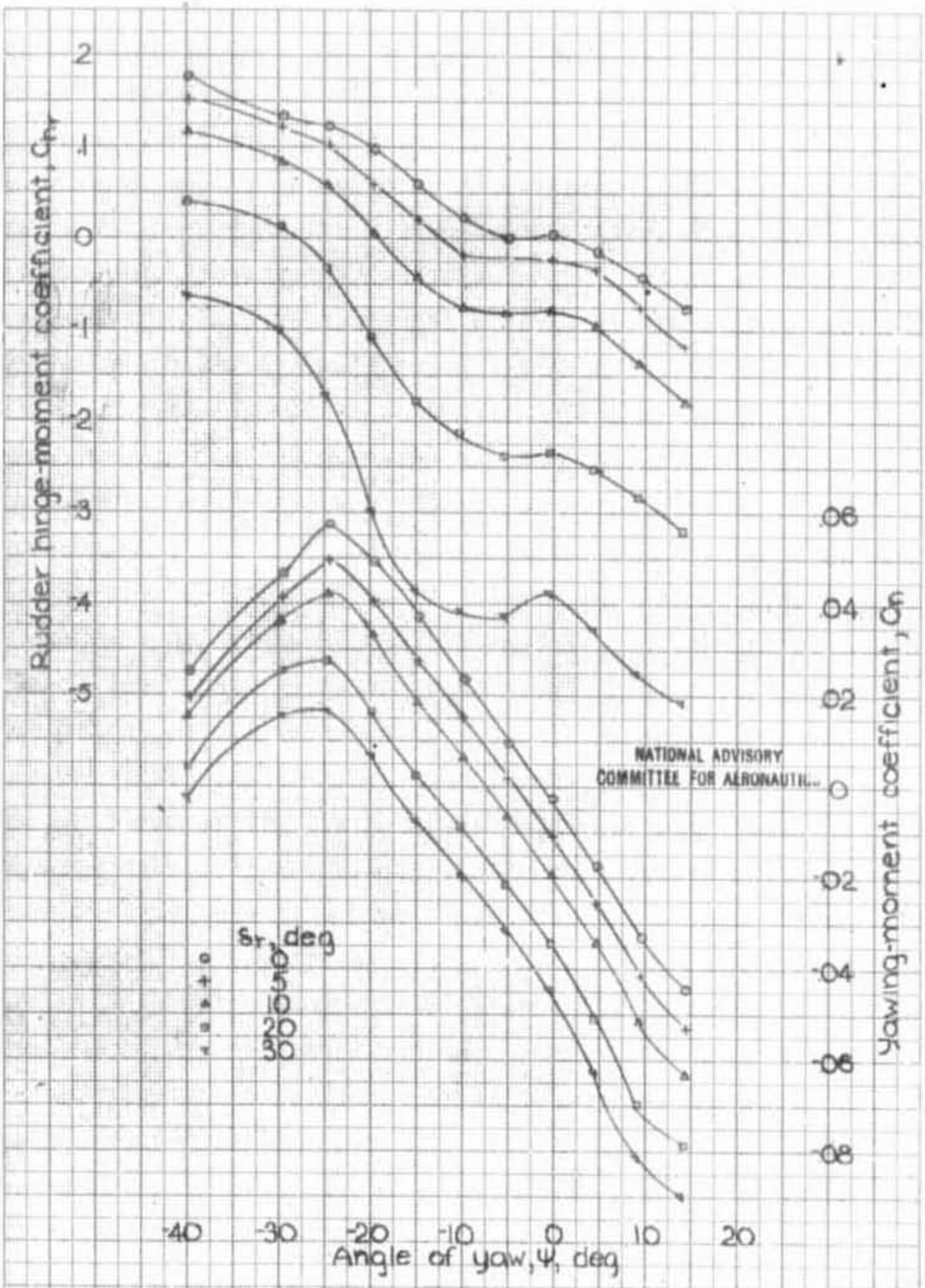

Figure 44.-Effect of rudder deflection on the aerodynamic characteristics in yaw of the XP-62 model (1/4-scale) with vertical tail V"R", δ_f=45°. Take off power, α=7.5 Anti-spin fillets, Dorsal D_{41}

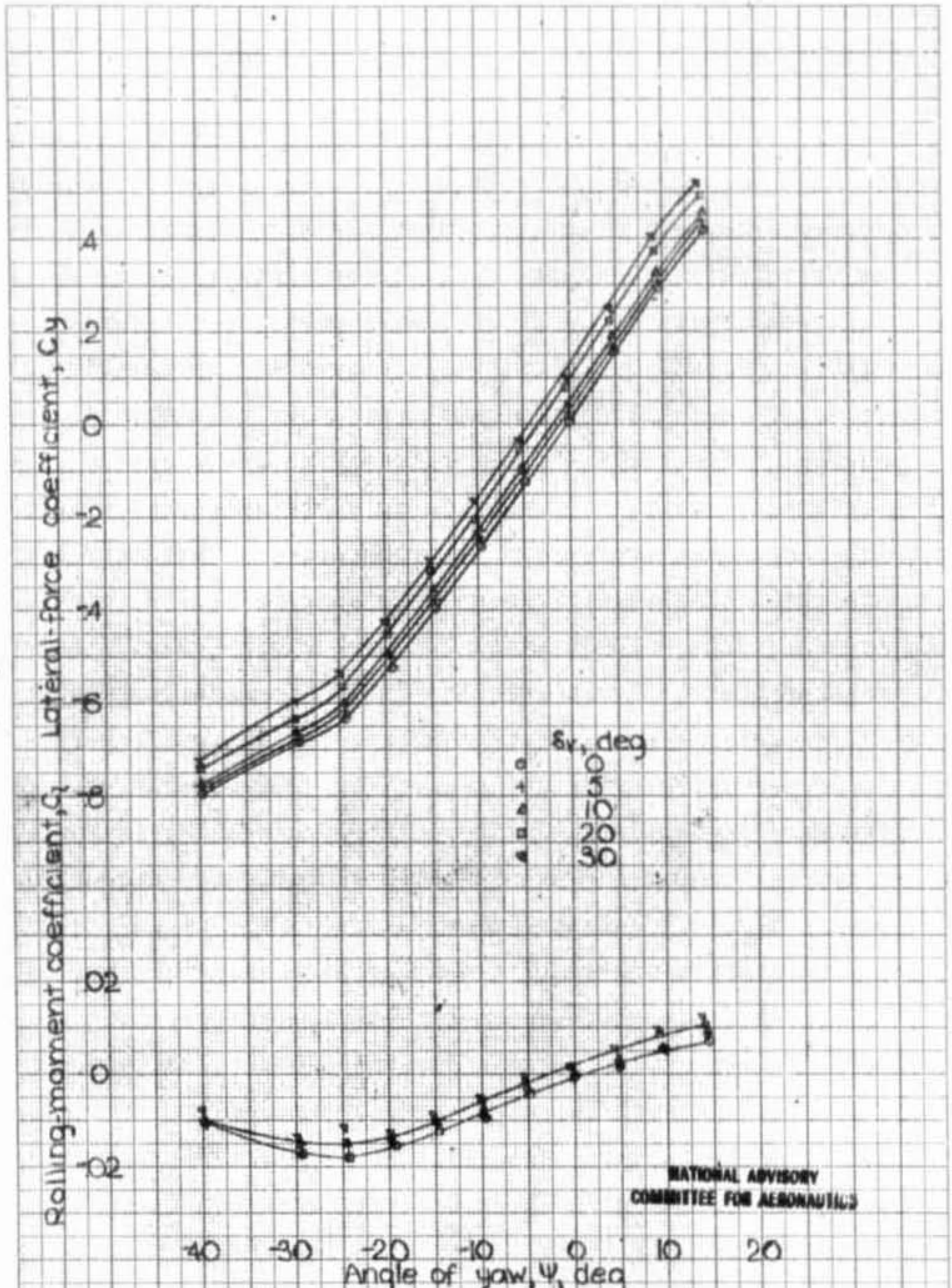

Figure 44.-continued.

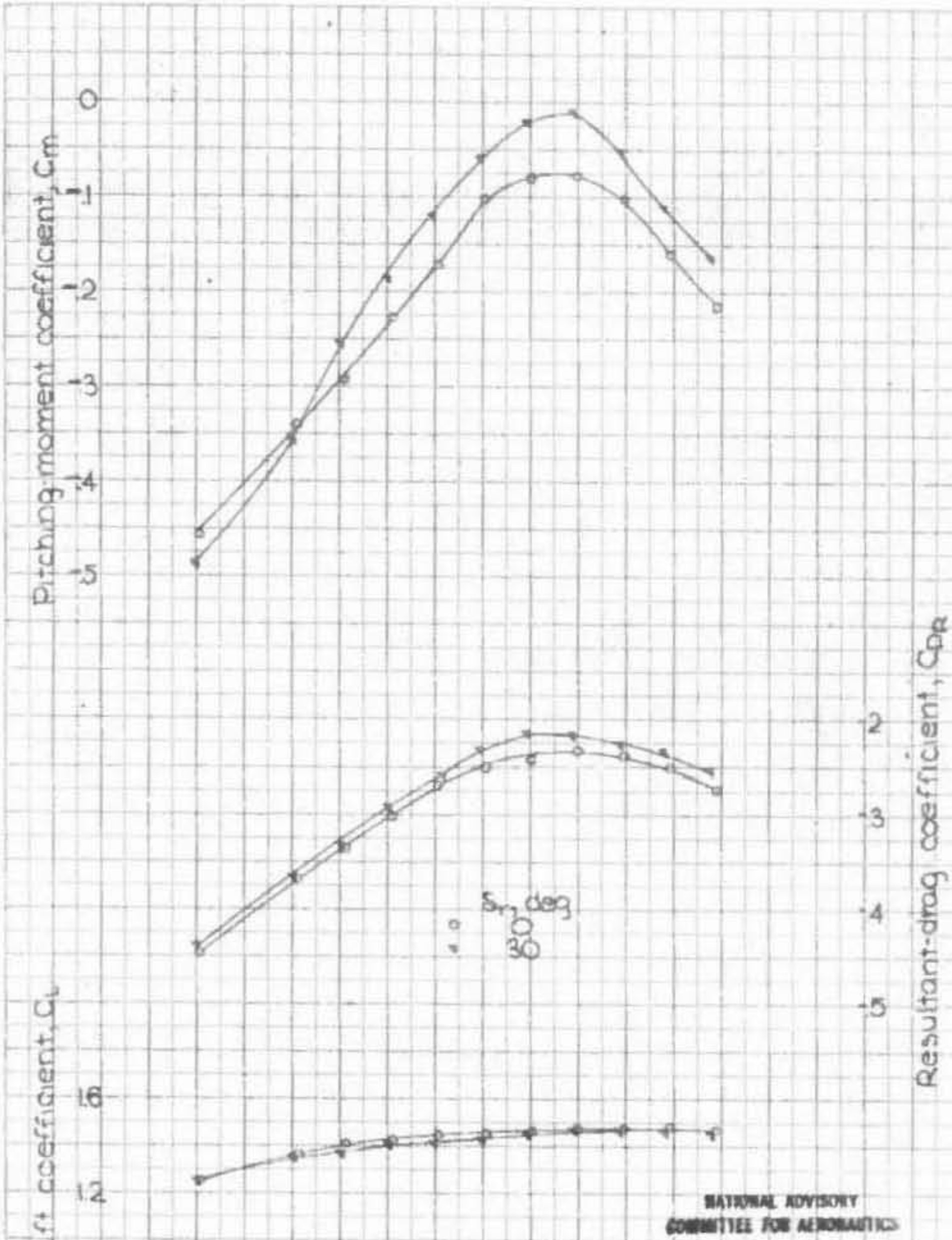

Figure 44-concluded.

L-779

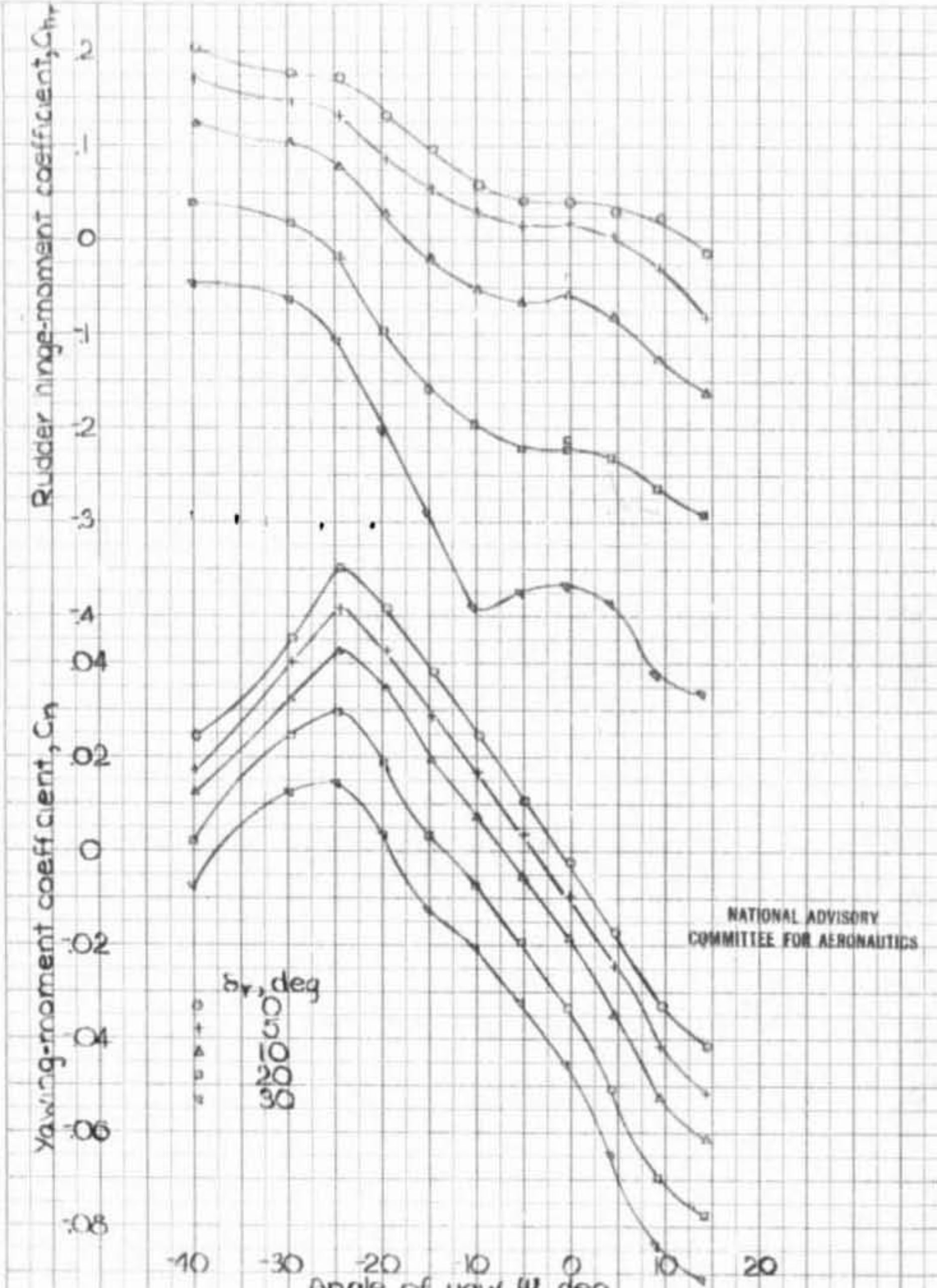

Figure 45.- Effect of rudder deflection on the aerodynamic characteristics in yaw of the XP-62 model (1/4 scale) with vertical tail V^4R^3 a_r 45°. Take-off power. α = 7.5° Antispin fillets, Dorsal D_{11}.

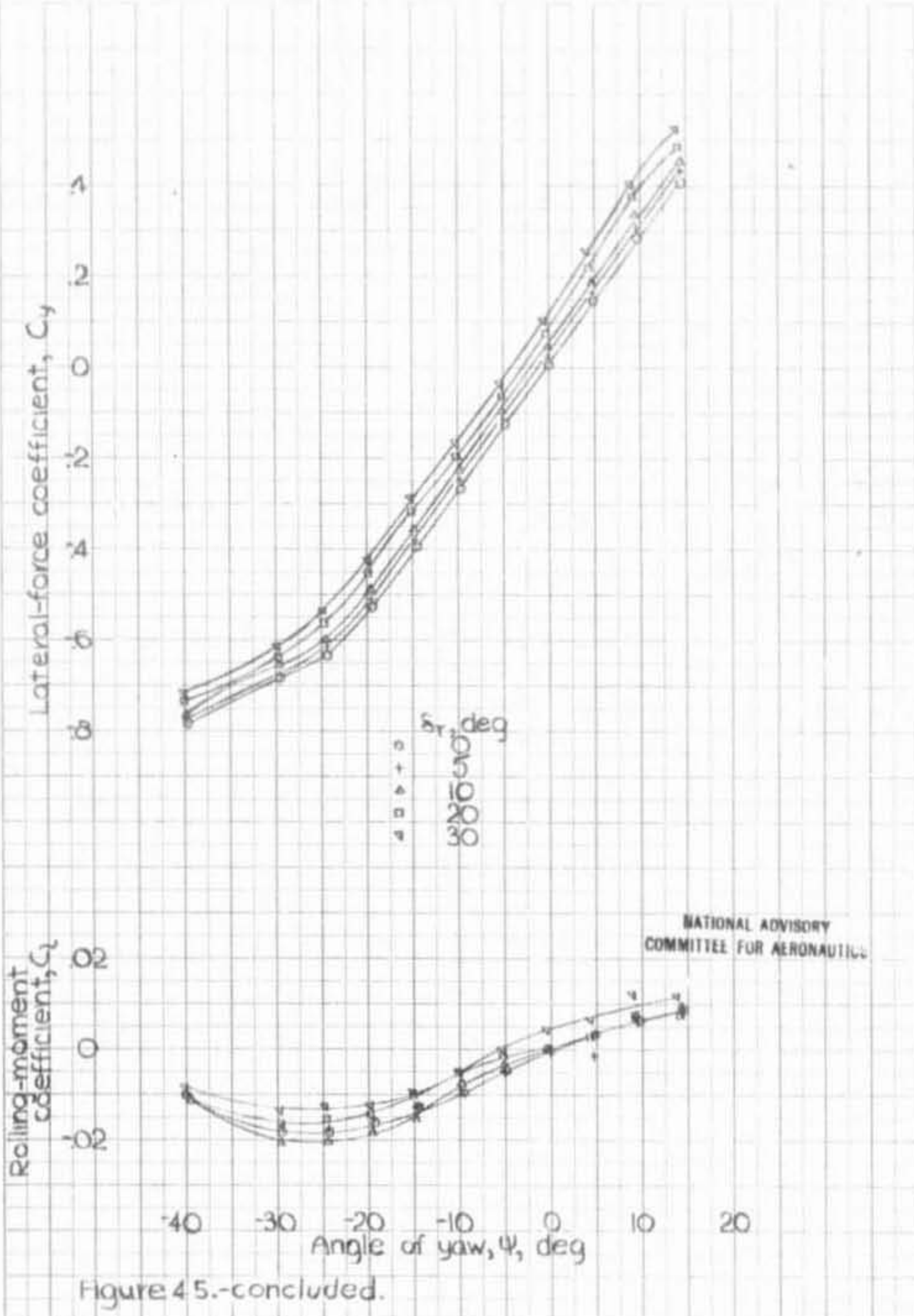

Figure 45.-concluded.

L-779

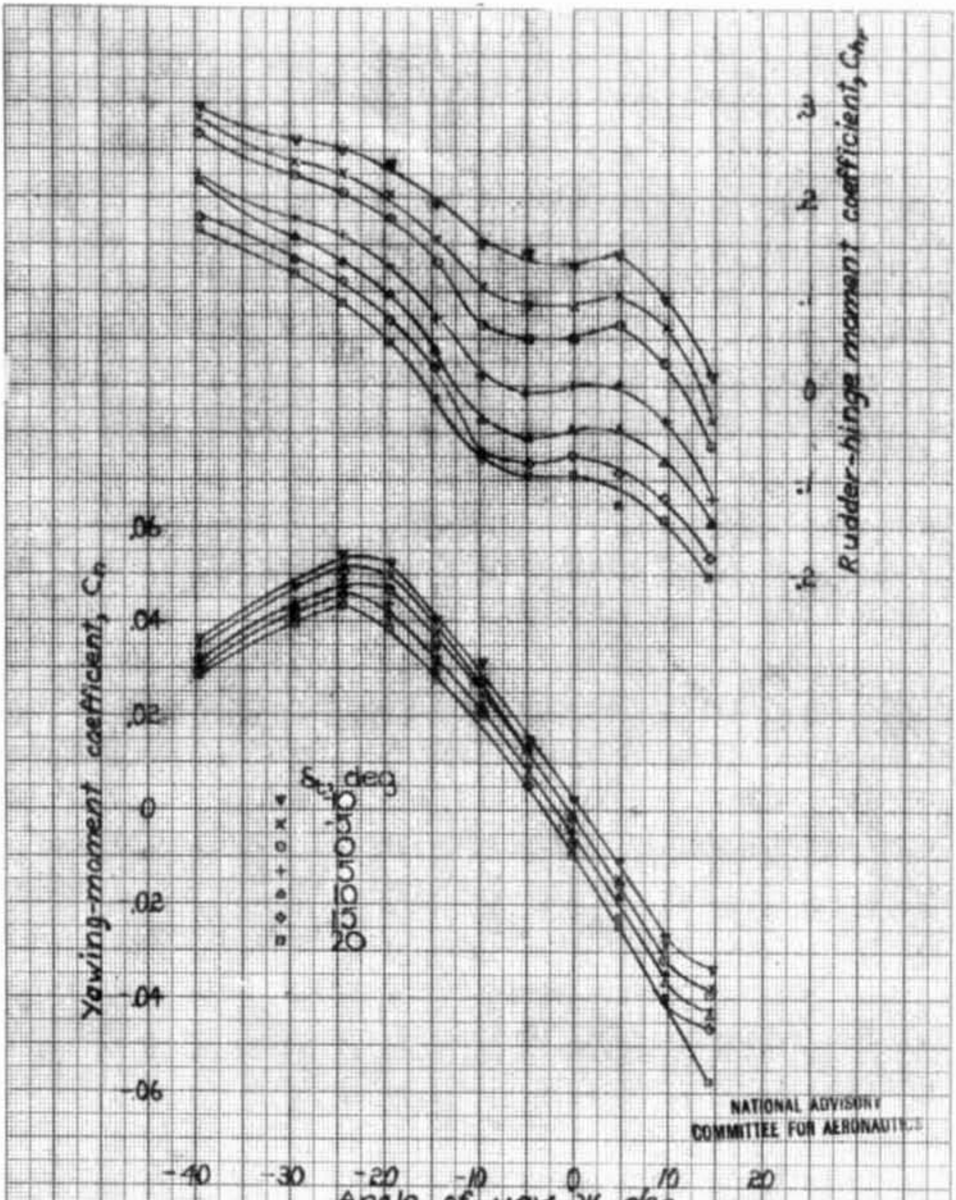

Figure 46.- Effect of tab deflection on yawing moment and rudder hinge moment characteristics in yaw of the XP-62 model (1/4-scale) with vertical tail $V^{14}R^{14}T$ $\delta_f = 45°$ $\alpha = 7.5°$, $\delta_r = 0$, antispin fillets Dorsal D_{51a}.

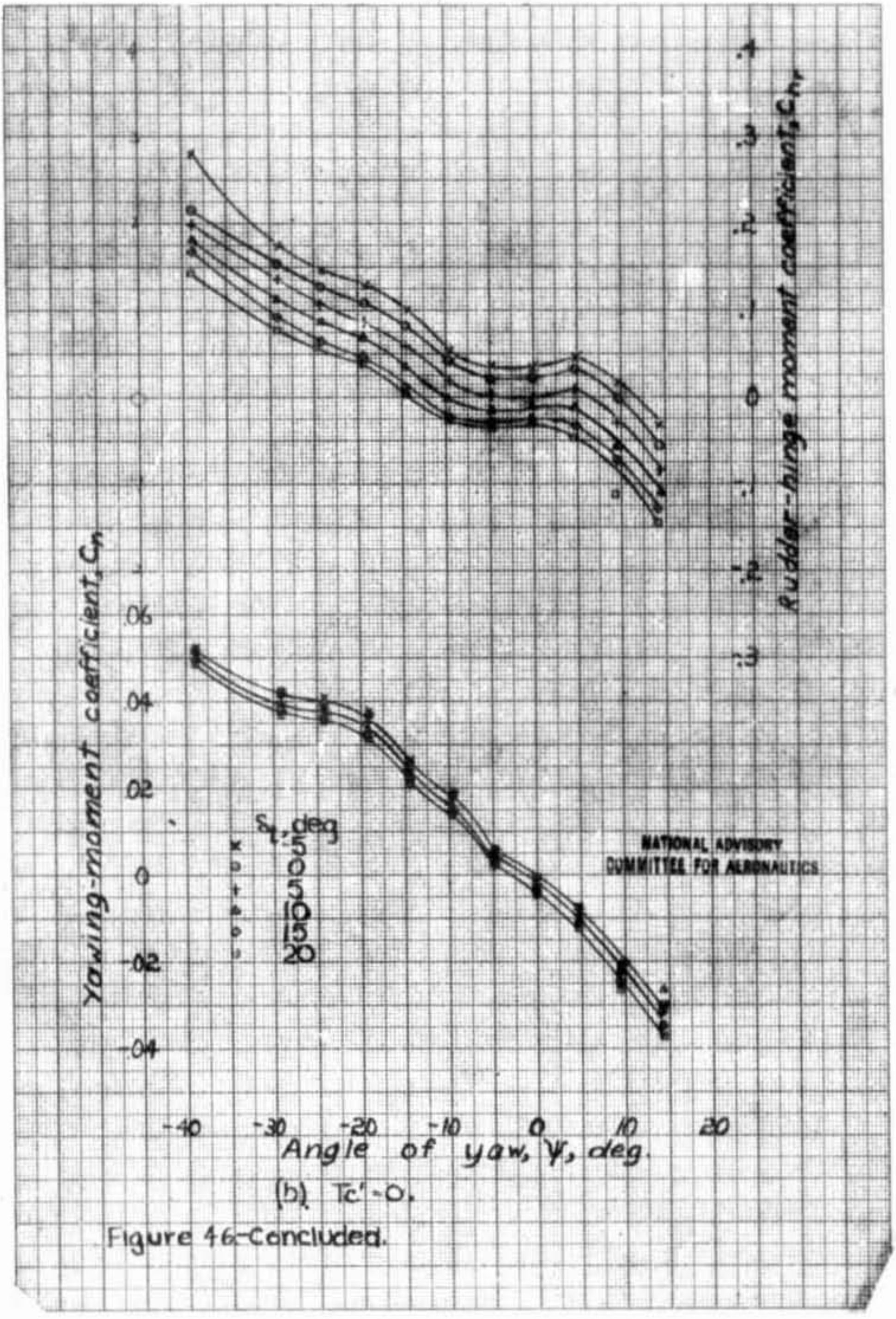

(b) $T_c' = 0$.

Figure 46-Concluded.

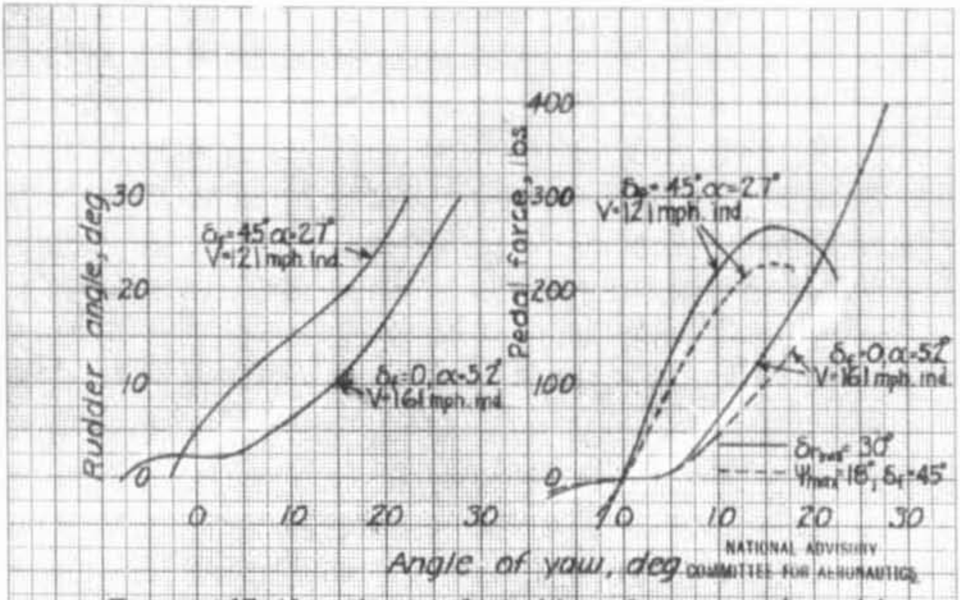

Figure 47.- Variation of rudder force and rudder deflection for trim with angle of yaw. XP-62 airplane with tail VR. Dorsal D_{32} Military power at 20,000 feet.

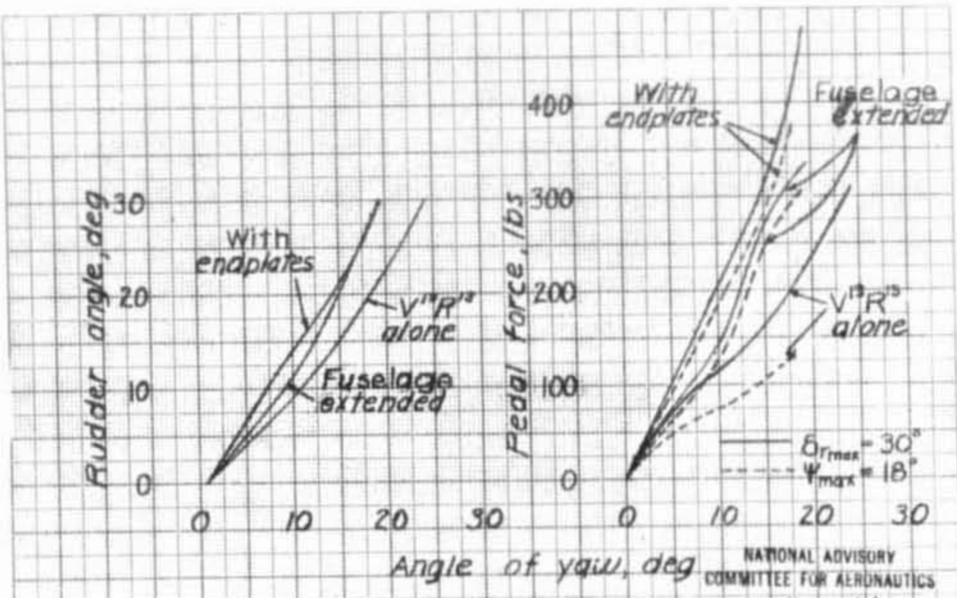

Figure 48.- Variation of rudder force and rudder deflection for trim with angle of yaw. XP-62 airplane with tail $V^{13}R^{13}$. Dorsal D_{41} Take-off power, δ_f= 45°, α= 7.5°, V= 96.5 mph. ind.

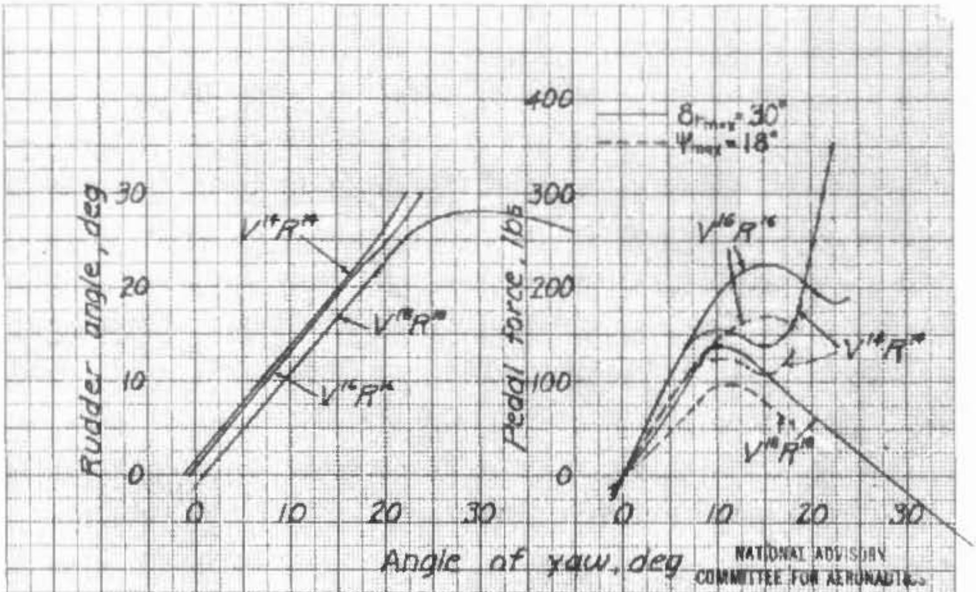

Figure 49. Variation of rudder force and rudder deflection for trim with angle of yaw. XP-62 airplane with tails $V^{14}R^{14}$, $V^{16}R^{16}$, $V^{18}R^{18}$. Dorsal D_{S14}. Take-off power, $\delta_f = 45°$, $\alpha = 7.5°$, $V = 96.5$ mph. ind.

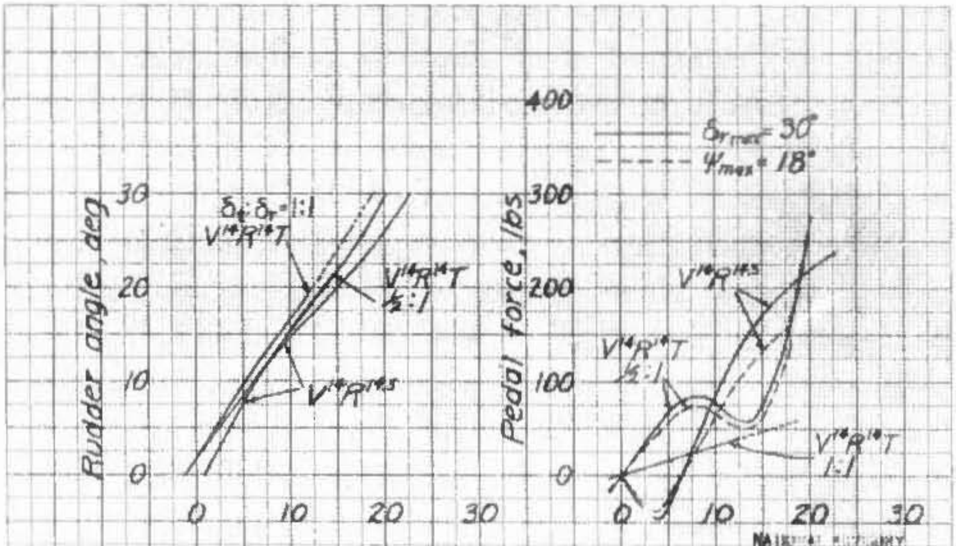

Figure 50.-Variation of rudder force and rudder deflection for trim with angle of yaw. XP-62 airplane with tails $V^{14}R^{14.5}$ and $V^{14}R^{14}T$ with balancing tab linkage. Dorsal D_{S14}, Take-off power, $\delta_f = 45°$, $\alpha = 7.5°$, $V = 96.5$ mph. ind.

L-779

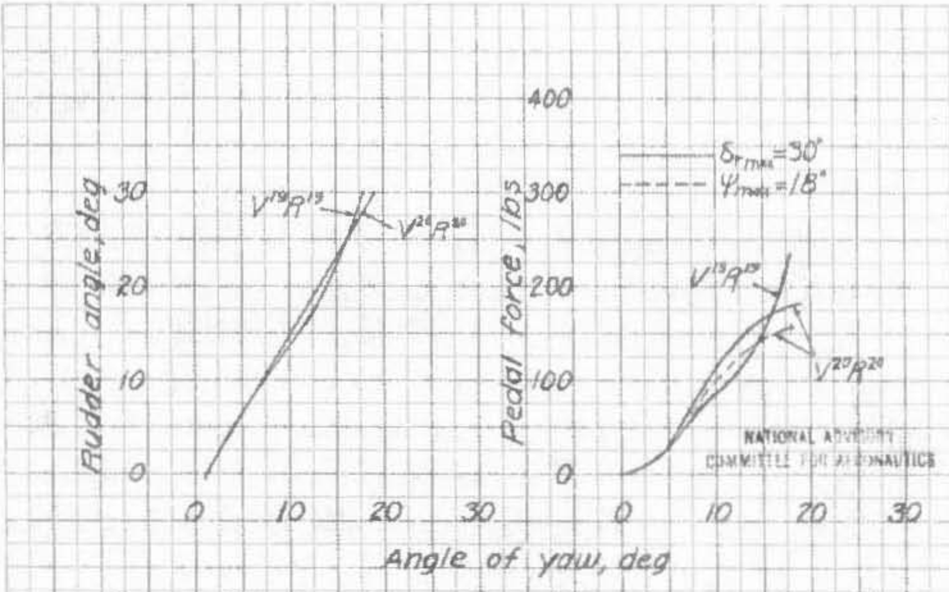

Figure 51.- Variation of rudder force and rudder deflection for trim with angle of yaw. XP-62 airplane with tails $V^{19}R^{19}$, $V^{20}R^{20}$ Dorsal D_{41}, Take off power, $\delta_f = 45°$, $\alpha = 7.5°$, $V = 96.5$ mph. ind.

ROLL FORM (10 OCT 47)

Recant, I. G.
Wallace, A. R.

AUTHOR(S)

DIVISION: Aerodynamics (2)
SECTION: Stability and Control (1)
CROSS REFERENCES: Airplanes - Tail configurations (08490.3); Airplanes - Control characteristics (08393); Airplanes - Performance (08478.6);*

ATI- 20709
ORIG. AGENCY NUMBER
MR L-779
REVISION

AMER. TITLE: Wind-tunnel tests of the 1/9-scale model of the Curtiss XP-62 airplane with various vertical tail arrangements
FORG'N. TITLE:

ORIGINATING AGENCY: National Advisory Committee for Aeronautics, Washington, D. C.
TRANSLATION:

COUNTRY	LANGUAGE	FORG'N.CLASS	U. S.CLASS.	DATE	PAGES	ILLUS.	FEATURES
U.S.	Eng.		Unclass.	Jul'43	120		photos, tables, diagrs, graphs

ABSTRACT

The effect of various vertical tail arrangements upon the stability and control characteristics of an XP-62 fighter model was investigated. Rudder-free yaw characteristics with take-off power and flaps deflected were satisfactory after dorsal fin modifications. Directional stability was obtained with all modified vertical tails. Satisfactory rudder effectiveness resulted partly because the dual-rotation propellers produced no asymmetric yawing moments. Pedal forces in sideslips were undesirably large but may be easily reduced.

* Airplane models - Wind tunnel testing (08321.3); XP-62 (08321.3)

NOTE: Requests for copies of this report must be addressed to: N.A.C.A., Washington, D. C.

RICTED

SHEET NO: R-2-1-19

TSDIN FORM 60 (13 MAR 47)

AUTHOR(S)		ATI- 20709
Recant, I. G. Wallace, A. R.	DIVISION: Aerodynamics (2) 1-9 SECTION: Stability and Control (1) 2-61 CROSS REFERENCES: Airplanes - Tail configurations (08490.3); Airplanes - Control characteristics (08393); Airplanes - Performance (08478.6);*	ORIG. AGENCY NUMBER MR L-779 REVISION

AMER. TITLE: Wind-tunnel tests of the 1/9-scale model of the Curtiss XP-62 airplane with various vertical tail arrangements

FORG'N. TITLE:

U

ORIGINATING AGENCY: National Advisory Committee for Aeronautics, Washington, D. C.

TRANSLATION:

COUNTRY	LANGUAGE	FORG'N.CLASS	U. S.CLASS.	DATE	PAGES	ILLUS.	FEATURES
U.S.	Eng.		Unclass.	Jul'43	120		photos, tables, diagrs, graphs

ABSTRACT

The effect of various vertical tail arrangements upon the stability and control characteristics of an XP-62 fighter model was investigated. Rudder-free yaw characteristics with take-off power and flaps deflected were satisfactory after dorsal fin modifications. Directional stability was obtained with all modified vertical tails. Satisfactory rudder effectiveness resulted partly because the dual-rotation propellers produced no asymmetric yawing moments. Pedal forces in sideslips were undesirably large but may be easily reduced.

* Airplane models - Wind tunnel testing (08321.3); XP-62 (08321.3)

NOTE: Requests for copies of this report must be addressed to: N.A.C.A., Washington, D. C.